

THE SIGNIFICANCE OF N-METHYLATION OF BACILLITHIOL ON ITS BIOLOGICAL ACTIVITY AS A REDOX COFACTOR

Hazel Nicole Moxham

A thesis submitted for the Degree of Master of Science by Research



University of East Anglia

School of Pharmacy

September 2018

This copy of the thesis has been supplied on condition that anyone who consults it is understood to recognise that its copyright rests with the author and that use of any information derived therefrom must be in accordance with current UK Copyright Law. In addition, any quotation or extract must include full attribution.

Abstract

Low molecular weight thiols play a crucial role in a multitude of biological processes such as maintaining redox homeostasis and the detoxification of chemical stressors. Different classes of microorganisms utilise different low molecular weight thiols. For example: glutathione is found eukaryotes and most gram-negative bacteria, mycothiol is found in the actinomycetes, and bacillithiol is found in the firmicutes. This study focused on N-methyl-bacillithiol, the novel low molecular weight thiol found in the green sulfur bacteria. Due to the unavailability of the thiol, the biophysical properties of a series of related derivatives were analysed and compared. Six thiols were examined so that each of their macroscopic and microscopic pK_a values as well as their thiol-disulfide exchange rate constants and their copper catalysed autoxidation rates were isolated. The results determined that each thiol maintains its own set of biophysical properties that are unique to each compound. These were then observed alongside others within the literature to compare and contrast. Predictions were made regarding the properties of N-methylated bacillithiol by associating the data of those with similar structural differences. The data presented here improves upon the knowledge of the individual properties of specific thiols, provides insight into the potential properties of a novel thiol and discusses its significance within the green sulfur bacteria.

Table of Contents

Abstract.....	2
List of Tables	5
List of Figures	5
List of Figures - Appendices	7
Acknowledgements.....	8
Chapter 1: Introduction	9
1.1 Overview	9
1.2 Low Molecular Weight Thiols and their Roles as Redox Cofactors.....	10
1.2.1 Overview	10
1.2.2 Glutathione	13
1.2.3 Trypanothione.....	15
1.2.4 Glutathione Amide.....	18
1.2.5 Mycothiol	19
1.2.6 Cysteine.....	21
1.3 The biological activity of Bacillithiol in <i>Bacillus subtilis</i>	23
1.3.1 Identification.....	23
1.3.2 Biosynthesis	23
1.3.3 Cellular Functionality	24
1.4 Green Sulfur Bacteria and its novel low molecular weight thiol	26
1.4.1 Green Sulfur Bacteria.....	26
1.4.2 The Role of Sulfur.....	26
1.4.3 The Discovery of N-Methyl-Bacillithiol	27
1.4.4 N-Methyl-Bacillithiol Biosynthesis	28
1.4.5 N-Methyl-Cysteine and Homocysteinyl-Bacillithiol	30
1.5 LMW Thiol Data Comparison	31
1.6 Aims of the project.....	33
1.6.1 Determining the Macroscopic and Microscopic pK_a 's of LMW thiols.....	33
1.6.2 Determining the pH Independent Thiol-Disulfide Exchange Rate Constants of LMW thiols.....	33
1.6.3 Determining the Copper Catalysed Autoxidation Rates of LMW thiols.....	33
Chapter 2: Determining the Macroscopic and Microscopic pK_a 's of LMW thiols.....	34
2.1 Introduction	34
2.2 Materials and Methods.....	37
2.2.1 Materials and Instruments.....	37

2.2.2	Thiol Quantification	37
2.2.3	Thiol and Amine Macroscopic pK_a Determination	37
2.2.4	Thiol and Amine Microscopic pK_a Calculations and Equations	38
2.3	Results and Discussion	39
Chapter 3: Determining the pH Independent Thiol-Disulfide Exchange Rate Constants of LMW thiols		46
3.1	Introduction	46
3.2	Materials and Methods	50
3.2.1	Materials and Instruments	50
3.2.2	Thiol-Disulfide Exchange Assay	50
3.2.3	Obtaining the pH-Independent rate constant (k_1)	50
3.3	Results and Discussion	51
Chapter 4: Determining the Copper Catalysed Autoxidation Rates of LMW thiols		56
4.1	Introduction	56
4.2	Materials and Methods	61
4.2.1	Materials and Instruments	61
4.2.2	Cu^{2+} Catalysed Autoxidation	61
4.2.3	Data Analysis	61
4.3	Results and Discussion	62
Chapter 5: Conclusions and Future Work		68
Appendices		69
1.1	Additional pK_a graphs and standard errors	69
Abbreviations		73
Bibliography		75

List of Tables

Table 1. The known properties of select LMW thiols.	31
Table 2. Macroscopic and microscopic pK _a values of the thiol and amino groups for various LMW thiols. Data errors for each pK _a were calculated to <0.36 pK _a values using Grafit.	41
Table 3. The predicted values for the macroscopic and microscopic pK _a 's of N-Me-BSH.	44
Table 4. Gathered vs published data of thiol-disulfide exchange reactivities between LMW thiols and DTNB.	52
Table 5. The autoxidation rates of LMW thiols with and without CuSO ₄ , their rates relative to Cys when normalised to 100%, and their standard errors.	64

List of Figures

Figure 1. Common LMW thiols produced by various organisms and their Cys components (blue).	11
Figure 2. LMW thiol cellular functions: i) as redox buffers, ii) in reactive carbonyl electrophile detoxification, iii) in the detoxification of xenobiotics, iv) in metal ion homeostasis, v) as an intracellular Cys reservoir, and vi) in protein function redox protection and regulation [7, 146, 3].	12
Figure 3. NADPH-dependent disulfide-reducing pathways: a) glutathione reductase, glutathione and glutaredoxin and b) thioredoxin reductase and thioredoxin [36, 148].	14
Figure 4. The biosynthesis of GSH.	15
Figure 5. NADPH-dependent disulfide-reducing pathway: trypanothione reductase and trypanothione followed by tryparedoxin and tryparedoxin peroxidase [3, 36].	16
Figure 6. The biosynthetic pathway of T(SH) ₂ following on from the biosynthesis of GSH... 18	
Figure 7. The metabolism of MSH: 1) NAD/MSH-dependent formaldehyde dehydrogenase, 2) MSH disulfide reductase (mycothione reductase), 3) MSH S-conjugate amidase, 4) MSH biosynthesis [1].	20
Figure 8. The biosynthesis of MSH [3].	21
Figure 9. The Biosynthesis of BSH.	23
Figure 10. The inactivation of fosfomycin catalysed by FosB, a BSH-S-transferase [3].	25
Figure 11. An overview of the sulfur metabolism pathways in <i>Cba. Tepidum</i> [88].	27
Figure 12. HPLC traces of the bimane labelled novel LMW thiol in <i>Cba. tepidum</i> , A) the thiol with a homocysteine sidechain, B) the thiol with an n-methylated cysteine sidechain, C) original sample isolated from <i>Cba. Tepidum</i> , D) the combination of B) and C) [85].	28
Figure 13. The Biosynthetic Pathway of N-Me-BSH.	29
Figure 14. Structure of Thiocoraline and its Cys residues (colour) [91].	30

Figure 15. The four deprotonation pathways of a cysteinyl thiol that dictate the four microscopic dissociation constant values [83].	36
Figure 16. The structure of BSH and its the relation of each of its functional groups to each macroscopic dissociation constant shown in table 2: a) pK_{a1} , b) pK_{a2} , c) pK_{a3} and d) pK_{a4} .	39
Figure 17. The absorbance (at 232nm) vs pH plot determining the thiol and amino pK_a values of Cys. The standard error for each one was also calculated. Y was calculated using equation (7) in chapter 2.2.3.	40
Figure 18. The percentage of thiolate present in Cys and BSH at different pH's as well as the predicted thiolate concentrations of N-Me-BSH.	45
Figure 19. The formation of sulfenic, sulfinic and sulfonic acids through the oxidation of thiols.	46
Figure 20. Mechanism of thiol-disulfide exchange.	46
Figure 21. A thiol-disulfide exchange reaction with DTNB reacting with a thiol to produce TNB ⁻ . The reaction then continues to ensure that all thiol is reacted. For $\lambda_{max} = 412nm$ and $\epsilon = 14150M^{-1}cm^{-1}$.	48
Figure 22. Graphs depicting the rate (k_1) of TNB formation (k_{obs}) vs thiolate concentration for Cys and N-Me-Cys when reacted with DTNB (40mM). Each data point was conducted in triplicate and the errors shown as error bars.	51
Figure 23. The differences in the thiol-disulfide exchange rates for Cys depending on the pK_a values used: with the pK_a data obtained from this study: pK_s at 8.49 and pK_{ns} at 10.33 (●), the pK_a data from Sharma et al: pK_s at 8.38 [83] and pK_{ns} at 9.94 (•) and the pK_a data from Benesch et al: pK_s at 8.53 and pK_{ns} at 10.03 (◻) [101].	53
Figure 24. The copper catalysed autoxidation of Cys. Phase I is represented with solid lines and phase II is represented with dotted lines [130].	58
Figure 25. The copper catalysed autoxidation of GSH. The two possible pathways are either peroxide-dependent or superoxide-dependent [124].	60
Figure 26. Differences in autoxidation rates for each thiol when incubated with and without CuSO ₄ . The gradient of the linear fit gives the rate of autoxidation.	63
Figure 27. Rates of thiol autoxidation when incubated with and without CuSO ₄ when compared to Cys (normalised to 100%).	65
Figure 28. Graphs depicting the relationship between the relative rates of autoxidation and the microscopic pK_a values of Cys, HCys, N-Me-Cys, BSH, HCys-BSH and GSH.	67

List of Figures - Appendices

Appendix 1. The absorbance (at 232nm) vs pH plot determining the thiol and amino pK _a values of HCys. The standard error for each one was also calculated.	69
Appendix 2. The absorbance (at 232nm) vs pH plot determining the thiol and amino pK _a values of N-Me-Cys. The standard error for each one was also calculated.	69
Appendix 3. The absorbance (at 232nm) vs pH plot determining the thiol and amino pK _a values of BSH. The standard error for each one was also calculated.	70
Appendix 4. The absorbance (at 232nm) vs pH plot determining the thiol and amino pK _a values of HCys-BSH. The standard error for each one was also calculated.....	70
Appendix 5. The absorbance (at 232nm) vs pH plot determining the thiol and amino pK _a values of GSH. The standard error for each one was also calculated.....	71
Appendix 6. Graphs depicting the rate (k ₁) of TNB formation (k _{obs}) vs thiolate concentration for the remaining LMW thiols when reacted with DTNB (40mM). Each data point was conducted in triplicate and the errors shown as error bars.	72

Acknowledgements

I would like to thank my primary supervisor Dr. Chris Hamilton for giving me the opportunity to work on this project as well as the opportunity to be a part of his team. With your endless enthusiasm for your work and your excitement when discussing potential avenues to explore made this research such an adventure. Thank you for accepting an inexperienced biologist into your lab and letting me learn from your vast knowledge and experience of the world of thiol biochemistry. I would also like to thank my secondary supervisor Prof. Nick Le Brun for his patience and for helping me improve my chemistry knowledge. Thank you both for your support, advice, and for pushing me out of my comfort zone when I needed it. You have both been invaluable to me and I thank you for every discussion and questioning.

My thanks also go to Dr. Ryan Tinson for teaching me all the vital chemistry knowledge that has led me here, I learnt so much from you and I enjoyed every minute of it. When I first entered the lab, I had so little experience, but you made me feel comfortable from the very beginning and took the time to ensure that I knew what I was doing. I must also thank Dr. Dominic Rodrigues for discussing and testing each other in the areas where our projects overlapped and for teaching me the techniques required for thiol detection. You both made it easy to share a good laugh whenever we were together or ask for advice when things didn't quite go to plan, and we didn't know what to do next. I couldn't have done it without you.

To everyone at UEA who helped me along the way, whether in aid of my research or as moral support, you have my unending gratitude for keeping me sane and for making my experience here so amazing.

I dedicate this thesis to my parents who have never stopped believing in me. Thank you for the support and the funding you have so generously provided throughout this project. Finally, thank you to Chris Aris for being my rock and my shoulder to cry on. Your faith in me has got me further than I ever thought possible.

1.1 Overview

Bacteria are microscopic organisms that are essential to our existence. These prokaryotic organisms are believed to be among the first forms of life to appear on Earth and can be found in almost every environment on the planet. The role that each bacteria play can range from very helpful to very harmful. For example, probiotic bacteria can have a positive effect on the body or alternatively pathogenic bacteria can cause a varying number of diseases. Outside the body, bacteria aid us in the food industry by fermenting foods. By converting compounds such as methane into energy and helping scientists produce antibiotics in order to combat diseases. The total biomass of all bacteria is thought to exceed that of plants and animals collectively, making the need to understand as many species as we can a necessity. There are many species of bacteria that have yet to be characterised and many that may never be identified.

All organisms, without exception, sustain at least one low molecular weight thiol (LMW) in high concentrations to maintain an intracellular reducing environment. Although most tend to rely on glutathione (GSH) for this purpose, many alternatives have been identified in certain organisms. In relation to this, this project focused on the newly characterised N-methyl bacillithiol (N-Me-BSH) and how it differs from the non-methylated bacillithiol (BSH) as well as other LMW thiols found in different organisms. In order to achieve this the pK_a 's, thiol-disulfide exchange rate constants and autoxidation rates of six LMW thiols were isolated and compared. These results were then analysed to gain an understanding into the roles that they play in cell physiology. The following introduction outlines some of the most well-known LMW thiols, their functions, and their roles in each of their respective organisms. Following that, the current knowledge of BSH and N-Me-BSH are examined in detail.

1.2 Low Molecular Weight Thiols and their Roles as Redox Cofactors

1.2.1 Overview

LMW thiols are very reactive non-protein compounds that can be found in every organism (Fig. 1) and play a crucial role in a variety of cellular processes due to the versatile nature of their sulfhydryl group [1]. These include: maintaining redox homeostasis, detoxification of chemical stressors, metal ion homeostasis and the redox regulation and protection of protein function (Fig. 2) [2, 3]. These cofactors are also produced by cells to combat a multitude of reactive chemical species including reactive oxygen, nitrogen, and electrophilic species. The most basic thiol, hydrogen sulfide, is indicated to have played a part in chemistry that occurred prebiotically [4, 5]. It is found in iron-sulfur proteins as a bound cofactor [1]. The most commonly occurring LMW thiol is GSH, which can be found in most eukaryotes and many gram-negative bacteria. Organisms that do not produce GSH can produce a wide variety of other LMW thiols that serve the same functions. Gram-positive bacteria can produce trypanothione ($T(SH)_2$), mycothiol (MSH), and BSH as an alternative to GSH. As well as producing one major LMW thiol, organisms produce smaller quantities of other thiols to perform as redox regulators such as cysteine (Cys) or Coenzyme A (CoA).

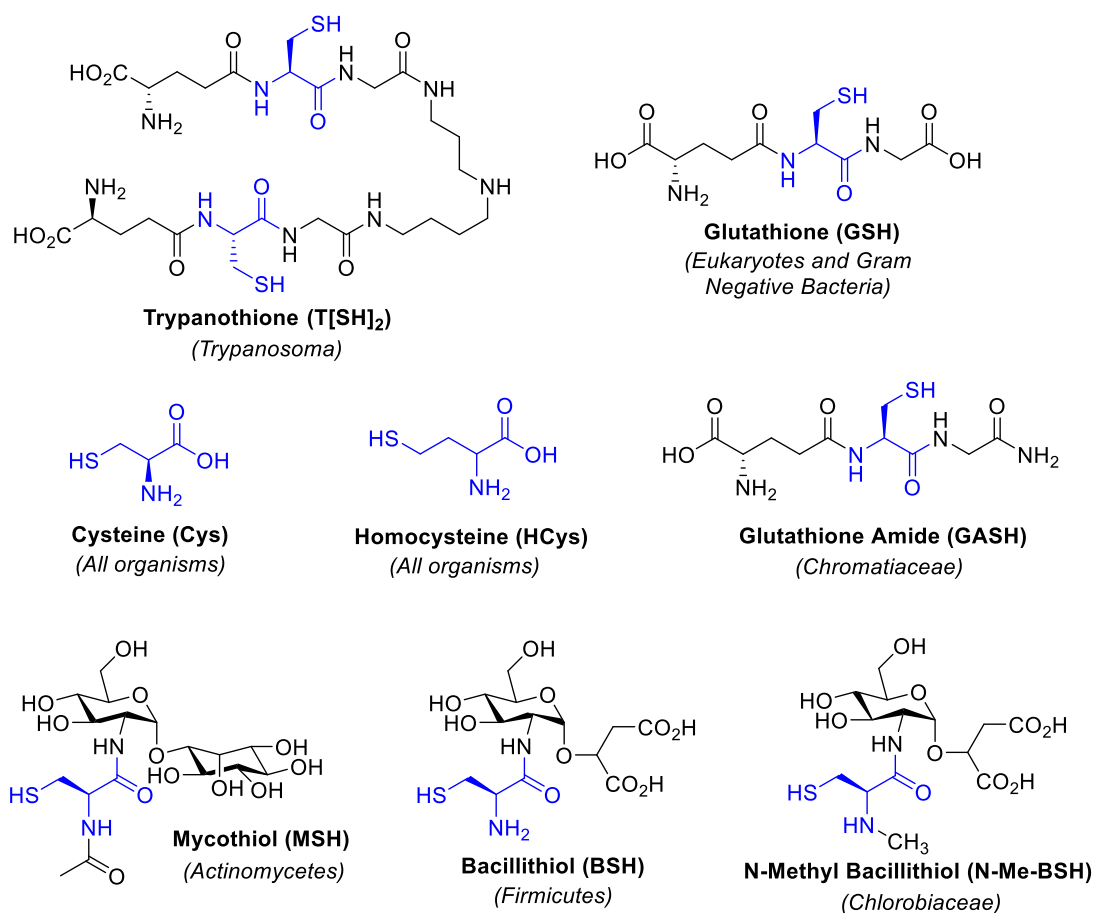


Figure 1. Common LMW thiols produced by various organisms and their Cys components (blue).

All thiols have certain similarities, including that each of their structures contain a cysteine component meaning that they have some consistency in the presence of certain functional groups like their thiol and amino groups which are important when looking at individual biophysical properties. They do, however, also have some very large differences between them which are thought to contribute towards the reason that different organisms produce different thiols. Specifically, their concentrations within the cell, their acid dissociation constants, rates of thiol disulfide exchange and autoxidation rates vary enough that these differences must be biologically important. Certain thiols have also been seen to have some of their own individual roles, providing a cause for the fact that organisms produce more than just one LMW thiol. Not all of their metabolic functions have yet been determined, leaving room for other possible roles within cells [6, 7].

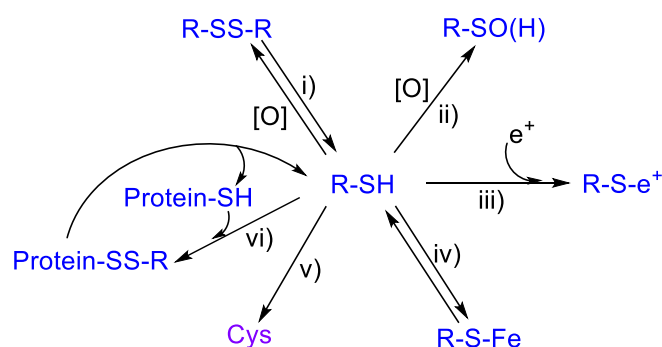


Figure 2. LMW thiol cellular functions: i) as redox buffers, ii) in reactive carbonyl electrophile detoxification, iii) in the detoxification of xenobiotics, iv) in metal ion homeostasis, v) as an intracellular Cys reservoir, and vi) in protein function redox protection and regulation [7, 146, 3].

Perhaps the most common reaction of the thiol group is their ability to form disulfide bonds between two thiols to produce a disulfide. A disulfide formed from two Cys molecules provides stability and helps provide structure for proteins present outside the cytoplasm of the cell. This does not happen during oxidative stress as a disulfide bond can only be formed between a protein thiol and a LMW thiol or between two protein thiols [8]. Oxidative stress is brought about via the overproduction of reactive oxygen species when the cell cannot combat it with antioxidants. This can change the structures of cell membranes, proteins, lipids and nucleic acids as well as disrupt cell signalling [9, 10, 11]. In response, most organisms produce enzymes such as peroxiredoxins, catalases and superoxide dismutases that neutralise harmful oxidants by reacting with them before they can cause irreparable damage [10]. Such damage can cause the alteration and inactivation of proteins through covalent modifications [11]. Carbonylation can occur to amino acids such as arginine, proline, threonine and lysine [12]. Tyrosine can form nitrotyrosine when reacted with reactive nitrogen species [13] and histidine forms oxo-histidine [14]. In humans, oxidative stress has been observed to play a role in ageing, cancer, diabetes mellitus, Alzheimer's disease, Parkinson's disease, atherosclerosis and rheumatoid arthritis [9]. Thiols also have a high affinity for metals and play a role in metal ion homeostasis by protecting the cell from their harmful effects on biological processes within the cytosol [8]. Each LMW thiol acts as a redox cofactor by influencing the redox potential of the organism which is crucial to the continued function of an organism's metabolic pathways. This can be achieved through the alteration of the ratio of thiol and disulfide concentrations, which are not in equilibrium intracellularly (Fig.2.i) [6]. As well as this, thiols can form S-conjugates due to their ability to act as nucleophiles. This allows them to protect against electrophiles and alkylating agents by acting as a buffer or by altering them enzymatically through the production of adducts so that they become less harmful [15]. For example, glutathione-S-transferases acts as a catalyst during the formation of S-conjugates which are produced to detoxify xenobiotics [16, 17]. Literature implicates that S-transferases play a role in resistance to herbicides, insecticides, drugs and toxic heavy metals [18, 19, 20, 21].

1.2.2 Glutathione

Otherwise known as L- γ -glutamyl-L-cysteinyl-glycine, GSH is the most abundant LMW thiol found in eukaryotes. These include plants, animals and fungi as well as most gram-negative bacteria [22]. The biosynthetic pathway for GSH has been identified in cyanobacteria and purple bacteria [23] as well as all eukaryotes not lacking chloroplasts and mitochondria [1]. As its name suggests, the thiol is a tripeptide made up of three amino acids: glutamate, cysteine and glycine. It's found in varying concentrations throughout each organism but in animals it ranges from 0.5mM to 10mM [22, 24]. The cytosol contains the majority of cellular GSH, around 85-90%, while the remainder can be found in organelles such as the mitochondria and nuclear matrix. Concentrations of its disulfide (GSSG) are very low intracellularly compared to that of GSH and so the levels are difficult to ascertain through experimental means. Extracellular concentrations of GSH however are low in comparison as, for example, they vary from 2-20 μ M in plasma. The only exception being the amount of the thiol found in bile acid which is thought to be anywhere up to 10mM. Transport of extracellular GSH and GSSG into cells is thermodynamically unfavourable due to the extreme concentration gradient [22]. Due to the presence of the Cys residue in its structure, GSH is easily oxidised into its disulphide form (Fig.2). This is achieved by reacting with different electrophilic substances including various reactive species and free radicals. These include: selenium-containing GSH peroxidase catalysing the reduction of hydrogen peroxide (H_2O_2) as well as other peroxides, reacting with oxygen (O_2) to form H_2O_2 and transhydrogenation [24]. GSH peroxidase catalysis of the reduction of H_2O_2 and other peroxides is an important metabolic pathway as it is coupled with the oxidation of both 6-phosphogluconate and glucose-6-phosphate and protects membrane lipids from oxidation [24, 25]. In biology, the production of H_2O_2 and O_2^- are a common occurrence and they tend to introduce reactive oxygen species into the cell that then go on to form organic peroxides [26].

The reduction of GSSG is controlled by GSSG reductase. The production of GSSG and its efflux from cells influences the decrease in pool size of GSH found intracellularly. Many factors affect the intracellular concentrations of the thiol: oxidative stress, certain pathological conditions, and protein malnutrition [22]. GSH and GSSG tend to make up the total cell content of the thiol, with up to 15% bound to proteins and most free GSH existing in its reduced state [9]. The ratio of thiol to disulfide is used as an indicator to determine the redox state of the cell [22]. GSH is a good redox buffer because it does not bear the same toxicity as Cys [27]. This state is maintained by a flavoenzyme called GSH reductase that utilises nicotinamide adenine dinucleotide phosphate (NADPH) to reduce GSSG [6]. The pathway for intracellular disulfide reduction is outlined in Fig 3. The pathway not only utilises GSH reductase, but glutaredoxin as well as thioredoxin and thioredoxin reductase. The GSH-GSSG ratio in resting cells under physiological conditions tend to exceed 100:1 whereas in models demonstrating oxidative stress it has been observed to drop to ratios of 10:1 [9]. Thiol disulfide exchange reactions, catalysed by glutathione-insulin transhydrogenase [28], promote the formation of protein-disulfides, as well as their reduction or isomerisation depend on the imposed redox potential [29]. The standard redox potential of GSH and GSSG at pH 7 is -240 mV [6]. In terms of products produced by reactions involving GSH, the formation of disulfides, thioethers and thioesters are the most common. A large number of thioethers are created by a group of enzymes known as GSH transferases. These thioethers are called GSH S-conjugates and use GSH to produce compounds that have an affinity for detoxification and elimination [27].

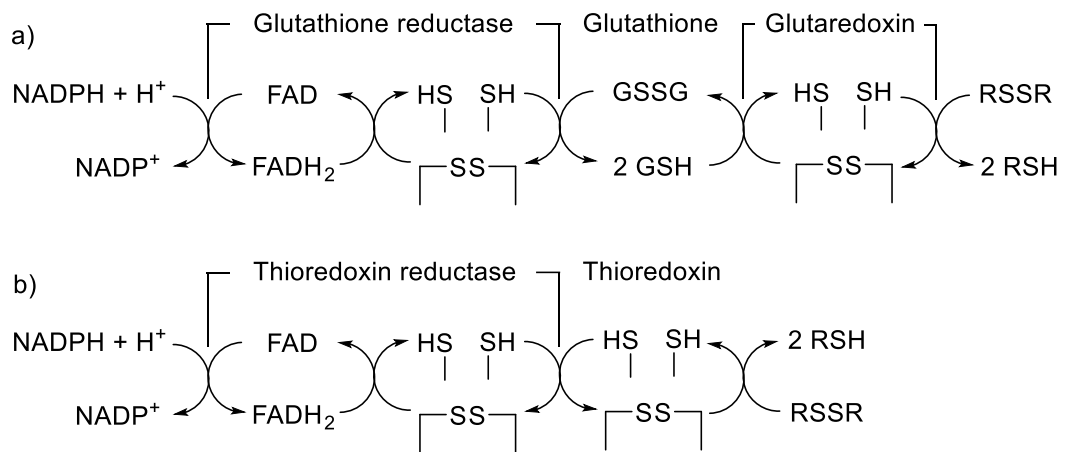


Figure 3. NADPH-dependent disulfide-reducing pathways: a) glutathione reductase, glutathione and glutaredoxin and b) thioredoxin reductase and thioredoxin [36, 148].

The liver's perivenous hepatocytes and periportal cells are where most of the thiol is produced and exported. GSH is synthesised from its three amino acid components (Fig 4.) intracellularly and is catalysed via GSH synthase and γ -glutamylcysteine synthetase (GCS), two cytosolic enzymes. Glutamate forms a peptidic γ -linkage on its γ -carboxyl group to the amino group of Cys [22]. The γ -linkage of the peptide is predicted to prevent degradation of GSH by aminopeptidases [22, 27]. In all cells throughout each different organism that can produce GSH, it is synthesised via the same pathway. The transport of Cys in the body is mainly undertaken in the form of GSH. Most of the Cys required for GSH synthesis is obtained from intracellular protein degradation or endogenous synthesis. GCS transcription and activity in cells can be affected by various factors which ultimately affects the production of GSH. Antioxidants, heavy metals, GSH depletion, GSH conjugation, heat shock, cancer, chemotherapy, inflammatory cytokines and oxidant stress can increase GCS levels whereas GCS phosphorylation, hyperglycaemia, dietary protein deficiency, dexamethasone and erythropoietin can decrease levels. GSH homeostasis is altered by the balance of amino acids in the diet as it affects protein nutrition in cells. Specifically, the intake of Cys, methionine (Met), glutamine and glycine is essential for optimising GSH synthesis [22]. As soon as synthesis is complete, the resulting thiol can be transported to take part in an inter organ transport network. Both the liver and the kidneys are the two major organs that are involved in the inter-organ flow of GSH [24, 30]. The GSH produced in the liver requires transportation through the bloodstream to other tissues. The thioesters, or S-conjugates, are transported the same way through the canalicular membrane for biliary excretion [27]. When transported across cell membranes, GSH interacts with γ -glutamyl transpeptidase which is responsible for the formation of γ -glutamyl amino acids. The reactions involving γ -glutamyl transpeptidase make up the γ -glutamyl cycle, the process responsible for the formation and degradation of GSH [24]. In mice and rats GSH synthesis can be inhibited by buthionine sulfoximine, which inhibits γ -glutamylcysteine synthetase, as well as other sulfoximines [31].

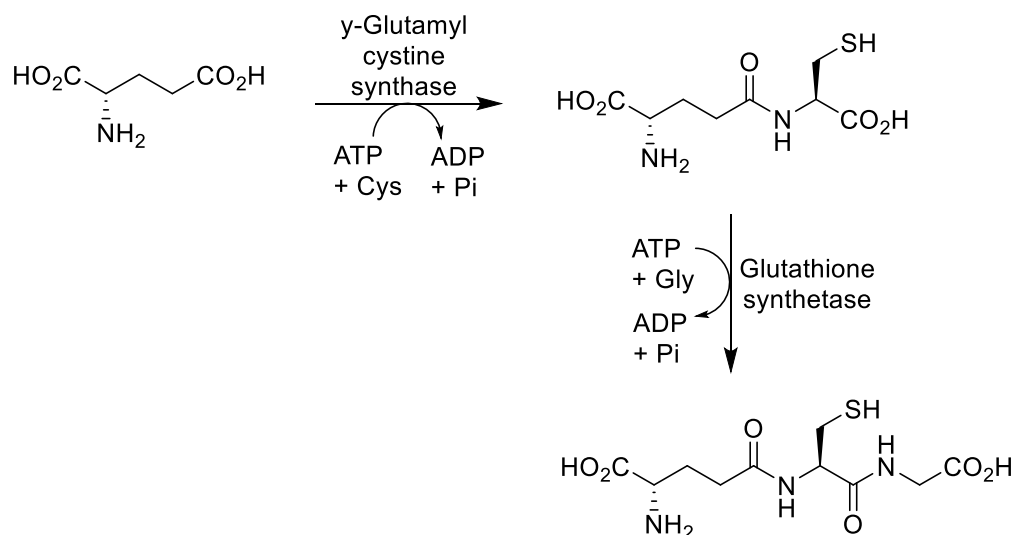


Figure 4. The biosynthesis of GSH.

GSH has a wide range of roles in various processes in cells including gene expression, cell proliferation, signal transduction and apoptosis. In addition to these roles the thiol has the same roles as all other LMW thiols. It is suggested that the glutathionylation of proteins, a post-translational modification where glutathione binds to Cys residues in proteins, may play a crucial role in the control of such processes. The process also protects exposed Cys residues from oxidative stress and damage that may be irreversible [32, 33]. Many proteins including: GSH transferase, phosphorylase, creatine kinase and carbonic anhydrase were observed to undergo glutathionylation. For example, Cys modification regulates human immune deficiency virus (HIV) protease activity [27]. One way to achieve this is through the application of oral or intravenous Cys or Cys precursors to enhance the synthesis of GSH and prevent GSH deficiency in patients with pathological and nutritional conditions including those with HIV. GSH is also required for cytokine production as well as the activation of polymorphonuclear leukocytes and T-lymphocytes [22]. In certain bacteria, GSH is involved in the gentisate pathway as a cofactor to aid in the decomposition of aromatic compounds [3]. It has been speculated that the thiol predates the appearance of eukaryotes [1]. Eukaryotes are thought to have gained GSH metabolism during endosymbiotic events that led to the formation of chloroplasts and mitochondria due to the thiols metabolism being linked to aerobic respiration and oxygenic photosynthesis [34, 35].

1.2.3 Trypanothione

T(SH)₂ or N¹, N⁸-bis(glutathionyl)spermidine is a LMW thiol that is made up of two GSH molecules that are attached via a spermidine linker (Fig. 1). It is found in the kinetoplastida, a group of parasitic eukaryotes that inhabit animals and plants [6]. The family includes the trypanosoma and leishmania genera which are responsible for causing select tropical diseases such as African sleeping sickness and leishmaniasis [3]. It was identified after studies were conducted on *Trypanosoma brucei brucei*, an African trypanosome that was observed to have unusual GSH reductase activity [36, 37]. T(SH)₂ acts as an alternative to GSH within

these organisms to meet their redox requirements as well as its other functions depicted in Fig 2. As with GSH, $T(SH)_2$ is oxidised to produce its disulfide (TS_2) in order to maintain the intracellular reducing environment. The cell maintains this high intracellular redox ratio by utilising the NADPH-dependent flavoprotein $T(SH)_2$ reductase (TR) to reduce TS_2 back into $T(SH)_2$ [3, 6]. GSH forms an intermolecular disulfide whereas the dithiol state of $T(SH)_2$ is that of an intramolecular disulfide. Although GSH is present in organisms that produce $T(SH)_2$, GSSG is not recognised by TR and is therefore kept in its reduced state. This is achieved through thiol-disulfide exchange reactions amid GSSG and $T(SH)_2$ that are catalysed by thiol-S-transferases [38].

The redox potential is determined by the relationship between TS_2 and $T(SH)_2$ and is very similar to that of GSH and its disulfide, GSSG. Although, in thiol-disulfide exchange reactions under physiological conditions, GSH is less reactive than $T(SH)_2$ which means that there is significantly more $T(SH)_2$ present than GSH in their thiolate forms. This is due to the pK_a values of each of the thiol groups: $T(SH)_2$ has a lower pK_a than GSH, which allows for better conditions for thiol-disulfide exchange as well as increasing its reactivity towards electrophiles. Both $T(SH)_2$ and TS_2 have a net charge of +1 at physiological pH whereas GSH and GSSG have a net charge of -2 [36]. Due to its dithiol nature, $T(SH)_2$ can react with trivalent organic arsenicals to form stable complexes [39]. The reduction of intracellular disulfides is achieved through the mechanism in Fig 5. Organisms utilising GSH have a disulfide-reducing pathway utilising thioredoxin. This redox protein has not been found within organisms producing $T(SH)_2$ and therefore trypanothione (TxN) along with trypanothione peroxidase ($TxNPx$) were discovered within cells that reduce toxic peroxides as an alternative to thioredoxin and thioredoxin reductase [3]. $T(SH)_2$ has the ability to scavenge H_2O_2 , radiation induced radicals and peroxyntirite as well as provide reducing equivalents to oxidoreductases and ribonucleotide reductase [6, 40, 41]. Cytosolic redox homeostasis is maintained through this TR/ $T(SH)_2$ / TxN disulfide-exchange system which passes electrons to peroxidases through intermediate molecules. Concentrations of the thiol range between 0.2mM and 1.5mM intracellularly [6], and approximately 98% of this is present in its thiol form as opposed to its thiolate form [42]. The culmination of all these characteristics allow the organisms to flourish in harsh (oxidative) conditions during pathogenic interactions with the host [3].

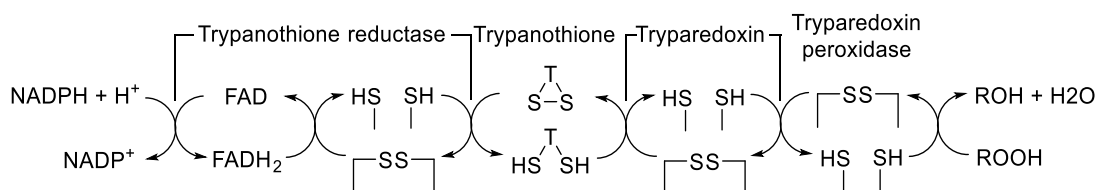


Figure 5. NADPH-dependent disulfide-reducing pathway: trypanothione reductase and trypanothione followed by trypanothione and trypanothione peroxidase [3, 36].

The biosynthetic pathway for the production of the thiol is an extension of the pathway that produces GSH (figure 6.). Four steps are required in total but after GSH is formed there are only two remaining. Spermidine in African trypanosomes is produced via the same pathway

within mammals: from Met and ornithine [36]. Ornithine decarboxylase [43], S-adenosylmethionine synthetase [44], S-adenosylmethionine decarboxylase [45], and spermidine synthase [46] are all enzymes required for the production of spermidine. The enzyme glutathionyl-spermidine synthetase is required for the attachment of spermidine to GSH resulting in the production of N₁-monoglutathionyl spermidine. T(SH)₂ is then formed from the reaction of N₁-monoglutathionyl spermidine and an additional GSH molecule in the presence of trypanothione synthetase. The similarities between the pathways for GSH and T(SH)₂ were determined after buthionine sulfoxide was introduced to organisms that produce the dithiol [36, 47]. The biosynthesis of GSH, and therefore of T(SH)₂, can be inhibited by this L-γ-glutamyl-L-cysteine synthetase inhibitor [48] because the inhibited enzyme is required for the first step of biosynthesis for both thiols. There are several ways the pathway can be disrupted to either reduce or halt the production of T(SH)₂. The pathway can be hindered using D,L-α-difluoromethylornithine, a drug synthesised to treat human African trypanosomiasis [49], to inhibit ornithine decarboxylase resulting in the loss of putrescine and therefore stopping the production of spermidine and T(SH)₂ [50].

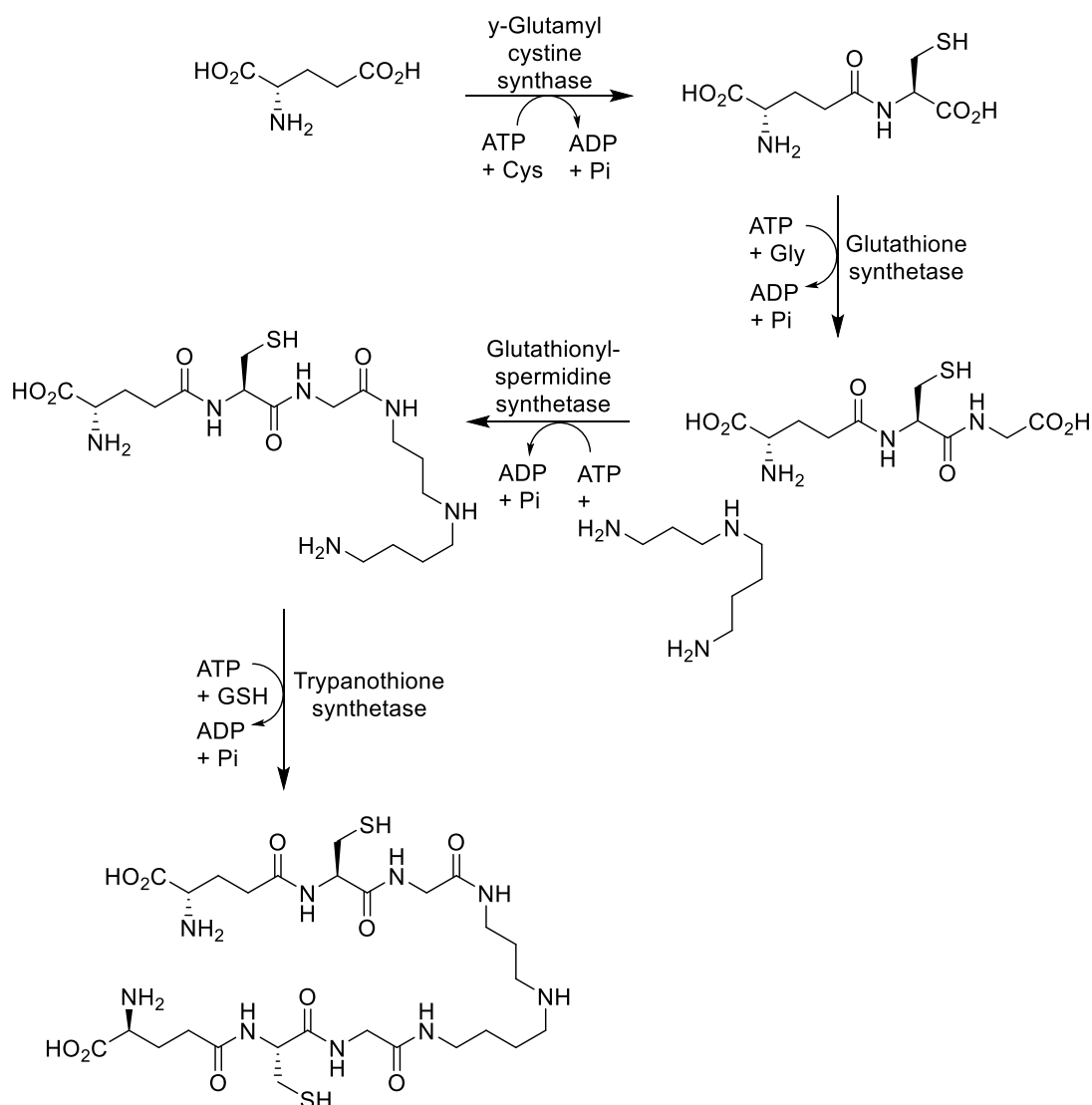


Figure 6. The biosynthetic pathway of T(SH)₂ following on from the biosynthesis of GSH.

1.2.4 Glutathione Amide

It is believed that GSH metabolism was present within an anaerobic ancestor of the purple bacteria as well as the cyanobacteria in whom it provided a different function [35]. When grown photoheterotrophically, the chromatium species of the purple sulfur bacteria (PSB) were discovered to utilise glutathione amide, otherwise known as γ -L-glutamyl-L-cysteinylglycine amide (GASH), as an alternative to GSH. An examination of its structure yielded the knowledge that while the α -carboxyl group of glutamate was present, the carboxyl group of glycine was absent and had been replaced by an amino group [51]. The thiol is thought to play a role in anaerobic sulfur metabolism as during photoautotrophic

growth on sulfide, GASH is mostly converted into its corresponding perthiol [51]. This particular species of bacteria store sulfur in globules intracellularly [52] which can account for a large portion of total cell mass when grown in sulfide [53]. When sulfur levels in the cell are low this accumulation of globules is mobilised for further oxidation [54]. GASH perthiol has been shown to form during growth on sulfide and it was concluded that this suggests it has a role in the transfer of elemental sulfur during sulfide metabolism [51, 55]. While many things have been speculated, the specific role of GASH has not yet been established [52, 54, 56] but it is likely that the thiol carries sulfur into the cytoplasm from the periplasm [57]. It is thought that GASH's ability to resist air oxidation, alongside GASH disulfide reductase activity, contributes to certain members of the *Chromatium* species maintaining the ability to survive in oxygenated environments [58] and potentially even undergo chemoautotrophic growth (either on sulfide or thiosulfate) under microaerophilic conditions [59, 60]. It is speculated that if GASH was present in the ancestors of purple bacteria and cyanobacteria, then findings would suggest an antioxidant-protective role which enabled the development of oxygenic photosynthesis and subsequently, aerobic respiration [51].

1.2.5 Mycothiol

MSH, or 1-D-*myo*-inosityl-2-(*N*-acetylcysteinyl)amino-2-deoxy- α -D-glucopyranoside, is the GSH equivalent LMW thiol found in the actinomycetes. The actinomycetes are a family of bacteria that include the mycobacteria (e.g. *Mycobacterium tuberculosis*), *Corynebacteria* (e.g. *Corynebacterium diphtheria*) and *Streptomyces* (e.g. *Streptomyces griseus*). Collectively, they are described as gram-positive bacteria that are recognised to be high G + C bacteria due to the high content of both guanine and cytosine in their DNA. The mycobacteria contain some of the highest levels of MSH with *M. tuberculosis* having one of the highest levels of the thiol [61]. This particular bacterium can defend itself against oxidative stress initiated by mammalian macrophages to kill unwanted organisms. It has been considered that MSH plays a role in both its survival and replication within the macrophage [1] and that further study may yield new targets for drugs to combat the bacterium [61, 62]. The biochemistry of MSH is important due to the fact that approximately half of the bacterial species found in soil belong to the *Actinomycetes* [1].

MSH bears the same functions as all other LMW thiols and is produced in millimolar concentrations in cells [6, 63]. Its metabolic functions are summarised in figure 7. In organisms that produce GSH, formaldehyde is removed by GSH-dependent formaldehyde dehydrogenase. However, in gram-positive bacteria, there is more than one type of formaldehyde dehydrogenase present, which lead to the conclusion that there is more than one LMW thiol produced by them, such as MSH and BSH [63]. NAD/MSH-dependent formaldehyde dehydrogenase was the first MSH-dependent enzyme to be identified [64, 65]. This dehydrogenase detoxifies formaldehyde via oxidation to produce formic acid (figure 7, reaction 1). During this reaction MSH is both consumed and regenerated [1]. MSH disulfide reductase, identical to GSH reductase, is the enzyme responsible for maintaining the thiol's reduced state. [63] MSH disulfide reductase (or mycothione reductase) utilises NADPH to facilitate the conversion of MSH disulfide back to MSH (figure 7, reaction 2) [1]. Although it is known that MSH exists both in its reduced state as well as in disulfide form, the thiol-redox potential has not yet been determined due to the limited availability of the thiol. At present, the only way to produce it is to isolate it from cell cultures as the chemical synthesis is a very long and elaborate process. [6] MSH, much the same as other LMW thiols, plays a role in the detoxification of electrophilic alkylating agents such as select antibiotics and their metabolites [66]. When an alkylating agent such as monobromobimane (mBBr) is reacted

with MSH, it is converted to its conjugate MSmB. This is then degraded to form GlcN-Ins and AcCySmB in which the latter is transferred from cells into the medium and the former is utilised in the resynthesis of MSH (figure 7, reaction 3) [1]. *Mycobacteria* can cope with a wider range of electrophiles due to their more general MSH-dependent detoxification system. The most important enzyme in the pathway is MSH S-conjugate amidase. MSH-dependent detoxification is suggested to aid in the bacteria's antibiotic resistance, as MSH S-conjugate amidase homologs are generally located in the same operons as those responsible for antibiotic production. [63]

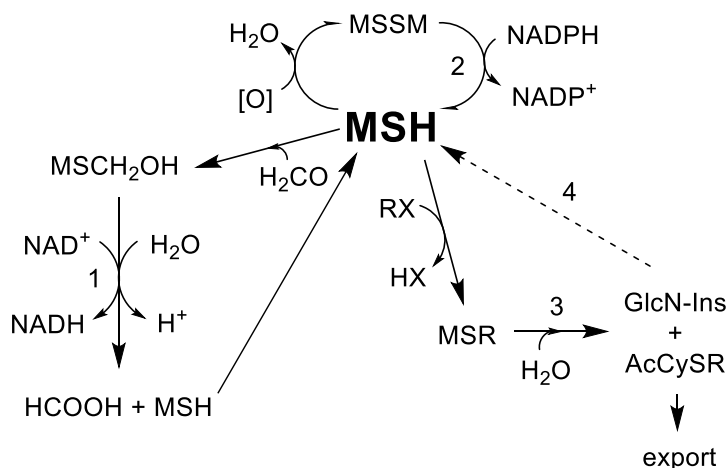


Figure 7. The metabolism of MSH: 1) NAD/MSH-dependent formaldehyde dehydrogenase, 2) MSH disulfide reductase (mycothione reductase), 3) MSH S-conjugate amidase, 4) MSH biosynthesis [1].

In figure 7, reaction 4 represents the biosynthesis of MSH and the full biosynthetic pathway is given in figure 8. The initial step in the biosynthetic pathway is catalysed by the UDP-GlcNAc-dependent retaining glycosyltransferase (MshA). This allows the formation of the glycosidic linkage between UDPGlcNAc and the acceptor substrate L-*myo*-inositol-1-phosphate. MshA2, a currently undefined phosphatase, removes the phosphate group from GlcNAc-Ins-1-P and a divalent metal-dependent N-acetyl hydrolase (MshB) catalyses the N-acetyl groups hydrolysis to form GlcN-Ins [67, 68]. MshC, or ATP-dependent cysteine ligase, catalyses the bonding of the Cys sidechain. The acetyl-CoA-dependent acetyltransferase (MshD) mediates the acetylation of the cysteinyl amine resulting in the formation of MSH [69, 70]. The crystal structures and the catalytic mechanisms of each of the catalysts (MshA-D) have been identified [71].

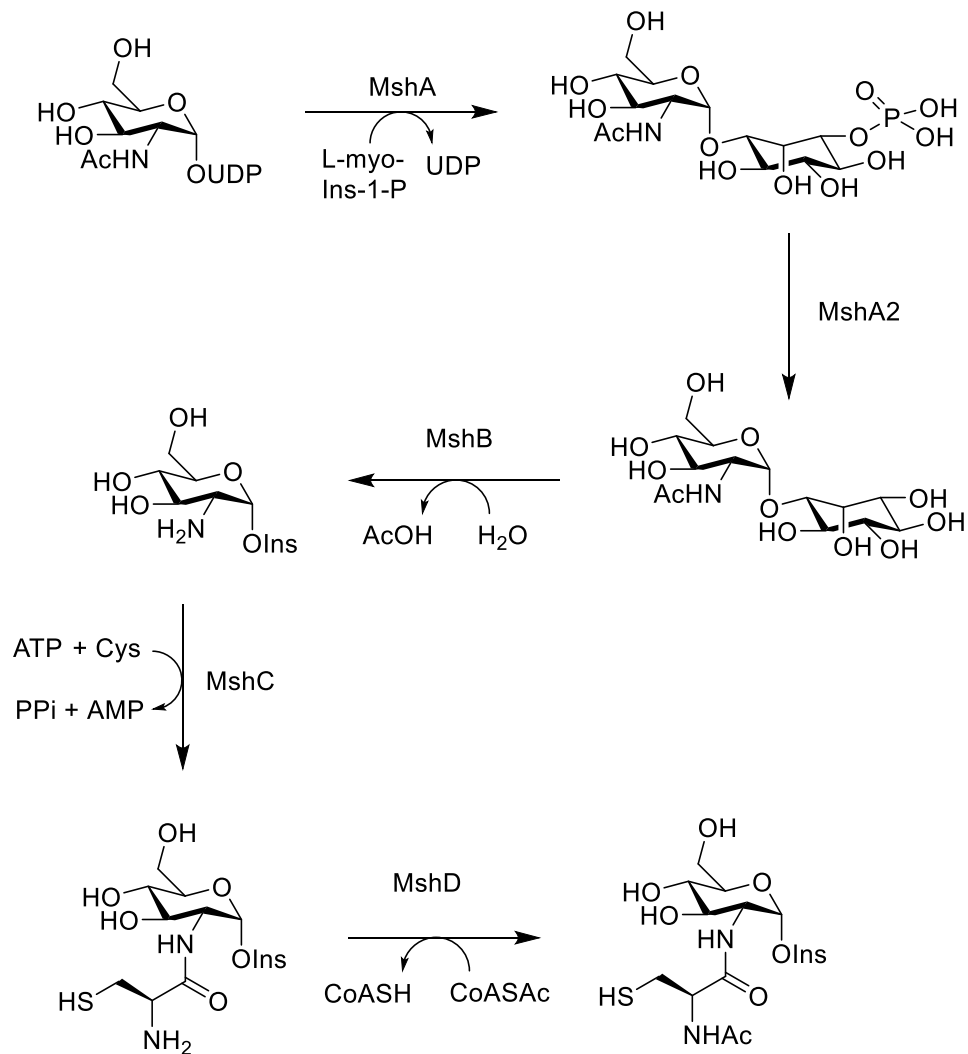


Figure 8. The biosynthesis of MSH [3].

1.2.6 Cysteine

Cys is one of the least abundant amino acids that can be found in all cells and many proteins that are important for various biological functions of the cell [72]. Its extensive functionality is due to the presence of its reactive thiol sidechain which when deprotonated to a thiolate anion enhances the nucleophilicity of the molecule [73]. It is one of only two amino acids that contain sulfur, the other being Met [7]. Its sulfhydryl group isolates it from other amino acids as its presence alters its chemical functionality [2] and increases its reactivity whereas the sulfur in Met is in thioether form which is less reactive. Therefore, the thiolate group can react with reactive species, either by alkylation (electrophiles) or oxidation (oxygen and nitrogen), resulting in modified forms of Cys that can perform different functions. Cys is also a key amino acid in proteins due to its ability to maintain a protein's folded state through the formation of covalent disulfide bonds [74]. It can be found at points that are structurally and functionally important. This means that the amino acid takes part in numerous cellular functions including: catalysis, structure stabilisation, signal transduction, metal binding,

protein splicing and post-translational modifications [6]. Cys residues, however, are known to cluster close to one another. This distribution pattern can be observed in organisms that thrive in difficult environments and are localised in areas of metal binding or redox sensitivity that can lead to the formation of disulfides. These residues are highly polarisable, which affects their reactivity and in turn, their state of protonation and accessibility [7].

During the biosynthesis of most thiols, Cys is used as a source of sulfur [1]. Due to its central role in the synthesis of LMW thiols, factors that affect Cys uptake in cells such as insulin and growth factors also affect the intracellular concentrations of each thiol [22]. These concentrations of the thiol are micromolar which are small when compared to other LMW thiols [6]. This is due to its toxicity to the cell and instead, is transported through the interorgan metabolism of GSH and reversed back to Cys when required (Fig.2.v) [22, 27]. Extracellularly, cystine is produced during the oxidation of Cys where a bond is formed between the two sulfur atoms. This keeps the concentration of Cys in the plasma quite low at 10-25 μ M. In contrast, this means that the levels of cystine are much higher at 50-150 μ M [22]. These levels are much higher than the levels of GSH and GSSG. The redox potentials of each of these pairings relate to their concentrations. Cys and cystine have a redox potential of -223mV and the GSH/GSSG pair have a redox potential of -240mV [75]. This measurement, also referred to as the reduction potential, relates to the susceptibility of a compound to the accepting of electrons, which reduces the compound. In humans that are affected by cardiovascular and age related diseases as well as infants that are new-born or premature, Cys is a vital amino acid as changes in the redox balance can have a negative effect on the body [6, 22].

Cys is very sensitive to autoxidation catalysed by heavy metals when concentrations of the thiol are too high intracellularly. Unbound cysteine is especially sensitive due to the presence of its free amino and carboxyl groups enhancing the thiolate residues ability to bind to metals [72]. The most effective catalysts of autoxidation are iron (Fe^{2+} and Fe^{3+}) and copper (Cu^+ and Cu^{2+}) [76]. Submicromolar concentrations of copper greatly increases the oxidation rate of Cys. For example: Half of the intracellular Cys concentration can be oxidised within thirty minutes by 0.2 μ M Cu^+ or Cu^{2+} [6]. Autoxidation utilising Cu^+ or Cu^{2+} as catalysts is faster than when using Fe^{2+} or Fe^{3+} . The autoxidation rates with Cu^+ and Cu^{2+} bear no difference whereas Fe^{3+} is a slower oxidant than Fe^{2+} at concentrations above 10 μ M [76]. The products of such reactions are toxic reactive oxygen species which include hydrogen peroxide and superoxide (chapter 4.1, figure 24.). Due to this, even the smallest occurrence of autoxidation is undesirable. The concentrations of Cys are kept low in the cell in order to minimize its oxidation and a supply of the thiol is maintained in a form that is more resistant to autoxidation such as GSH. Another way to minimize this reaction is to control the availability of transition metals. Iron is found in iron-sulfur proteins in both aerobic and anaerobic bacteria [77]. Copper is found in the cyanobacteria, within its electron transfer agent plastocyanin [78].

1.3 The biological activity of Bacillithiol in *Bacillus subtilis*

1.3.1 Identification

BSH was first discovered in 2009 and found to be present in many firmicutes or low-G + C gram positive bacteria. These include many Bacilli and some Staphylococci and Streptococci such as *Bacillus anthracis*, *Bacillus cereus*, *Staphylococcus aureus* and *Streptococcus agalactiae*. These bacteria do not produce either GSH or MSH but are known to produce BSH in a similar biosynthetic pathway utilised in the production of MSH. The structure of BSH is also similar to that of MSH, bearing the same GlcN-Cys group but differing in its addition of L-malate and loss of the N-acetylation of the Cys side chain (figure 1.) [6]. Other thiols can be found in the bacteria however, suggesting that each one has a specific role. Intracellularly, the majority of BSH is found in its reduced state with ratios of BSH and BSH disulfide (BSSB) varying from 400:1 in *B. subtilis* [79] and 40:1 in *B. anthracis* [80]. The major LMW thiol in *B. subtilis* was originally thought to be Cys until BSH was identified [79]. Apart from forming disulfides with a copy of itself, BSH can create mixed disulfides that contain proteins in a process called bacillithiolation. The process is reversible, however, when interacting with bacilliredoxins. BSH levels in *Firmicutes* (up to 400 μ M) are more similar to the levels of Cys than that of GSH in gram-negative bacteria (up to 5mM) [6]. Under physiological conditions, approximately 22% of BSH is present in its thiolate form which is more than the 14.5% for the Cys thiolate. The redox potential of BSH and BSSB is -221 mV compared to the GSH value of -240 mV and that of Cys at -223 mV [75].

1.3.2 Biosynthesis

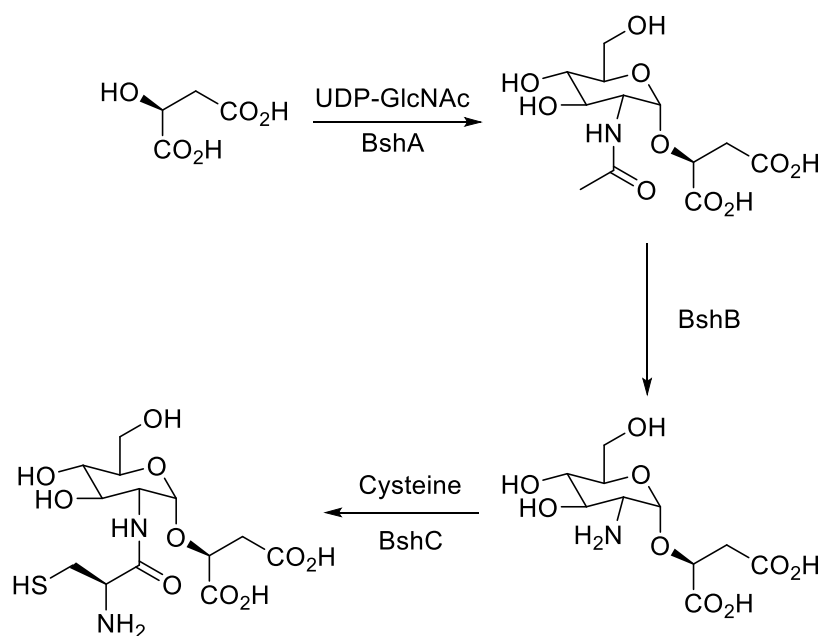


Figure 9. The Biosynthesis of BSH.

The biosynthetic pathway for the formation of BSH consists of three steps. L-malate reacts with uridine diphosphate n-acetylglucosamine (UDP-Glc-NAc), a glucosamine donor substrate, to form N-acetylglucosaminyl-malate (Glc-NAc-Mal). BshA (encoded by gene CT0548), a retaining GT4 class glycosyl transferase enzyme [81], catalyses the reaction. BshB (encoded by gene CT1419), a metal-dependent deacetylase, hydrolyses the acetyl group in Glc-NAc-Mal to produce glucosaminyl-malate (Glc-N-Mal). Glc-N-Mal then reacts with Cys which is catalysed by BshC (encoded by gene CT1558), the BSH synthase enzyme, to produce BSH (figure 9.) [8].

BshA, isolated from *B. anthracis*, has been crystallised and when the gene that encodes for it is removed from the genome no BSH is produced [81, 82]. BshA and its orthologs are present in all BSH synthesising species and are part of a distinctive group of glycosyltransferases. BshB1 is located directly upstream of BshA and was knocked out to form a mutant that produced 2-fold less BSH than the wild type. This led to the conclusion that BshB1 was not vital for BSH synthesis and that there was another deacetylase with the same function, BshB2. BshB2 is a paralog of BshB1, and when knocked out on its own produced the same levels of BSH as the wild type [8]. When both BshB1 and BshB2 were removed together, however, no BSH was detected in the mutant. It was deduced that both can operate separately as there is enough deacetylase activity for BSH synthesis but BshB1 is the most effective of the two. A BshC lacking mutant was also created and was discovered to halt the production of BSH as well as producing a large pool of Glc-N-Mal, indicating its essential role in BSH biosynthesis.

There are four more proteins that relate to BSH biosynthetic functions that are thought to be thiol-disulfide oxidoreductases: YpdA, YqiW, YphP and YtxJ. They are connected to genes that are present in species thought to produce BSH and are predicted to affect the concentration of disulfides inter- and intracellularly. Three operons contain members of the BSH biosynthetic genes. Downstream of one of these operons, an operon containing three genes encoding for the enzymes found in pantothenate biosynthesis suggesting a relation to CoA [8]. During times of disulfide stress, genes in *B. subtilis* are up-regulated by Spx transcription factor. In addition to this, reactive oxidants and electrophiles can trigger the up-regulation of genes required for BSH synthesis and detoxification [75].

1.3.3 Cellular Functionality

Like all other LMW thiols, BSH shares the same functions including detoxification of chemical stressors and redox regulation. It also has similar metabolic functions to GSH [83]. The thiolate anion can be utilised in detoxification pathways as a nucleophile. In organisms that produce BSH, these processes are mediated by BSH-S-transferases of which the most notable one is FosB [75]. Fosfomycin, a broad-spectrum antibiotic, acts as a covalent inhibitor of the first enzyme involved in peptidoglycan biosynthesis. Resistance to fosfomycin in *B. subtilis* is dependent on FosB, an S-transferase that is thiol-dependent and for which BSH acts as a cosubstrate (figure 10.). Mutants that don't produce BSH showed a large increase in sensitivity to fosfomycin and a small resistance to penicillin G and rifampin [75]. The mutant lacking FosB was found to be just as sensitive to fosfomycin as one that lacks BSH. One with both BshA and FosB knocked out, had the same sensitivity as the mutants with only one of each removed. This led to the conclusion that FosB is a BSH S-transferase. [8] BSH also plays a major role in the detoxification of methylglyoxal, a derivative of reduced pyruvic acid due to the location of the methylglyoxal synthase gene which is in the same operon as BshA and

BshB1. BSH is not required for the cell to function normally but its presence has a positive effect on the stress conditions of organisms [75].

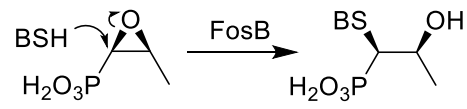


Figure 10. The inactivation of fosfomycin catalysed by FosB, a BSH-S-transferase [3].

1.4 Green Sulfur Bacteria and its novel low molecular weight thiol

1.4.1 Green Sulfur Bacteria

Since prokaryotes have evolved throughout time to produce such versatile natures, they can be found in more and more volatile environments on the planet and still thrive. Where aerobic bacteria have adapted to their need for oxygen and learnt to combat thiol autoxidation, anaerobic bacteria do not need to do the same and could potentially retain characteristics, specifically thiol biochemistry, from earlier forms of life [1]. Phototrophic sulfur bacteria are anaerobic bacteria that are distinguished by their ability to utilise reduced sulfur compounds as electron donors during photosynthesis. Each of these bacteria belong to either the PSB or green sulfur bacteria (GSB). The PSB and GSB have very similar ecology and sulfur metabolism but differ in their phylogeny. GSB, or the chlorobiaceae, are a family of anaerobic bacteria comprised of organisms that utilise electron donors that have a standard potential lower than that of water [84]. Examples of these include *Cba. tepidum* and *Cba. thiosulfatophilum*. These electrons are found in sulfur compounds and are inserted into the electron transport chain in order to reduce ferredoxin and therefore partake in reducing NAD(P)^+ , as well as carbon dioxide (CO_2) and nitrogen (N_2) fixation. [85] Various forms of these compounds can be utilised including: sulfide, thiosulfate and elemental sulfur. Hydrogen and ferrous iron are also used as electron donors as oxygen is not produced during anoxygenic photosynthesis [86]. Most GSB are non-motile and due to their restricted physiological attributes can only be located in environments that are sulfide-rich, typically in water where light touches anoxic water or littoral sediments [84, 86]. The bacteria are important to these areas due to their role in the transformations of sulfur and carbon compounds. The family have a particular cytological feature that distinguishes them from other bacteria. They contain chlorosomes, light-harvesting complexes that shelter carotenoids and bacteriochlorophylls [86]. Carotenoids can capture light very efficiently which allows them to adapt and thrive in ecosystems that are of very low light intensity [84, 86].

1.4.2 The Role of Sulfur

Sulfur can be found in the environment in its elemental form (S_8) and is present in all organisms mostly as organosulfur compounds. It can be utilised in a variety of ways: in fertilisers and pesticides, as a preservative of foods, in cement and in natural gas supplies to detect leaks. Some forms of sulfur such as sulfide and sulfate are not harmful but hydrogen sulfide, carbon disulfide and sulfur dioxide are examples of sulfur containing compounds that are toxic which can have dire consequences for living organisms. Plants and algae absorb sulfate from soil or water and humans consume some through proteins in their diet. It is an essential part of the makeup of two amino acids, Cys and Met, that are required for protein synthesis. Thiamine and biotin are vitamins that are classed as organosulfur compounds and are present in organisms. Cofactors containing sulfur vary from organism to organism depending on the requirements of the cells although none require sulfur more than the bacteria that require the element to photosynthesise.

It has been suggested that the thiols specific to the chlorobi are involved in the movement of sulfur between the periplasm and the cytoplasm in order to insert sulfide into the biosynthetic pathways in the bacteria [85]. Sulfur is obtained from outside the cell and once inside, sulfide:quinone oxidoreductases (SOX) oxidise sulfide and thiosulfates in the

periplasm are oxidised by the sulfur oxidation enzyme system (figure 11). Sulfide is oxidised in preference over thiosulfate but when most of it has been oxidised, thiosulfate and elemental sulfur is oxidised to sulfate. A putative oligosulfide pool is produced from both of these oxidation processes. The pool is thought to be equilibrium with a pool of elemental sulfur or S^0 (figure 11). The oligosulfide pool is oxidised by the dissimilatory sulphite reductase enzyme (DSR) system which contains at least 15 subunits. Intracellular sulphite is formed by the DSR system that is then oxidised by the presence of Sat, Apr and Qmo proteins that are part of a different enzyme system [87]. Menaquinone and cytochrome C, two electron acceptors, are then oxidised by the photosynthetic reaction centre [88].

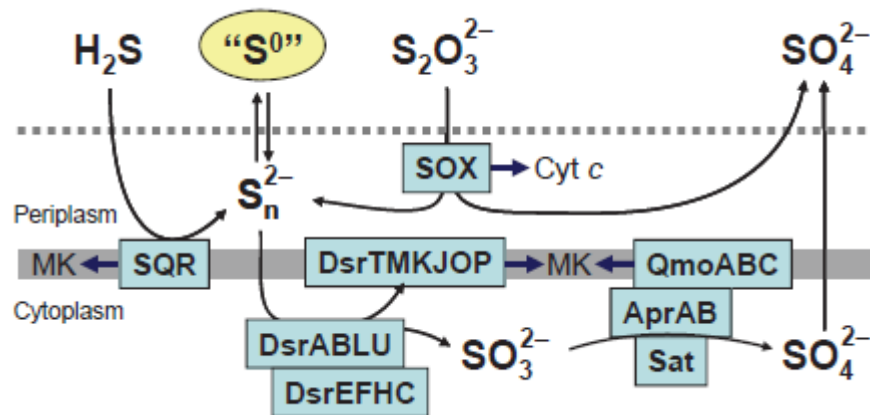


Figure 11. An overview of the sulfur metabolism pathways in *Cba. tepidum* [88].

1.4.3 The Discovery of N-Methyl-Bacillithiol

Of the many GSB, *Cba. tepidum* is commonly used as a model system for the family of bacteria due to its rapid growth rate, genetic system and complete genome sequence. In order to identify the LMW thiols native to this particular bacterium, thiol extraction and derivitisation with mBBr were performed. The bacteria were grown with additional sulfide and thiosulfate present to utilise as electron donors. The result of this produced a peak that corresponded to a unique biman derivative. When compared to known LMW thiols, this derivative possessed a different retention time and could not be found when exposed to N-ethylmaleimide, a compound that blocks the sulfhydryl group of the thiol, before derivitisation. This method was used to confirm that the *Cba. tepidum* genome does not encode a biosynthetic pathway for the production of GSH and that other GSB also do not produce GSH as no peak was present at the correct retention time for the thiol. To determine the structure, a sample of it was observed using Fourier transform ion cyclotron resonance mass spectrometry. The resulting mass suggested that it differed from BSH merely by the addition of a methyl group. Two possible structures were derived from this information, a thiol that replaces the cysteine sidechain with either HCys ((figure 12.a) hCys-BSmB) or N-methyl-cysteine (N-Me-Cys) ((figure 12.b) N-MeBSmB). In order to decipher the true sidechain, both possibilities were synthesised and derivatised to observe the peaks via HPLC (figure 12.). Each sample was added to a sample of the original thiol ((figure 12.c) U7mB) to

determine which structure matched. N-Me-Cys co-migrated with the sample containing the N-Me-Cys sidechain and when mixed together gave a single peak confirming the structure [85].

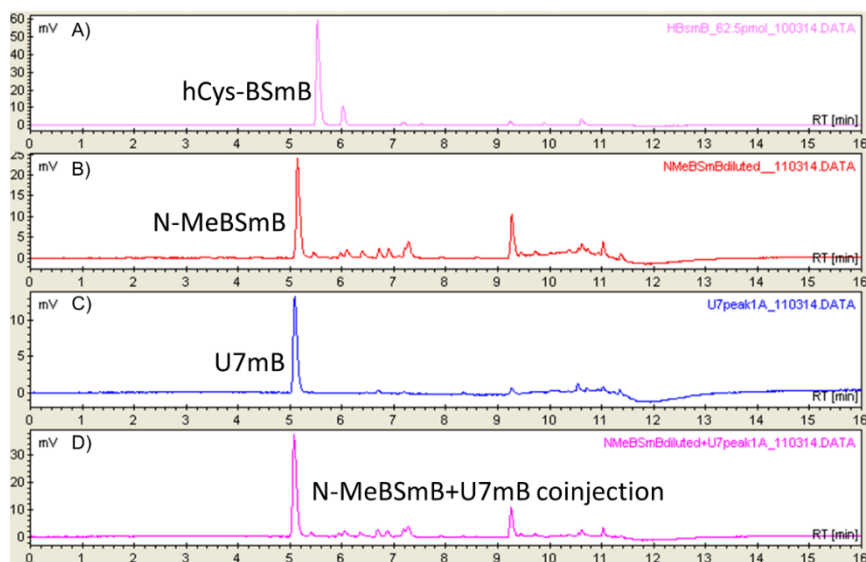


Figure 12. HPLC traces of the bimane labelled novel LMW thiol in *Cba. tepidum*, A) the thiol with a homocysteine sidechain, B) the thiol with an n-methylated cysteine sidechain, C) original sample isolated from *Cba. Tepidum*, D) the combination of B) and C) [85].

The first paper on N-Me-BSH is as yet unpublished (in review) as the thiol has only recently been characterised [85, 89]. The N-methylation of metabolites is rarely seen in biology and the significance of the production of N-Me-BSH as opposed to BSH is as yet unknown. Of all the bacteria that have been analysed for N-Me-BSH production, the volume of the thiol produced is greater than that of BSH. Even though environmental conditions effect the growth rate and production of N-Me-BSH, the bacteria produce the thiol regardless of growth phase. While the N-Me-BSH seems to be the thiol that is suggested to play a role in the movement of sulfur between the periplasm and the cytoplasm in the GSB, it has been concluded that the thiol must play another role due to its production in other non-sulfur bacteria such as *Polaribacter* sp. MED152, as well as certain members of the bacteroidetes, acidobacteria, and firmicutes [85].

1.4.4 N-Methyl-Bacillithiol Biosynthesis

It was originally proposed that N-Me-BSH could be synthesised in one of two ways: by the fusion of N-Me-Cys or alternatively by the methylation of BSH. The latter synthesis was concluded due to the fact that N-Me-BSH has never been detected in *Cba. tepidum* alongside N-Me-Cys but has been observed alongside BSH. The N-Me-BSH biosynthetic pathway in *Cba. tepidum* is very similar to that of BSH due to the presence of orthologs of genes that encode

three critical proteins found in the BSH biosynthetic pathway in *B. subtilis*; BshA, BshB and BshC (figures 9. and 13.). Therefore, it was deduced that the biosynthesis of N-Me-BSH incorporated the BSH biosynthetic pathway into its own with the addition of a step following the synthesis of BSH. NmbA or N-Me-BSH synthase A (encoded by gene CT1040), an S-adenosyl-methionine (SAM)-dependent methyltransferase enzyme, catalyses the reaction between BSH and SAM to form N-Me-BSH (figure 13.).

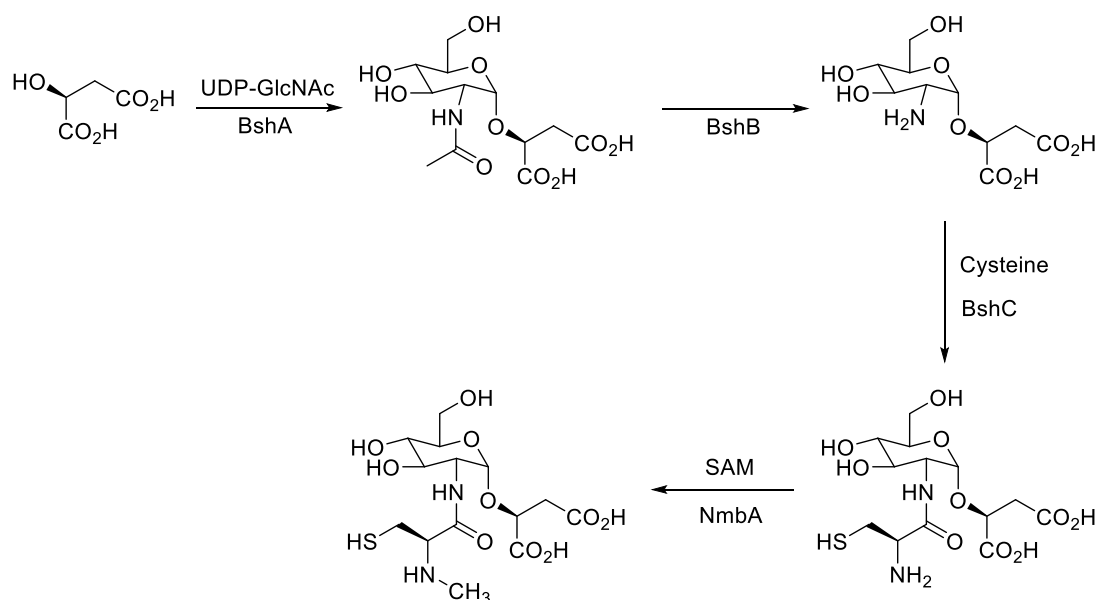


Figure 13. The Biosynthetic Pathway of N-Me-BSH.

CT1040 is not the only gene found in the *Cba. tepidum* genome that encodes for SAM-dependent methyltransferase as CT1213 also encodes the enzyme. Both of these genes can be found in every bacterium in the *Chlorobi* family. Knockout mutants of CT1040 and CT1213 were created in *Cba. tepidum* to determine which of them is part of the N-Me-BSH biosynthetic pathway. Of the two mutant strains that were created, the one that did not contain CT1040 had no N-Me-BSH present whereas the strain without CT1213 contained the same volume of the thiol that the wild type contained. The strain lacking CT1040 had volumes of BSH present similar to that of the volumes of N-Me-BSH found in the wild type suggesting that the presence of SAM-dependent methyltransferase is pivotal to the production of the thiol in all GSB. To prove that the proposed pathway for N-Me-BSH is almost identical to that of BSH, BshB or CT1419 was removed from the *Cba. tepidum* genome which developed a strain of the bacteria that no longer produced N-Me-BSH or BSH. The chlorobi are not the only bacteria to contain the biosynthetic pathway for N-Me-BSH. The ignavibacteriae as well as certain bacteroidetes, acidobacteria, and firmicutes also contain the pathway. A percentage of each of these bacteria that contain the BSH biosynthetic pathway also possess an ortholog of NmbA; 33% of *Bacteroidetes*, 31% of *Acidobacteria* and 7% of *Firmicutes*. However, there is one member of the *Chlorobi* that possesses BshA-C but not NmbA, NICIL-2, which is presumed to be the most basal of the family. Orthologs of genes

found in BSH can also be found in many other types of bacteria and the dispersal of these genes indicates that both N-Me-BSH and BSH could be two of the most predominant LMW thiols [85, 89].

1.4.5 N-Methyl-Cysteine and Homocysteiny-Bacillithiol

N-methylation is a common post-translational modification [74]. Amino acids that are methylated on the amide nitrogen have become popular due to their presence in a multitude of natural bioactive molecules as well as due to their versatile physical and chemical properties [90]. Peptides containing these compounds have better metabolic stability, higher hydrophobicity and a more stable conformational structure [74].

N-Me-Cys can be found in thiocoraline peptides which contain six residues that are Cys derivatives, two of them being N-Me-Cys (figure 13, Blue) [74]. Thiocoraline is a thiodepsipeptide, a natural marine compound derived from *Micromonospora marina* [91], an actinomycete, that has been observed to have anticancer activity [92]. There is no evidence of N-Me-Cys being isolated from the source and due to it not being available commercially, a method has been produced for synthetic production [74]. The thiol has not been identified as a cofactor in any organism and therefore may play a much smaller role in biology than other LMW thiols. For the purpose of this study it was used alongside Cys to compare and contrast against BSH and its methylated version to determine the significance of the extra methyl group.

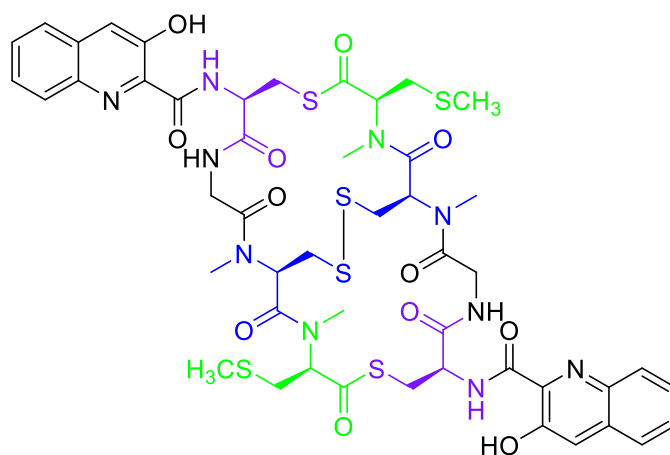


Figure 14. Structure of Thiocoraline and its Cys residues (colour) [91].

Homocysteiny-bacillithiol (HCys-BSH) was created in a laboratory for the sole purpose of identifying the structure of N-methylated BSH as it maintains the same molecular weight. It consists of a HCys sidechain as opposed to a Cys sidechain (Fig. 1) [85]. It has not been identified in any organism and thus far, has had no published research conducted on it. It remains a mystery as to whether it is produced biologically by an organism, and whether it bears any significance among its counterparts. For this study, it was used because its structure so closely resembles that of BSH and N-Me-BSH.

1.5 LMW Thiol Data Comparison

Due to the numerous functions and properties of LMW thiols, isolating their individual properties is becoming more critical for them to be better understood. Unfortunately gathering data can be quite tricky due to their instability in solution as well as the ease at which they can be oxidised to disulfides. Each experiment in this study was designed to be quick and efficient but still be specific enough to allow for accurate measurements. Table 1. outlines some of the properties of LMW thiols found in the literature. The intracellular concentrations vary between organisms containing different thiols as well as organisms containing the same thiols hence why there is not one singular concentration for each thiol. Since there are such a vast number of organisms in existence it is impossible to predict that all cellular concentrations lie within the boundaries given in the table. At present, GSH has been noted to have concentrations of up to 10mM intracellularly, far more than any other thiol. The levels of MSH within cells have also been noted to be more considerable than the others in certain organisms with concentrations of up to 6mM. T(SH)₂ has up to 1.5mM but the remainder have concentrations far smaller than 1mM, which is quite a difference compared to the high levels of GSH. Quantities of N-Me-BSH have been isolated but not in mM concentrations. The chlorobi were found to contain 65-700 pmol thiol per mg of dry weight (dw⁻¹) [85]. When this was compared to BSH (200-2600 pmol thiol per mg dw⁻¹), it was found to be a much smaller quantity [79].

Table 1. The known properties of select LMW thiols.

Thiol	Intracellular Concentration (mM)	Extracellular Concentration (μM)	Thiol-Disulfide Ratio (under physiological conditions)	Redox Potential (mV)
GSH	0.5 - 10 [22]	2-20 [22]	100:1 [9]	-240 [93]
T(SH) ₂	0.2 - 1.5 [6]	-	-	-252 [36]
GASH	0.033 - 0.165 [51, 55]	-	-	-
MSH	0.1 - 6.27 [94]	-	-	-
Cys	0.1 - 0.2 [95]	10-25 [22]	-	-223 [96]
BSH	0.04 [6]	-	400:1 [79] 40:1 [80]	- 221 [75]
N-Me-BSH	-	-	-	-

The extracellular concentrations have only been recorded for GSH and Cys. Both thiols concentrations are much lower extracellularly (in μM not mM) than when compared to their intracellular concentrations. The external thiols react to form disulfides and therefore the levels of each of their corresponding disulfides is much higher. Under physiological conditions the levels of GSH and GSSG are around 100:1. The thiol is always present in much larger quantities than its disulfide except during times of oxidative stress, under certain pathological conditions, or during protein malnutrition [22]. The variances between

organisms is evident when observing the differences between the ratios of thiol-disulfide within *B. subtilis* and *B. anthracis*. *B. subtilis* has a ratio of 400:1 whereas the in *B. anthracis* the difference is not so drastic with a ratio of 40:1. When comparing the values for redox potential (E^0) T(SH)₂ is more electronegative than GSH, Cys and BSH. It relates to the susceptibility of a compound to the accepting of electrons, which reduces the compound. In other words, the more positive the value the more readily the thiol is reduced.

1.6 Aims of the project

The overall aim of this project was to build upon the little knowledge of N-Me-BSH [85], and to determine the significance of its N-methylated sidechain. To date, only two N-methylated LMW thiols have been observed and produced in a laboratory. By combining the current knowledge of LMW thiols and the results in this study, it was estimated that accurate predictions of the biophysical properties of N-Me-BSH were obtainable by observing the changes to their biophysical properties and comparing them. The specific goals of this project were as follows:

1.6.1 Determining the Macroscopic and Microscopic pK_a 's of LMW thiols

The intracellular ratio of thiols and their reduced forms vary between organisms. The macroscopic and microscopic pK_a 's provide insight into the protonation states of each thiol at certain pH's. Chapter 2 reports the pK_a values for six LMW thiols and discusses the impact of structure on the differences between them. The conclusions made from these results allowed predictions to be made for N-Me-BSH which could give insight into the significance of its structure.

1.6.2 Determining the pH Independent Thiol-Disulfide Exchange Rate Constants of LMW thiols

Thiol-disulfide reactions are a common occurrence in cells and are responsible for redox regulation. As redox buffers, their role in combatting reactive species is crucial to the normal functionality of the cell. Chapter 3 reports on the thiol-disulfide exchange rates for six LMW thiols and discusses the potential reasons for the differences between each of them. The conclusions made from these results allowed predictions to be made for N-Me-BSH which could give insight into the significance of its structure.

1.6.3 Determining the Copper Catalysed Autoxidation Rates of LMW thiols

Autoxidation occurs during oxidative stress and can very quickly consume certain thiols when in the presence of copper. Copper acts as a catalyst, increasing the speed of the reaction and the rate at which the thiol is consumed. Due to certain thiols only being available in specific organisms, the rate at which autoxidation occurs could depend on whether they are found in aerobic or anaerobic organisms. Chapter 4 reports on the rates of the six LMW thiols and the potential reasons for the differences between each of them. The conclusions made from these results allowed predictions to be made for N-Me-BSH which could give insight into the significance of its structure.

Chapter 2: Determining the Macroscopic and Microscopic pK_a 's of LMW thiols

2.1 Introduction

Compounds containing both a sulfhydryl and ammonium group have long been a subject of great interest due to the ionic equilibrium that occurs when they are deprotonated. The former are the most chemically active group within cells and can react with many different thiophilic reagents (such as metal ions to form stable complexes) [97]. All LMW thiols are classed as weak acids due to the presence of the sulfhydryl group and are far more likely to donate their proton than act as a proton acceptor (although they can act as both [98]) [99]. The nonpolar covalent bond binding the sulfur and hydrogen atoms is relatively easy to break due to the similar electronegativities of the two atoms. This results in a thiolate ion with a negative charge. This in turn greatly increases the nucleophilicity of the thiol as when it deprotonates it becomes far more reactive towards electrophiles:



Thiolate anions are generally more stable than their oxygen anion equivalents due to the sulfur atoms larger electron cloud with a smaller electron density compared to oxygens smaller cloud with a higher electron density. In terms of acidity, thiols are most commonly compared to alcohols due to the presence of O^- atoms which are in the same group in the periodic table as S^- atoms. The reactivity of a sulfhydryl containing compound is more than five hundred times more nucleophilic than that of an alcohol [100]. O^- is more electronegative than S^- and will less readily donate an electron pair to an electrophile. However, it is less nucleophilic than S^- because of its smaller size. Therefore, the greater the spread of the negative charge the greater the stability. These factors make thiols stronger acids and better nucleophiles than alcohols. It also allows them to be fully reacted to form their conjugate-base anion when reacted with one equivalent of alkoxide or hydroxide.

The sulfhydryl group is not the only functional group within LMW thiols that can be deprotonated. The carboxylic groups can also lose a proton but at the same time the amino group can be protonated to give NH_3^+ . These occur, however, at different pH's depending on different factors including: molecular structure, bonding, inductive effects, resonance, and temperature. The pK_a of a molecule is determined from the pH of the solution. pH is used to identify acidity or basicity depending on the molar concentration of hydrogen ions (H^+) in solution. It is defined as:

$$\text{pH} = -\log_{10}(\text{H}^+) \quad (2)$$

To determine the strength of an acid, the acid dissociation constant (K_a), can be measured based on equation (1):

$$K_a = \frac{[\text{RS}^-][\text{H}^+]}{[\text{RSH}]} \quad (3)$$

Where RS^- represents the thiolate concentration, H^+ the hydrogen ion concentration and RSH the thiol concentration. When the concentrations of each of them do not change over time they are said to be in equilibrium. The value of K_a is increased by producing a more stable

product from the acid-base reaction. The pK_a is therefore defined as the logarithmic constant of K_a :

$$pK_a = -\log_{10}(K_a) \quad (4)$$

The pK_a values dictate which side the equilibrium is shifted in equation (1) and can be calculated using the Henderson-Hasselbalch equation:

$$pH = pK_a + \log_{10} \frac{[RS^-]}{[RSH]} \quad (5)$$

Since pK_a is affected by change in temperature, thermodynamics play a role in each reaction and therefore each value is directly proportional to Gibbs free energy change. This is defined as the largest quantity of reversible work possible within a thermodynamic system when temperature and pressure are kept constant. In an endothermic reaction when temperature is increased, K_a values increase and pK_a decreases. The exact opposite occurs within exothermic reactions.

pK_a values can distinguish strong acids from weak acids. For monoprotic acids in water, values below -2 are very strong acids that cannot be accurately measured due to the almost complete dissociation of the acid. The opposite can be said for weak acids above a pK_a of 12 as the acids are almost completely protonated. Therefore, the measurable area lies between pK_a -2 and pK_a 12. Amino thiols are referred to as polyprotic acids because they can lose more than one proton at a time. Previous data has demonstrated that when two thirds of the sulfhydryl group have ionised in Cys, one third of the ammonium group has also ionised making the acid strength of the sulfhydryl group twice that of the ammonium group [101]. This means that when the amine is fully protonated it has a different effect on the rest of the molecule as it does when its only just started to deprotonate. Its positive charge increases the likelihood of the deprotonation of the thiol group. Therefore, each thiol can have multiple pK_a values due to the different functional groups that can be deprotonated as well as having pK_a values when more than one functional group is deprotonated at the same time. These are described as macroscopic and microscopic acid dissociation constants.

The number of macroscopic pK_a 's can vary depending on the number of functional groups that can lose a proton. When the macroscopic dissociation constants are set apart by approximately four pK_a units, each deprotonated state could be regarded as a different acid. If this is not seen, then when in equilibrium there is an overlap of species present at the stated pH. In this study each thiol had three or four macroscopic values due to the presence of some of the following functional groups: CO_2H , SH, NH_2 , and $NHCH_3$. The microscopic values were then calculated to give the four individual pK_a values of the thiol and amino groups. These four exist due to the sequential deprotonation of both groups occurring in two possible ways as depicted in figure 15. The pK_s and pK_{ns} values represent the thiol groups acidity and the pK_n and pK_{sn} values represent the amino groups acidity. This dissociation interrelationship is the same within all compounds where the acidic strengths of the two functional groups are of similar extent [101]. The pK_a of the thiol differs depending on whether the neighbouring amino group itself is either protonated or deprotonated. When the amine is protonated, its positive charge helps stabilise the negatively charged thiolate anion explaining why the thiol is more acidic when the amine is protonated.

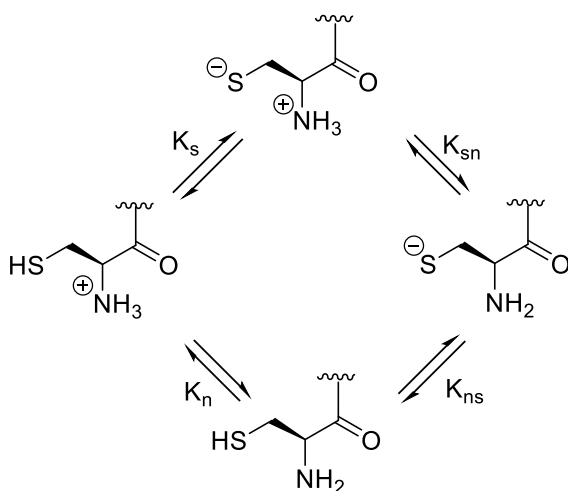


Figure 15. The four deprotonation pathways of a cysteinyl thiol that dictate the four microscopic dissociation constant values [83].

The macroscopic and microscopic pK_a values for each thiol were determined using the equations above. Following on from this, the data was analysed and compared to known literature as well as to each other in order to identify the causes behind the different pK_a 's that were calculated for each thiol. Methods in this chapter were adapted from those reported previously [83].

2.2 Materials and Methods

2.2.1 Materials and Instruments

All chemical reagents were obtained from appropriate suppliers including Sigma-Aldrich and Fisher Scientific. Thiols were obtained from Sigma-Aldrich and lab stocks. Levels of pH were measured on a Hanna HI-2002 Edge pH Meter. Absorbance was measured on a Perkin Elmer Lambda 25 UV/VIS spectrometer using either 1ml disposable plastic cuvettes or quartz cuvettes. Cuvettes were obtained from Star Labs. The data was plotted and analysed using Grafit and Excel software programmes.

2.2.2 Thiol Quantification

For accuracy, each thiol was quantified using a buffer solution containing 5,5'-dithio-bis-[2-nitrobenzoic acid] (DTNB or otherwise known as Ellman's reagent). A disposable cuvette (1ml) containing 2mM DTNB dissolved in 50mM HEPES buffer, at pH 7.4, was blanked at 412nm. 0.05mM of thiol was added and the absorbance measured. The Beer-Lambert Law was used to determine the true concentration of the thiol in solution:

$$A = \epsilon lc \quad (6)$$

Where A is measured absorbance, ϵ is the extinction coefficient ($\epsilon = 14150 \text{ M}^{-1}\text{cm}^{-1}$), l the path length, and c the concentration of the substance being analysed [102].

2.2.3 Thiol and Amine Macroscopic pK_a Determination

A range of sodium phosphate buffers were prepared at approximate intervals of 0.25 between pH 4.8 and pH 12.8 at a concentration of 100mM by combining sodium phosphate dibasic (Na_2HPO_4) and sodium phosphate monobasic (NaH_2PO_4). Each buffer was blanked in a quartz cuvette before adding thiol (dissolved in Milli-Q water) to a final concentration of 40 μM [101, 103, 104]. Absorbance of the thiolate anion was immediately measured at 232nm using a UV/VIS spectrometer [101]. pK_a was determined after plotting absorbance against pH in Grafit.

To determine the macroscopic acid dissociation constants a graph containing the non-linear regression plot of fractions of thiol in its thiolate form (α_s as calculated from equation (7)) versus pH was produced (see figure 17.):

$$\alpha_s = \frac{\text{lim} \times 10^{(\text{pH} - pK_a)}}{10^{(\text{pH} - pK_a)} + 1} - \frac{(\text{lim} - 100) \times 10^{(\text{pH} - pK_a')}}{10^{(\text{pH} - pK_a')} + 1} \quad (7)$$

Absorbance is converted to α_s using estimated Lim values produced by Grafit from each data point inserted into the software. Lim represents the inflection point on the biphasic curve and the macroscopic constants are represented by pK_a and pK_a' .

2.2.4 Thiol and Amine Microscopic pK_a Calculations and Equations

Each separate microscopic pK_a value (K_s , K_n , K_{sn} and K_{ns}) were calculated from the following equations. K_s was calculated first using the data obtained from equation (7) (α_s):

$$K_s = \alpha_s([H^+] + K_a) - \frac{K_a K_{a'}}{[H^+]} (1 - \alpha_s) \quad (8)$$

K_n was then determined by rearranging the following equation:

$$K_a = K_s + K_n \quad (9)$$

Following this, equations (9) and (10) were rearranged and inserted into equation (11) so that K_{sn} and K_{ns} could be determined:

$$\frac{1}{K_{a'}} = \frac{1}{K_{sn}} + \frac{1}{K_{ns}} \quad (10)$$

$$K_a K_{a'} = K_{sn} K_s + K_{ns} K_n \quad (11)$$

[83, 101].

2.3 Results and Discussion

All thiols can be deprotonated leading to the formation of thiolate ions in the form RS^- . This allows each charged compound to exhibit distinctive properties and reactivities that differ from their non-ionised forms. The pK_a of each depicts at what pH the levels of thiol and thiolate are in equilibrium [7]. Using this knowledge, the macroscopic pK_a values of Cys, HCys, N-Me-Cys, BSH, HCys-BSH, and GSH's thiol and amino groups were determined by observing the changes in absorbance of the thiolate anion at 232nm at varying pH's between pH 4.8 and pH 12.8 [101]. Since each thiol bears different numbers of functional groups, some have more macroscopic values than others. For example: Cys contains a carboxylic group, a sulfhydryl group and an amino group and has a value for each: pK_{a2} , pK_{a3} and pK_{a4} . BSH on the other hand, contains four separate functional groups: two carboxylic groups, a sulfhydryl group, and an amino group. The thiol therefore, has four macroscopic constants, pK_{a1} , pK_{a2} , pK_{a3} and pK_{a4} (figure 16.).

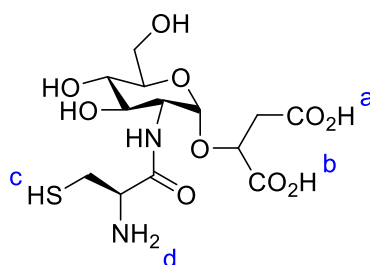


Figure 16. The structure of BSH and its the relation of each of its functional groups to each macroscopic dissociation constant shown in table 2: a) pK_{a1} , b) pK_{a2} , c) pK_{a3} and d) pK_{a4} .

In this study, macroscopic values were only obtained for the thiol and amino groups and not for any of the carboxylic groups. This is due to the more acidic nature of carboxylate pK_a 's as they can only be determined below pH 4.6 via nuclear magnetic resonance (NMR) spectroscopy. BSH contains two carboxylic groups and therefore has two pK_a values representing them. The carboxylate pK_a 's were previously determined for BSH at 3.14 and 4.38 [83]. These values do not affect the pK_a 's for the thiol and amino groups as they are always fully ionised at higher pH values [101]. The work done here focused on data obtainable using UV/VIS spectroscopy. These values were plotted on a graph that produced a double sigmoidal curve depicting the relationship between absorbance and pH (figure 17.).

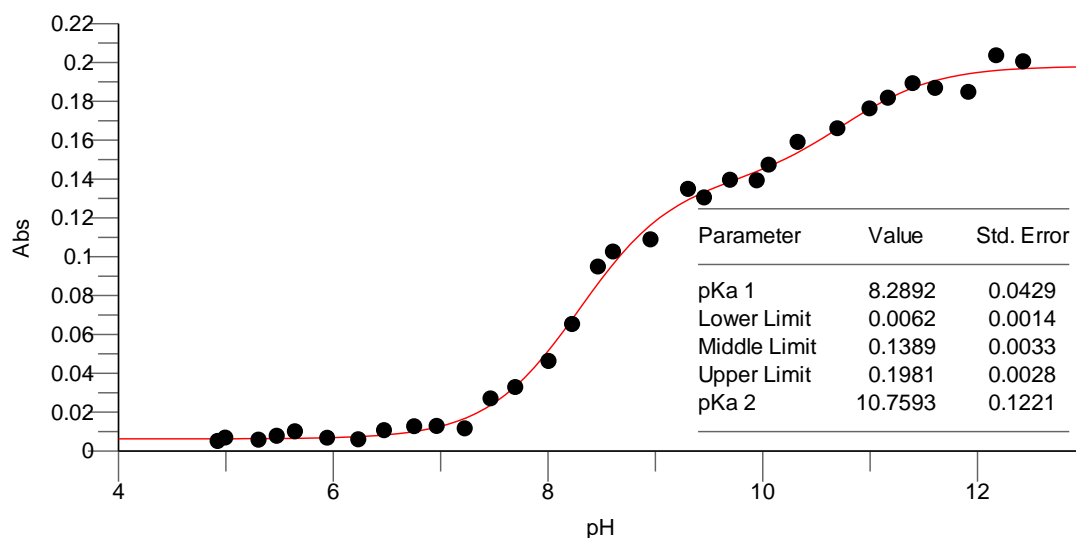


Figure 17. The absorbance (at 232nm) vs pH plot determining the thiol and amino pK_a values of Cys. The standard error for each one was also calculated. Y was calculated using equation (7) in chapter 2.2.3.

Once the macroscopic values were obtained from the graph, they were then used to calculate the corresponding microscopic pK_a values. The macroscopic dissociation constants are not representative of the individual thiol and amino groups as they differ depending on the protonation state of the other, allowing four different microscopic deprotonated forms of each thiol exist. The four microscopic pK_a values were then calculated using the relevant equations (7-11), representing the four individual deprotonation states (pK_s , pK_n , pK_{ns} and pK_{sn}) for each LMW thiol. The values obtained for Cys, HCys, BSH, and GSH (table 2.) were comparable to those found in the literature (table 3.). Overall, the strength of each thiol compared to the others as weak acids depends on which pK_a value is being observed. In terms of the thiol groups acidity (pK_{a3}), BSH has the lowest value (7.54) and is therefore more readily deprotonated followed on by N-Me-Cys, Cys, GSH, HCys and HCys-BSH with the highest value at 10.03. It is more beneficial, however, to compare each differing functional group within each thiol than observing them as a whole. Both the data gathered and previous data depicting microscopic pK_a tell that Cys' thiol group is more acidic than its amino group ($pK_s < pK_n$ and $pK_{ns} < pK_{sn}$) whereas the data for BSH indicates the opposite: that its amino group is more acidic than its thiol group ($pK_s > pK_n$ and $pK_{ns} > pK_{sn}$). HCys, N-Me-Cys and HCys-BSH follow the same trend as Cys but GSH follows that of BSH. This was originally thought to be due to the two carboxylate groups within BSH stabilising the positive charge of the ammonium group in its protonated form [83]. However, if that were the case then HCys-BSH would also follow the same trend where instead it is reversed. It may be that the carboxylate groups do influence the stabilisation of the ammonium group when protonated but because the thiol group is further along the carbon chain from the other functional groups their influence upon it is reduced as is the effect of steric hindrance.

Table 2. Macroscopic and microscopic pK_a values of the thiol and amino groups for various LMW thiols. Data errors for each pK_a were calculated to <0.36 pK_a values using Grafit.

Thiol	Results and Errors						Published								Reference
	pK_{a3}	pK_{a4}	pK_s	pK_n	pK_{ns}	pK_{sn}	pK_{a1}	pK_{a2}	pK_{a3}	pK_{a4}	pK_s	pK_n	pK_{ns}	pK_{sn}	
Cys	8.29	10.76	8.49	8.72	10.33	10.55	-	-	8.28	10.45	8.38	8.77	9.94	10.40	[83]
	(± 0.04)	(± 0.12)	(± 0.11)	(± 0.20)	(± 0.20)	(± 0.12)	-	-	8.33	10.70	8.53	8.86	10.03	10.36	[101]
HCys	9.14	10.94	9.36	9.61	10.47	10.73	-	2.22	8.87	10.86	-	-	-	-	[105]
	(± 0.07)	(± 0.09)	(± 0.13)	(± 0.30)	(± 0.30)	(± 0.15)									
N-Me-Cys	8.16	10.20	8.28	8.63	9.72	10.08	-	-	-	-	-	-	-	-	-
	(± 0.03)	(± 0.20)	(± 0.08)	(± 0.07)	(± 0.08)	(± 0.09)									
BSH	7.54	10.09	8.00	7.64	9.99	9.64	3.14	4.38	7.46	9.72	7.97	7.63	9.55	9.21	[83]
	(± 0.10)	(± 0.05)	(± 0.19)	(± 0.14)	(± 0.17)	(± 0.21)									
HCys-BSH	10.03	12.41	10.09	10.93	11.51	12.35	-	-	-	-	-	-	-	-	-
	(± 0.04)	(± 0.35)	(± 0.02)	(± 0.30)	(± 0.30)	(± 0.04)									
GSH	8.67	9.77	9.00	8.76	9.68	9.44	2.12	3.59	8.75	9.65	-	-	-	-	[106]
	(± 0.14)	(± 0.14)	(± 0.16)	(± 0.13)	(± 0.18)	(± 0.21)									

The equilibrium shift between different forms of a thiol depends upon the stability of each of them at a specific pH. The more stable the product in a reaction (in this case the conjugate base), the more favourable the reaction and the higher the acidity of the deprotonating molecule. The removal of a proton is easiest when the overall charge on a molecule is +1 but becomes more difficult when the overall charge becomes negative. A molecule is considered stable when there is either no charge throughout the molecule or there is equal charge (i.e. a positive and a negative charge cancelling each other out). The charge can be spread over a large or small area within the molecule and yet still influences the overall stability of the molecule. A small charge spread over a large area is far more stable than a small charge spread over a small area. This comes about through the delocalisation of electrons where the charge is shared by more than one atom. Sometimes delocalisation can lead to resonance: the sharing of a charge between two atoms so that more than one Lewis structure can be drawn to represent a molecule's structure. Within thiols, this can occur within their carboxylic groups as its charge can be shared between adjacent oxygen atoms. Every reaction undertaken by either a thiol or disulfide depends upon the electronic structure surrounding the sulfur atoms and the atoms closest to them.

When observing the structure of thiols, the bond lengths and angles of the S-H and S-S bonds are fundamentally important. They lead not only to the determination of the pK_a values (through their light absorption properties and their ability to ionize), but also their redox potentials (through their ability to oxidise) as well as their ability to form free radicals [97]. This is especially important because the GSB contain chlorosomes, light-harvesting complexes that shelter carotenoids and bacteriochlorophylls [86]. Carotenoids can capture light very efficiently which allows them to adapt and thrive in ecosystems that are of very low light intensity [84, 86]. The S-H bond has less dissociation energy and a longer bond length than that of an O-H bond which can be explained by observing its size and electronegativity. As mentioned previously, sulfur is less electronegative than oxygen due to its larger atomic radius which gives the S-H bond these properties. Electronegative groups within the structure of the thiol have a polar effect on the deprotonated group. This can vary depending on which elements are present (some are more electronegative than others) as well as the distance between them and the deprotonated group.

Orbital hybridisation is also an important characteristic that plays into the acidity of a molecule. The acidity (or basicity) can be predicted through the amount of p and s characters within the structure. Hybridisation occurs when the ground state of an atom cannot explain its bonding tendencies. For example, carbon's ground state does not explain its tendency to form four equal energy bonds. It can, however, be explained through four hybrid sp^3 orbitals containing four unpaired electrons that are produced through the fusing of carbon's 2s and three 2p orbitals. Each sp^3 orbital expresses 25% s character and 75% p character and has the same bond energy as the 2s orbital did before hybridisation. This configuration defines the tetrahedral structure of certain molecules. Each time hybrid orbitals are produced; their bond energies are reduced. sp hybridisation is more acidic than sp^2 and sp^2 hybridisation is more acidic than sp^3 . sp^2 , on the other hand, defines molecules with a trigonal planar structure where the 2s and two 2p orbitals combine to produce three sp orbitals with 33% s character and 67% p character. Molecules bearing linear structure are defined as having sp hybridisation. One 2s and one 2p orbital combine to form two sp orbitals with 50% s character and 50% p character. The electrons exhibiting s character prefer to stay as close to the nucleus as possible. As the percentage of s character increases, the distance between the electrons and the nucleus decreases and the acidity of the molecule increases. This is due to the angular momentum of the orbitals as the greater the angular momentum, the further away the electrons are from the nucleus decreasing the electronegativity.

Sulfhydryl groups have a tendency to react with carbonyl oxygen atoms to form hydrogen bonds and therefore are more inclined to donate a proton rather than accept one. When taking into consideration the charge, polarisation, and electronegativity of the sulfhydryl group, it is defined as a 'soft' donor as opposed to the carboxylate group that is described as a 'hard' acceptor. This leads to a disparity between the two groups hydrogen bonding capabilities [107]. While the nonpolar bond between sulfur and hydrogen is easy to break, the polar bond between nitrogen and hydrogen is more difficult due to nitrogen's strong electronegativity. The bonding electrons gravitate towards the nitrogen atom and leave the singular hydrogen proton exposed with a partial positive charge, which in turn attracts non-bonding pairs of electrons on another electronegative atom in other molecules. Due to the presence of the sulfhydryl group they show little inclination for hydrogen bonding and therefore have lower boiling points and are less soluble in water than alcohols.

Thiols contain both oxygen and nitrogen, two very electronegative atoms that have differing effects on pK_a depending on where they are located in relation to the deprotonated group. For example, the difference in the structures of Cys and N-Me-Cys lie in the N-methyl group attached to the nitrogen atom. Since nitrogen is very electronegative, it can pull the surrounding electrons of either two H atoms in Cys or one H atom as well as the methyl groups in N-Me-Cys towards it giving it a partial negative charge. The negative charge is greater for the nitrogen within the methylated thiol due to the higher electron density. The pairings Cys and HCys as well as BSH and HCys-BSH differ from each other by the addition of one CH_2 group within the carbon chain between the thiol and amino groups. This increases the distance between the deprotonating groups and, in turn, alters the pK_a values of each thiol. All dissociation constants for Cys are lower than those for HCys, proving Cys to be the more acidic of the two. The same can be said for BSH and HCys-BSH, as all the values for BSH are lower than those of HCys-BSH. The thiolate anion of a Cys molecule is thermodynamically more stable as well as a better leaving group than the thiolate anion of HCys [108]. BSH is the same in comparison to HCys-BSH but the gap between the two pK_a values is much larger (by 2.5 pK_a values). Overall the difference in values is much larger between BSH and HCys-BSH than for Cys and HCys. The acidity of each of Cys deprotonated states are very similar to those of HCys, differing by approximately 0.14 to 0.89 pK_a values. The values of the other pair differ between 1.52 to 3.29 pK_a values which can be explained by the structures of each thiol. Within the group HCys and HCys-BSH are the most basic of the thiols leading to the conclusion that the addition of a CH_2 group within the carbon chain affects the thiol so that the electron withdrawing capabilities of the amino group become less influential as the distance between functional groups increases. This leads to a decrease in the acidity and the molecule becomes less inclined to lose a proton. The lower the pK_a of a thiol, the more likely it will be oxidised to form sulfenic acids by reactive oxygen species. Sulfenic acids tend to be an intermediate in reaction mechanisms due to their increased reactivity. Since the pK_a of GSH is quite high, it needs to be decreased by GSH S-transferases in order for the nucleophilicity of the thiol to increase and allow it to conjugate to electrophilic compounds. This leads to the thiolate form becoming more predominate at physiological pH [6].

Of all the data collected, the weak acid dissociation constants for Cys and N-Me-Cys are the most similar. The N-methylation of Cys has brought each of the pK_a values down very slightly, which when considering the errors (appendices, table 1.) is a negligible difference leading to the conclusion that the addition of the methyl group has no influence on the pK_a of the amine. From this data, it could be predicted that something similar would occur when observing the differences between BSH and its N-methylated counterpart. BSH's acidity can be explained through the inductive effects of the cysteinyl carboxylate group as its negative

charge has an electrostatic effect. Due to the presence of an uncharged amide group, this cysteinyl carboxylate group is capped so that the electrostatic effect is gone, and the inductive effect remains causing an increase in the acidity of both the amino and the thiol groups [83]. The same could also be said of those with similar structures such as N-Me-BSH and HCys-BSH, although as mentioned previously HCys-BSH is much less acidic than BSH for other reasons. This would also hold true for N-Me-BSH, but it would also have the added advantage of the methyl group as N-Me-Cys did to further increase the acidity of its functional groups. The percentages of thiolate present at physiological pH were calculated previously for BSH, Cys, and CoA. They are 22%, 15% and 1% respectively. The higher concentration of BSH thiolate allows for the thiol to participate in certain reactions involving electrophilic biomolecules within the cell [83]. Without being able to conduct the same experiment on N-Me-BSH, it is difficult to estimate the concentration of thiolate at physiological pH. It is speculated, however, that in certain bacteria the thiol traffics sulfur atoms throughout the cell. This is necessary for the bacteria to photosynthesise and therefore would require large concentrations of the thiol to be present in thiolate form. The pK_a values for BSH are more acidic than those for Cys which are more acidic than those for CoA. Following on from this, if the values for N-Me-BSH are indeed more acidic than those of BSH, then the percentage of the thiol in thiolate form at physiological pH may be higher than that of BSH.

Table 3. The predicted values for the macroscopic and microscopic pK_a 's of N-Me-BSH.

Thiol	pK_{a3}	pK_{a4}	pK_s	pK_n	pK_{ns}	pK_{sn}
Cys	8.29	10.76	8.49	8.72	10.33	10.55
N-Me-Cys	9.14	10.94	9.36	9.61	10.47	10.73
BSH	7.54	10.09	8.00	7.64	9.99	9.64
N-Me-BSH	7.41	9.55	7.78	7.57	9.39	9.2

From the data gathered above, the macroscopic and microscopic pK_a 's were estimated for N-Me-BSH (table 3.). They were determined using the collected data for Cys, N-Me-Cys, and BSH. The differences between the values for Cys and N-Me-Cys were taken away from the BSH values to give the estimated pK_a values. From this, a plot of the percentage thiolate vs pH was produced for N-Me-BSH alongside those of Cys and BSH. The y values were calculated using a rearranged version of equation (8) where α_s was made the subject. The equation was first tested using the values for Cys and BSH to ensure reliable results. The resulting curves were identical to those found in figure 18.

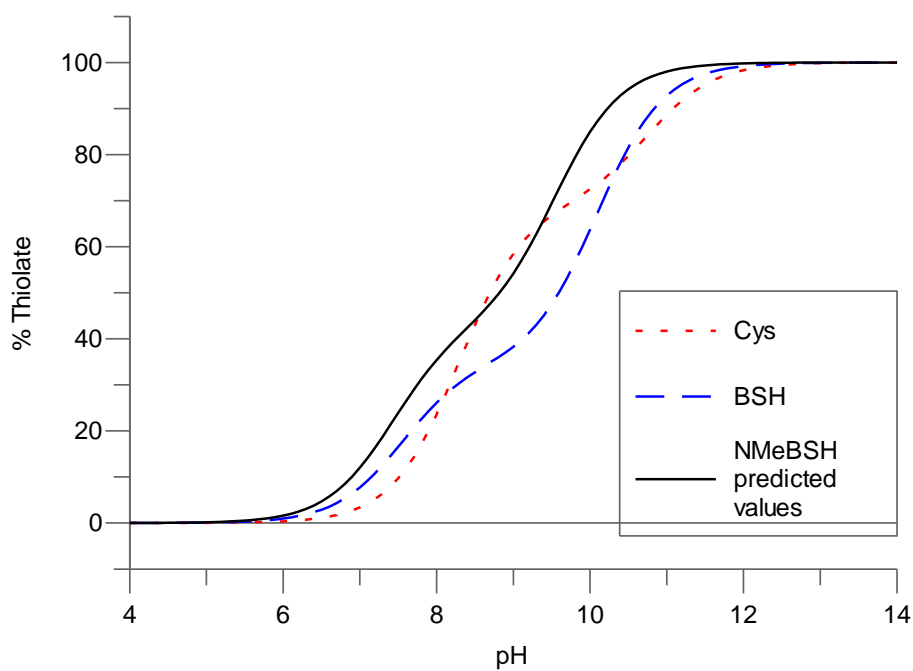


Figure 18. The percentage of thiolate present in Cys and BSH at different pH's as well as the predicted thiolate concentrations of N-Me-BSH.

In order to understand the importance of these acidity values and why each thiol produces all of their protonation states, properties that rely on these dissociation constants must also be evaluated. This would provide a broader scope of knowledge that helps indicate why each thiol differs in both their acidity and function. The following chapter explores the thiol-disulfide exchange rates that rely on the pK_a values determined above.

Chapter 3: Determining the pH Independent Thiol-Disulfide Exchange Rate Constants of LMW thiols

3.1 Introduction

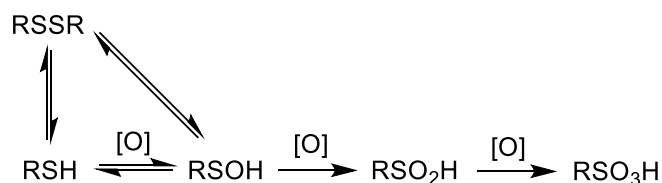


Figure 19. The formation of sulfenic, sulfinic and sulfonic acids through the oxidation of thiols.

When oxidised, thiols form reactive oxygen species. This includes the formation of sulfenic (RSOH), sulfinic (RSO₂H) and sulfonic acids (RSO₃H) (figure 19.). The reaction is only reversible during the first oxidation stage that forms sulfenic acid. The acid can then be converted into disulfide which protects the thiols from irreversible oxidative damage. Where most thiols contain a singular sulfur atom, a disulfide contains two sulfur atoms linked by a disulfide bond. Most of these molecules consist of two sulfur containing compounds bonded by this particular bridge and are known as intermolecular disulfides. However, there are those that are known as dithiols (such as T(SH)₂) that produce an intramolecular disulfide, which contain a bridge between two of its own sulfur atoms. Each disulfide can be either symmetrical (consisting of two identical R groups) or asymmetrical (consisting of two different R groups) that is also referred to as a mixed disulfide. Disulfide bonds are much stronger than the S-H bond in thiols but is weaker than any C-C or C-H bond. It is possible to cleave the bond using a polar reagent or by reacting it with a nucleophile. The bonds are generally formed in biology through sulfhydryl group oxidation. This is not always true for protein thiols, however, as they tend to be formed through thiol-disulfide exchange (figure 20.).



Figure 20. Mechanism of thiol-disulfide exchange.

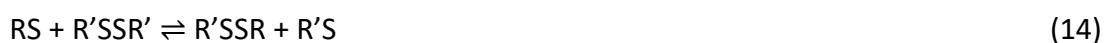
For each reaction defining rate there is a rate equation that corresponds to the concentrations and pressures of the reaction. These can be further defined as either zero order, first order or second order reactions depending on the conditions of the reaction. Zero order is where the rate is independent of the reactant concentration, first order is where the concentration of one reactant is key (the rest being zero order) and second order occurs

when the overall order of the reaction is two. Thiol-disulfide interchange reactions of a bimolecular nature display pseudo first order dependency on the reactant concentrations. The rate equation for these reactions is:

$$-\frac{d[A]}{dt} = k[A][B] \quad (12)$$

where k is the rate constant (1/time). If, like under biological conditions, the reactant concentrations are similar then the reaction follows a second order rate equation [109]. The full set of reactions are given in chapter 3.2.3. The rate constant can change depending on temperature, light irradiation, ionic strength, and surface area of an absorbent.

There are many functions that involve the exchange of thiols and disulfides both metabolically and physiologically. These biochemical processes include: the reduction, formation and cleavage of structural cysteines [24, 110, 111], the activation and inactivation of enzymes through the use of enzyme thiols and disulfides reversible redox reactions [112, 113], protein synthesis, protein degradation [24], thiol dependent redox processes [97], and the synthesis of deoxyribose intermediates needed for DNA synthesis [24]. The set of equations that relay the mechanism for the reaction is as follows:



To begin with the thiol is ionised to produce its thiolate anion (equation (13)). The thiolate anion then acts as a nucleophile and attacks one of the sulfur atoms within the disulfide bond (equation (14)), ultimately reforming the thiol by protonating the product thiolate anion (equation (15)) [111, 114]. It is always the thiolate that attacks the disulfide bond, not the thiol itself. The nucleophilic reaction is described as an S_N2 reaction, or a bi-molecular nucleophilic substitution reaction, where one bond is broken at the same time another is formed. During the transition state, their charge is spread over all three sulfur atoms, but it is concentrated on the atom being attacked [111]. These reactions can be controlled through the presence of enzymes or through equilibria. In order to understand the complexity of this process certain parameters must be ascertained: the rates behind each step of displacement, the dissociation constants for each thiol, and the equilibria positions between each thiol/thiolate and disulfide species for each step [114]. The reactivity of the thiolate depends on the pH of the reaction buffer and the acidity of the thiolate itself. When at physiological pH, the more acidic the thiol is the higher the concentration of thiolate present [83]. The pH of the solution is kept below the pK_a values of the thiol to ensure that the reaction is pH independent, meaning that the rate increases alongside the pH until the majority of the attacking thiol is deprotonated. In order for the reaction to be pH dependant, both the attacking and leaving sulfur atoms must have different pK_a values. Kinetically, the pH dependency occurs because the thiolate has far stronger nucleophilicity than the thiol. This difference is usually so drastic that the reaction occurs through the thiolate regardless of it being the minor species [109]. In this case, the equilibrium shifts towards the thiol with a lower pK_a as it is more favourable.

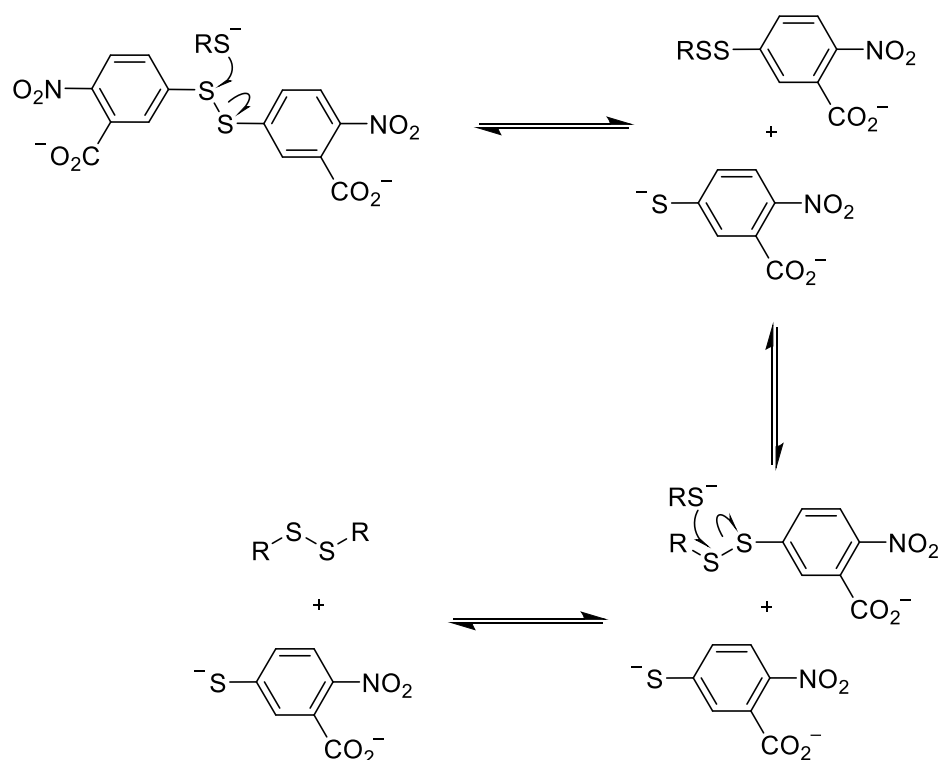


Figure 21. A thiol-disulfide exchange reaction with DTNB reacting with a thiol to produce TNB^- . The reaction then continues to ensure that all thiol is reacted. For $\lambda_{max} = 412nm$ and $\epsilon = 14150M^{-1}cm^{-1}$.

Observing this interchange reaction is quite simple in aqueous solutions. DTNB is commonly used as a model disulfide, as found in the literature, to determine rates of thiol reactivity [111, 115]. This is due to its useful properties: its water solubility, the ease at which it can be monitored spectrophotometrically, its commercial availability, its stability in a neutral solution when protected from light, and the fact that forward rates tend to not become more complex by the occurrence of back reactions [111]. When DTNB is reacted with aliphatic thiols to undergo thiol-disulfide exchange the reaction occurs at pH 7 under thermodynamic control to ensure the complete reaction of the reagent [114]. To characterise the thiol-disulfide equilibrium between dilute solutions of thiols, the pK_a values as well as the concentration of the thiol and disulfide present must be known. This is due to the S-H and S-S groups present in each molecule not being readily detectable intrinsically. Figure 21. depicts the reaction between the reagent and the thiol where the disulfide bond within DTNB is broken, which produces a disulfide with the reacting thiol attached as well as a thiolate molecule known as 2-nitro-5-thiobenzoate (TNB^-). The disulfide continues to react, producing more TNB^- until all the reacting thiol has been consumed. When ionised by water, TNB^- becomes TNB^{2-} which is yellow in colour and detectable at 412nm by UV/VIS spectroscopy. The more intense the yellow, the higher the concentration of TNB^{2-} present within the solution. The reaction produced a mixed disulfide, which are more favourably produced when the disulfide reactant is present in excess compared to the thiol reactant

[97]. This excess ensured that all the thiolate was consumed, and that the reaction continued until completion. Disulfides containing an electron withdrawing group (i.e. DTNB) react with aliphatic thiols to produce an aromatic thiol that is vividly coloured (TNB⁻). This colouration is due to the presence of an aromatic ring that has resonance with the thiol anion [97]. This resonance stabilises the charge of the thiolate anion due to the delocalisation of electrons which causes the equilibrium to shift to the right as it is the more favourable state hence why it is used to quantify thiols. It is possible, however, that the rates of thiol-disulfide exchange would differ greatly when utilising different disulfide substrates [83].

The structure surrounding the disulfide bond can affect the rate of the reaction. For example, if there is a positive charge in near proximity then it more readily attracts the attacking thiolate anion. It can also occur faster when the disulfide bond is under strain. The opposite can be said as well, as having a negative charge nearby can inhibit the reaction by repelling the incoming thiolate anion. The stability of the mixed disulfides formed can also influence the favourability of the reaction. Steric hindrance also affects the rate as bulky sidechains can block access to the thiol or disulfide.

3.2 Materials and Methods

3.2.1 Materials and Instruments

All chemical reagents were obtained from appropriate suppliers including Sigma-Aldrich and Fisher Scientific. Thiols were obtained from Sigma-Aldrich and lab stocks. Levels of pH were measured on a Hanna HI-2002 Edge pH Meter. Absorbance was measured on a Perkin Elmer Lambda 25 UV/VIS spectrometer using 1ml disposable plastic cuvettes. Cuvettes were obtained from Star Labs. The data was plotted and analysed using Grafit and Excel software programmes.

3.2.2 Thiol-Disulfide Exchange Assay

A 100mM solution of sodium phosphate buffer that was altered to pH 4.6 was blanked in a 1ml disposable cuvette. A solution of DTNB was added to a final concentration 40mM (1ml total assay volume). Each thiol was measured at five different concentrations: 2 μ M, 25 μ M, 50 μ M, 75 μ M and 100 μ M. The addition of the thiol initiated the reaction which needed to be quickly mixed in order to record the initial values. The absorbance was monitored at 412nm for 40 seconds, temperature was maintained at 30°C and each assay was performed in triplicate. Buffers were prepared at pH 4.6 so that the pH was lower than that of each thiol pK_a to enable measurable rates of reaction [83].

3.2.3 Obtaining the pH-Independent rate constant (k_1)

Initial rate was recorded during the first few percent of total thiol consumption which allowed the postulation that $[RS^-]_t = [RS^-]_0$ and enabled the following rate equations to be utilised. Each rate was determined from the initial thiol consumption:

$$v = \frac{\delta[TNB]}{dt} = k_1[RS^-][DTNB] \quad (16)$$

Which can also be expressed as:

$$v = \frac{\delta[TNB]}{dt} = k_{obs} ([DTNB]_0 - [TNB]_t) \quad (17)$$

where the reaction rate (s^{-1}) is represented by k_{obs} . The pH-independent rate constant (k_1) was then measured from plots of k_{obs} values. Each value, measured at varying concentrations, was plotted into $\ln \{([DTNB]_0 - [TNB]_t)/[DTNB]_0\}$ against time (t). From there, the gradient of each graph was plotted into another graph depicting k_{obs} versus $[RS^-]$ to give k_1 due to $k_{obs} = k_1[RS^-]$ (figure 22.) [83].

3.3 Results and Discussion

When compared to the reactivities of a thiol group, disulfides are far less reactive. They react with a variety of substances, most of which cleave them into two separate moieties. When oxidised they form sulfenic, sulfinic and sulfonic acids but when reduced, thiols are formed. The latter can occur in two ways: through heterolysis (attack by nucleophiles such as RS^- or electrophiles such as H^+ or metal ions) or homolysis. In this study, the nucleophilic cleavage of DTNB by a thiolate anion was the main focus. Since both the reactants and the products in the reaction were thiols and disulfides, the reagent DTNB (also a disulfide) was used in order for the resulting thiolate to be detected by UV/VIS spectroscopy. The absorbances were inserted into equations (16) and (17) to give the graphs depicted in figure 22. and appendix 6. The thiolate concentration was plotted against the k_{obs} values obtained from the equations and k_1 was determined from the gradient of the linear plot these values produce. The k_1 values were then compared to each other and those that have been published previously (table 4.) The results are not as close to the published data as was desirable. The overall trend within the published data tells that Cys reacts the slowest, closely followed by BSH (being almost two times faster than Cys) which is followed by GSH being more than two times faster than BSH. Within the data collected for this study, BSH proved to be the slowest of the three, with Cys approximately two times faster than BSH and GSH a fraction faster than Cys. When comparing the data of each individual thiol, the previously published k_1 value for Cys is more than 11 times slower than the data collected. Similar trends occur for the other two thiols: the published data for BSH is approximately 2.5 times slower and GSH's data is approximately 3 times slower. These discrepancies could be due to a number of reasons.

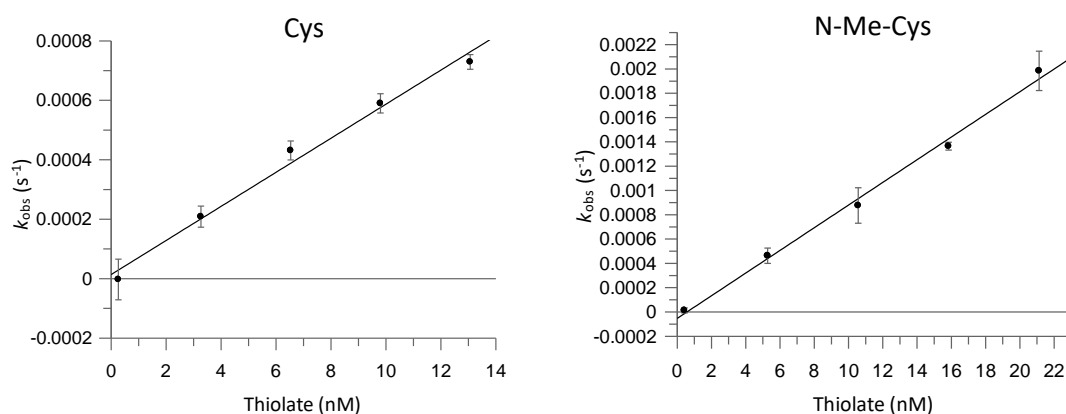


Figure 22. Graphs depicting the rate (k_1) of TNB formation (k_{obs}) vs thiolate concentration for Cys and N-Me-Cys when reacted with DTNB (40mM). Each data point was conducted in triplicate and the errors shown as error bars.

Since the rates of thiol-disulfide exchange rely so heavily upon the pK_a values determined in the previous chapters set of experiments there is a lot of room for error. Firstly, there must always be allowances for human error. However, in this case there is a chance that there could be a greater error due to the reliance of this experiment on the previous experiments results in chapter 2. Due to the accuracy required to produce so many buffers as select pH's, it is possible that minute errors could have occurred at different points during the experiment. In an attempt to counter this all experiments were run in triplicate.

Table 4. Gathered vs published data of thiol-disulfide exchange reactivities between LMW thiols and DTNB.

Thiol	$k_1 [s^{-1}m^{-1}]$	
	Presented here	Published [83]
Cys	5.73×10^{-5}	0.49×10^{-5}
HCys	0.3×10^{-5}	-
N-Me-Cys	9.33×10^{-5}	-
BSH	2.56×10^{-5}	0.95×10^{-5}
HCys-BSH	0.7×10^{-5}	-
GSH	6.68×10^{-5}	2.02×10^{-5}

Secondly, the published data used the pK_a values published in the same paper [83] and were therefore different to those used in this study since all rates were calculated using the data described in the previous chapter. The difference between each pK_a value for both data sets was significant enough that the results were altered. Three different sets of pK_a data were used to show this change and can be seen in figure 23. Since the linear fit had moved, so had the gradient, which gave a different k_1 value. The values for each plot were: $5.73 \times 10^{-5} s^{-1}M^{-1}$, $4.39 \times 10^{-5} s^{-1}M^{-1}$ and $6.18 \times 10^{-5} s^{-1}M^{-1}$ respectively. The changes in the dissociation constants used were no more than 0.39 pK_a units different but the reactivity of the thiol decreased by 23% in the first instance and increased by 8% in the second.

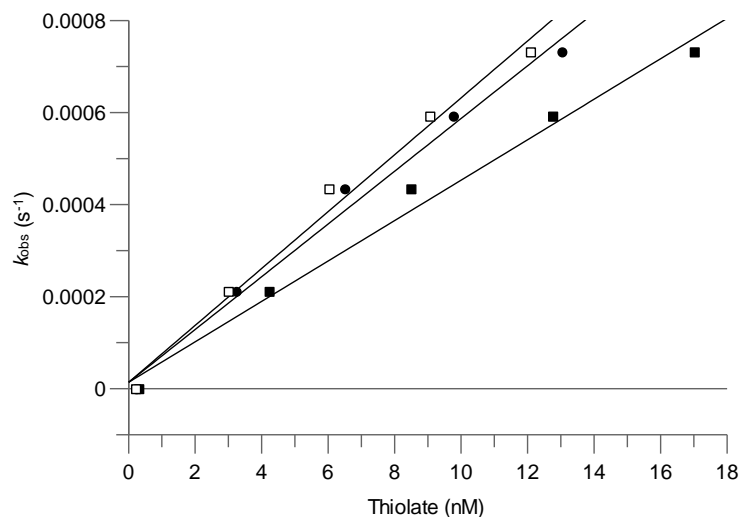


Figure 23. The differences in the thiol-disulfide exchange rates for Cys depending on the pK_a values used: with the pK_a data obtained from this study: pK_s at 8.49 and pK_{ns} at 10.33 (●), the pK_a data from Sharma et al: pK_s at 8.38 [83] and pK_{ns} at 9.94 (■) and the pK_a data from Benesch et al: pK_s at 8.53 and pK_{ns} at 10.03 (□) [101].

There are many factors known to have either inhibitory or rate enhancing effects on thiol-disulfide exchange reactions. These include factors that affect the reactivity of the attacking thiol such as pK_a and nucleophilicity as well as those that affect the electrophilicity of the central disulfide sulfur or the stability of the leaving group. The pK_a values of both the reducing thiol and the thiol formed from the disulfide contribute towards the thiol-disulfide equilibrium constants. This is proportional to the difference between values of pK_a for each specific thiol and is reliant upon the pH of the solution. Its contribution is bigger when each thiol is present only in its thiolate form and the equilibrium is between the thiolate and its disulfide. Monothiols that have similar dissociation constants also have similar equilibrium constants. Cyclic disulfide forming dithiols, however, can reduce more readily than monothiols [114]. The rate of equation (14) is affected by both the pK_a of the central group as well as the leaving group within the reaction. This can be observed through the use of the Brønsted equation, which indicates that the values for the central thiol (i.e. R'SH) have less influence than those of the attacking and leaving thiols (i.e. RSH and R''SH) [109]. In short, the rate of the reaction increases as the leaving thiols pK_a decreases and vice versa for the attacking thiols pK_a [109, 116]. As pK_a decreases the stability of the leaving thiol increases, resulting in a decrease of transition state energy [109]. This holds true for HCys and HCys-BSH as they have the highest dissociation constants and have the slowest thiol-disulfide exchange rates of all the thiols. However, HCys reacts slower than HCys-BSH but has a lower pK_a . The reactivities of N-Me-Cys and Cys also fit this pattern as N-Me-Cys has some of the lowest pK_a values and reacts quickly. Cys sits in-between N-Me-Cys and HCys-BSH within the rate table as well as the pK_a table. Both BSH and GSH, however, do not fit the pattern as BSH has the lowest pK_a values and yet has the third slowest k_1 value and GSH sits in the middle of the pK_a table but has the second fastest rate of reaction.

In polyprotic molecules kinetic analyses are more difficult due to the deprotonated state of the sulfur centre being determined by the microscopic dissociation constants as opposed to the macroscopic constants [109]. For example: GSH has four functional groups that can be deprotonated. Under physiological conditions its two carboxylic groups are deprotonated and therefore they bear no influence upon the kinetics of its thiol-disulfide reactions. Both its sulfhydryl and amino groups, however, are almost completely protonated under physiological conditions and can result in two forms of reduced GSH. These forms represent the macroscopic dissociation constants and are not definitive as each form represents a mixture of two protonation isomers. This is where the microscopic constants are required in order to determine the concentration of each thiolate functional group. This distinction is important due to the rate of equation (14) being less influenced by the overall protonation state of the thiol than of the protonation state of the thiol group. However, this does not mean that the protonation state of another functional group cannot influence the pK_a of the thiol as other charges present within the molecule can affect the overall reactivity [117]. The ionizability of protein thiols can be affected by many factors such as the inductive effects of adjacent functional groups, the positioning of the molecule, the charges present, and solvent accessibility [118]. Since proteins are so dynamic, altering the pH can result in small conformational changes which makes it difficult to determine the exact contribution of each functional groups deprotonation when measuring pK_a . As a result, protein thiols differ chemically to other small molecules. Therefore, the pH portion of the kinetics of protein thiols are best measured, where possible, with a partner that is biologically relevant [109].

There are additional factors, other than microscopic dissociation constants, that can affect the kinetics of a reaction. In reactions that utilise an S_N2 mechanism, steric factors are important due to their crowded transition state structure. Access of the attacking thiol can be hindered by bulky functional groups which also increases the activation energy for the reaction. These bulky groups can also be useful, however, as steric interactions can stabilise the binding of some substrates which is important for enzyme substrate specificity [109]. Some functional groups can cause strain on a disulfide bridge and make it more liable which speeds thiol-disulfide exchange. Overall, the data suggests that N-Me-Cys is the most reactive of all the thiols when it comes to thiol-disulfide exchange. This is followed by GSH, being approximately a third less reactive, which is closely followed by Cys. BSH is more than two times slower than Cys with HCys-BSH and HCys being the slowest at $0.7 \times 10^{-5} \text{ s}^{-1} \text{ m}^{-1}$ and $0.3 \times 10^{-5} \text{ s}^{-1} \text{ m}^{-1}$ respectively. When observing the structures of each thiol and the order of reactivity, it is clear that the presence of more bulky sidechains within each molecule do not affect the rates in the same way. For example, Cys sits roughly in the middle of all the k_1 values whereas the addition of a methyl group to the molecule increases its reactivity by 39%. The addition of a CH_2 group makes the molecule 95% less reactive and when BSH has a HCys sidechain, the reactivity increases more than two-fold when compared to that of HCys. When comparing HCys-BSH and BSH, the rate of reaction slows with the addition of the CH_2 group within the Cys sidechain. The same can be said when comparing HCys and Cys, as Cys is far more reactive than the other thiol.

Functional groups within the thiol that stabilise the charge distribution of the molecule during the transition state accelerate the reaction. The opposite occurs when the transition state charge distribution is unstable. The molecules containing electron withdrawing functional groups (those with positive charges) can stabilise the reacting thiolate or the leaving group and increase the rate of reaction, whereas those with negative charges have the opposite effect. The nucleophilicity of the reacting thiolate can be affected by the H-bonding interactions, ion pairing, or dipole interactions. For example: the increase of nucleophilicity through the presence of electron-donating functional groups and the

decrease in nucleophilicity through H-bond donation [119, 120]. When observing similarly structured thiols, the nucleophilicity increases with the pK_a of the conjugate acid. The pK_a of the conjugate acid is greater when the reactivity of the thiolate increases [121]. The presence of a hydrophobic environment during a direct thiol-disulfide reaction increases the rate [122, 123]. An aprotic environment is generally favoured by S_N2 reactions, as polar protic solvents have a greater stabilising effect on the reactants as opposed to the transition state complex. This was proven to be true as thiol-disulfide exchange reactions were seen to exhibit a more delocalised negative charge in their transition state when reacted in aprotic solvents compared to water. Those performed in aprotic solvents were approximately three orders of magnitude faster [123]. The activation of the disulfide bond through mechanical force can also trigger thiol-disulfide exchange [109].

According to the data, N-Me-Cys is far more reactive than any of the other thiols utilised in this experiment. As mentioned previously, the addition of the methyl group increased the speed of the reaction by 39%. This may hold true for N-Me-BSH since the bulkiness of the molecule when testing BSH did not seem to hinder its reactive capabilities. It is interesting to note, however, that HCys-BSH was not as reactive as BSH which could be down to the additional CH_2 group present within the Cys sidechain. However, these pH-independent k_1 values alone do not indicate how reactive a thiol would be under physiological conditions. To observe this, one paper describes the way they presented their data after factoring in thiolate concentrations during mid-exponential growth while at physiological pH. The results suggested that during these conditions, BSH would be eighteen times more reactive than Cys compared to the thiol-disulfide data predicting that BSH would be two times less reactive than Cys. These values would change further depending on different stages of growth [83]. The same can be said when the cell is under stressful conditions. When oxidative stress occurs, the thiol pool decreases so different rates would be obtained depending on the level of stress. Since thiol-disulfide exchange reactions occur often within biological systems, the kinetic forces that govern the dynamics of these reactions are vitally important. These are difficult to observe, however, as the chemical properties of sulfur mean that the reactions can occur through diverse pathways and produce various products and intermediates.

4.1 Introduction

Any molecule that undergoes oxidation in the presence of oxygen, and further goes on to form peroxides and hydroperoxides, are said to undergo autoxidation. As stated previously, thiols can react with oxygen to produce disulfides. When catalysed by transition metals such as copper or iron, this reaction can lead to the production of reactive oxygen species which include hydrogen peroxide as well as hydroxyl and superoxide radicals [124]. The most effective catalysts of autoxidation are iron (Fe^{2+} and Fe^{3+}) and copper (Cu^+ and Cu^{2+}) [76]. Interactions that occur between copper and thiols play a crucial role in the functionality of copper-containing metalloenzymes and have been of great interest for many years [125]. The effect of copper can be seen using micromolar concentrations of either Cu^+ or Cu^{2+} in the presence of Cys. Half of the intracellular Cys concentration can be oxidised within thirty minutes by $0.2\mu\text{M}$ Cu^+ or Cu^{2+} [6]. While Fe^{2+} and Fe^{3+} are also effective catalysts for autoxidation, they tend to react slower than Cu^+ or Cu^{2+} . The difference between Cu^+ and Cu^{2+} is negligible but Fe^{2+} reacts quicker than Fe^{3+} [76]. The redox-active natures of both the Cu^{2+} and thiol are very versatile and result in the formation of copper complexes that contain either terminal or bridging thiolates [125].

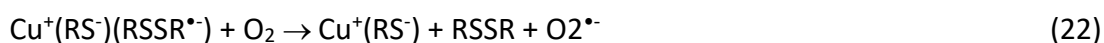
Potentially, the frequency of the reaction could be reduced by somehow controlling the availability of transition metals. Iron is found in iron-sulfur proteins in both aerobic and anaerobic bacteria [77] and copper is found in the cyanobacteria, within its electron transfer agent plastocyanin [78]. Poisonous heavy metals such as arsenic, lead, mercury, cadmium, silver, and gold will target protein thiol groups. Copper and zinc are required at low concentrations to play a role in enzymatic reactions but at higher concentrations are also toxic to cells. [36] The isolation of these metals often requires the presence of sulfhydryl groups such as GSH and its analogues, phytochelatins (fungi and plants) [126] and metallothioneins (proteins that are Cys-rich) [127].

Once oxidative stress occurs, the autoxidation cycle is continuous due to the regeneration of the catalyst. This in turn, reduces the cellular thiol pool which leads to autoxidation in the absence of thiol. As mentioned previously, free Cys is very sensitive to autoxidation catalysed by heavy metals when concentrations of the thiol are too high intracellularly due to the presence of its free amino and carboxyl groups enhancing the thiolate residues ability to bind to metals [72]. Therefore, concentrations of Cys are kept lower within the cell in order to minimize its oxidation. Other thiols, such as GSH and MSH, are much less susceptible. Both have been proven to act as Cys reservoirs due to their resistance to autoxidation. This is because their Cys residue amino groups are amides and are therefore less accessible for metal binding. The mechanisms of both GSH and Cys autoxidation have been widely explored. The mechanism of Cys's autoxidation in the presence of the copper catalyst Cu^{2+} is laid out in figure 24 and consists of two phases. Cys is a chelator of copper [128] and iron [129], suggesting that the catalyst for the reaction is the complex formed not the free metal ion itself [130]. The complex is formed from a 1:2 copper-thiol ratio. This complex was originally discovered by Cavallini *et al.*, who described its role in copper catalysed Cys oxidation [131]. The copper-Cys complex generation is as follows:

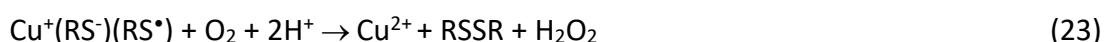




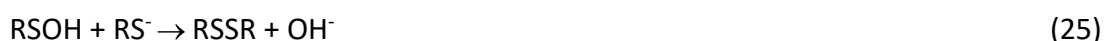
The rate limiting step is presumed to be the electron transfer from sulfur to copper since the same was found with GSH [124]. Subsequently, oxygen is consumed and converted. Approximately 40% of it is converted through the reactions:



In which no hydrogen peroxide or hydroxyl radicals are formed. Therefore, the remaining 60% is converted through the reaction:



The hydrogen peroxide that is produced is then reduced by free thiol:



In which no hydroxyl radicals are produced. Equations (21) to (25) make up the first reaction phase of thiol oxidation. The second phase is made up of reactions between thiol radicals and oxygen when free thiol is absent [130] and any excess of oxygen is consumed, and hydrogen peroxide is produced through a series of reactions [124, 132]:



The second phase is initiated only when there are equal concentrations of copper and free Cys in solution. The mechanism has practical applications due to the discovery of tumour cells containing high concentrations of Cys [133]. The mechanism also relates to Cys' neurotoxicity which may be mediated by its oxidative products [134].

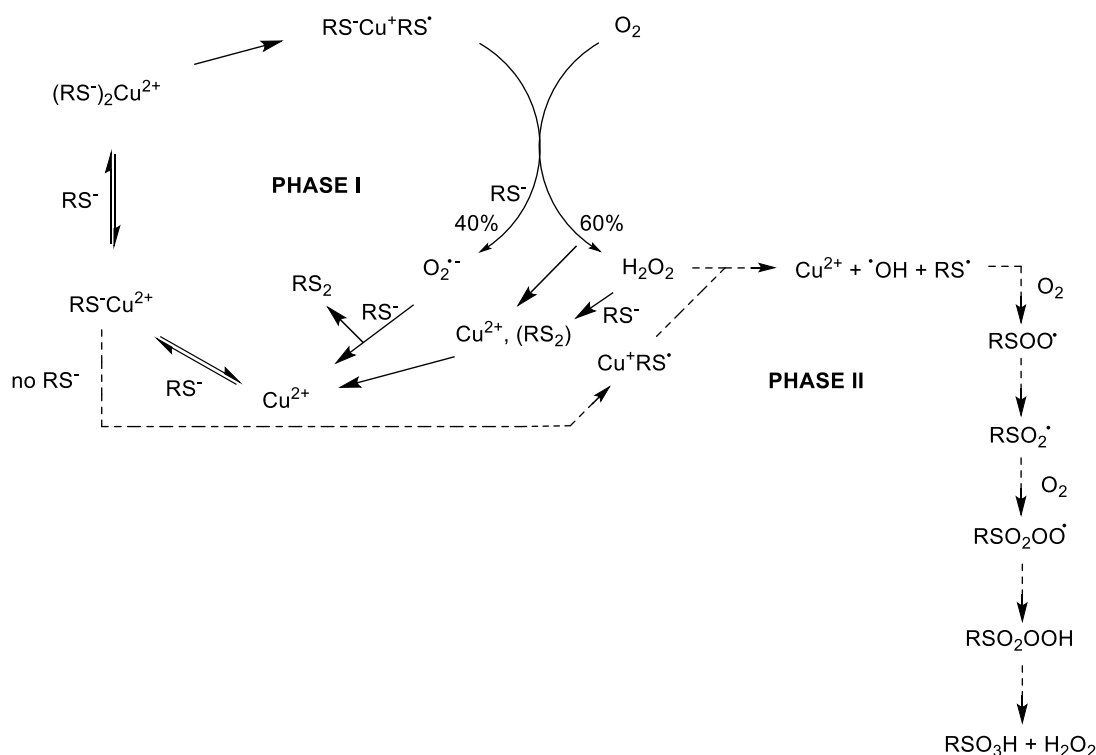


Figure 24. The copper catalysed autoxidation of Cys. Phase I is represented with solid lines and phase II is represented with dotted lines [130].

The mechanism for GSH's oxidation in the presence of copper is fundamentally different (figure 25.). Unlike Cys, GSH can undergo autoxidation through two independent but parallel pathways. To begin with, GSH forms both strong complexes with copper (with a 1:1 ratio) as well as weak complexes (with a 2:1 ratio) [124]. The higher the concentration of copper present in the solution, the quicker thiol-copper complexes are formed. The two complexes are part of the process that produces hydroxyl radicals in the presence of hydrogen peroxide. When GSH is in excess compared to copper, it is thought that a complex is formed between two GSH molecules and Cu^{2+} that is bound at the cysteine thiol moiety and the glutamine α -amino group moiety on both GSH molecules [124]. The complex is then activated through electron transfer from S^- to Cu^{2+} which leaves the complex open to attack at two different sites. Since the thiol sulfur on one of the GSH molecules is no longer bound to Cu^{2+} due to the loss of its negative charge, oxygen can now attack the complex via the thiol sulfur or the reduced metal. This electron transfer is irreversible and depending on where the oxygen attacks, the reaction can proceed via two different routes.

The first, known as the peroxide-mediated superoxide-independent pathway, begins through the reduction of oxygen by cupric ion [124]. This leads to the production of hydrogen peroxide which can then be reduced by GSH to form sulfenic acid followed by the formation of GSSG without producing any radical intermediates or oxygen depletion [135]. The second pathway, known as the superoxide-mediated peroxide-independent pathway, is initiated through the reaction of sulfur radicals with the exposed thiol sulfur of the thiol-copper

complex [136]. Sulfur radicals are not easily oxidised but when it occurs the reaction forms GSSG anion radicals which are strong reductants. The anion radicals then react with oxygen to produce superoxide anions as well as cuprous GSH [137, 138]. These two products then react with each other to form sulfenic acid which is consequently reduced to form GSSG as it does in the parallel pathway. This mechanism proves that GSH can act as both an antioxidant as well as a pro-oxidant in biology [124, 139]. When concentrations of GSH are high, superoxide and hydrogen peroxide are utilised and generate minimal hydrogen peroxide which prevents the next stage of GSH oxidation (unless severe oxidative stress conditions occur) [124]. For GSH to act as a pro-oxidant it would be when the thiol is at low concentrations in the presence of copper. This could happen during oxidative stress [140] or viral infection [141] after GSH is released from cells. The copper carrying protein ceruloplasmin is found in the blood and acts a source of copper for thiol autoxidation [142].

Rates that were previously reported for Cys described that approximately 80% of Cys was consumed within five minutes when reacted in the presence of copper [143]. However, these are not comparable to those published by Sundquist and Fahey who reported 100% of thiol consumption in approximately five minutes [144]. The same paper quoted 13% consumption of GSH within thirty minutes [144] but the previous paper claims a 75% drop in GSH during the same time [143]. MSH has been observed to be especially suitable as a cellular antioxidant as it undergoes autoxidation at a slower rate than GSH [143]. GASH was also found to have a slower autoxidation rate than GSH, as the thiol reacts at more than five times the speed of GASH [51]. The varying results of each paper made it difficult to predict how certain thiols would react in the presence of copper. In this chapter, the ease at which certain thiols oxidised in the presence of copper were determined and compared. The rate at which N-Me-BSH would oxidise in the presence of copper was then predicted.

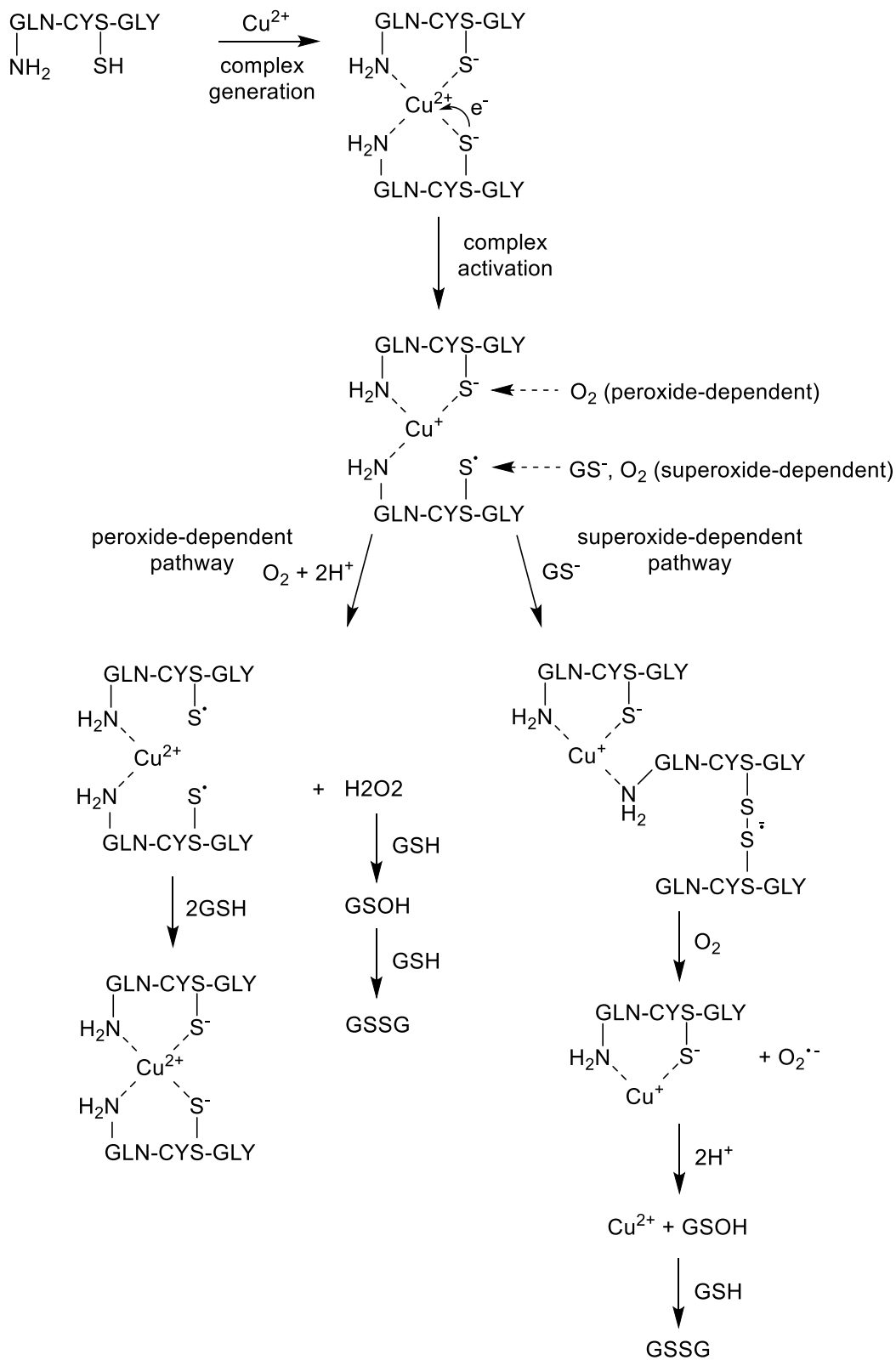


Figure 25. The copper catalysed autoxidation of GSH. The two possible pathways are either peroxide-dependent or superoxide-dependent [124].

4.2 Materials and Methods

4.2.1 Materials and Instruments

All chemical reagents were obtained from appropriate suppliers including Sigma-Aldrich, Fisher Scientific and Biorad. Thiols were obtained from Sigma-Aldrich and lab stocks. Levels of pH were measured on a Hanna HI-2002 Edge pH Meter. Absorbance was measured on a Perkin Elmer Lambda 25 UV/VIS spectrometer using 1ml disposable plastic cuvettes. Cuvettes were obtained from Star Labs. The data was plotted and analysed using Graft and Excel software programmes.

4.2.2 Cu²⁺ Catalysed Autoxidation

Buffer A was prepared containing 20mM imidazole desalted in the sodium form of Chelex and altered to pH 7.0. This ensured no metal ions were present for the thiol to react with. Buffer B was prepared containing 50mM NaH₂PO₄ and 1mM EDTA and altered to pH 7.5. EDTA also quenched the reaction by chelating any excess metal ions in buffer B. DTNB was added to buffer B to 2mM (from a 13.33mM stock solution in 50% dimethyl sulfoxide). A cuvette containing 1ml of buffer B and DTNB solution was used to blank the UV/VIS spectrometer and 200µl was subsequently removed. For the assay, a 1ml solution containing 200µM of thiol (from 10mM stock in MQ water) and 1µM copper sulfate (CuSO₄) dissolved in buffer A was prepared. Five aliquots of 200µl of the thiol and CuSO₄ solution were diluted five-fold into buffer B during a thirty-minute window. For time zero, 200µl was removed and tested before the CuSO₄ was added. Absorbance was read at 412nm and controls were conducted without the addition of CuSO₄ [144].

4.2.3 Data Analysis

Absorbance was converted into assay concentration using the Beer-Lambert Law:

$$A = \epsilon lc \tag{6}$$

so that graphs could be plotted between thiol concentration and time. A is measured absorbance, ϵ is the extinction coefficient ($\epsilon = 14150 \text{ M}^{-1}\text{cm}^{-1}$), l the path length, and c the concentration of the substance being analysed [102]. Rates were obtained from the gradient of the linear plot and compared. Graphs were plotted using Graft.

4.3 Results and Discussion

Autoxidation was measured by incubating each thiol with CuSO_4 and titrating thiol consumption at different timepoints using DTNB. The initial time point was taken before the addition of copper to ensure the measurement accounted for the total concentration of thiol present in solution when added. Controls were conducted without the addition of copper and run for 30 minutes. Samples of each thiol were run at up to five different time points over a period of 30 minutes or until all the thiol had been consumed. Each set of data was then analysed to produce a line graph depicting the differences in the rate of oxidation when incubated with and without copper (figure 26). Each graph shows a distinct difference in rate between the controls and the copper catalysed reactions. In all cases the copper increased the speed of the reaction and was most effective when reacted with Cys. The reactions containing N-Me-Cys, BSH and HCys-BSH as well as CuSO_4 were all completed within 30 minutes but HCys and GSH did not go to completion within that time.

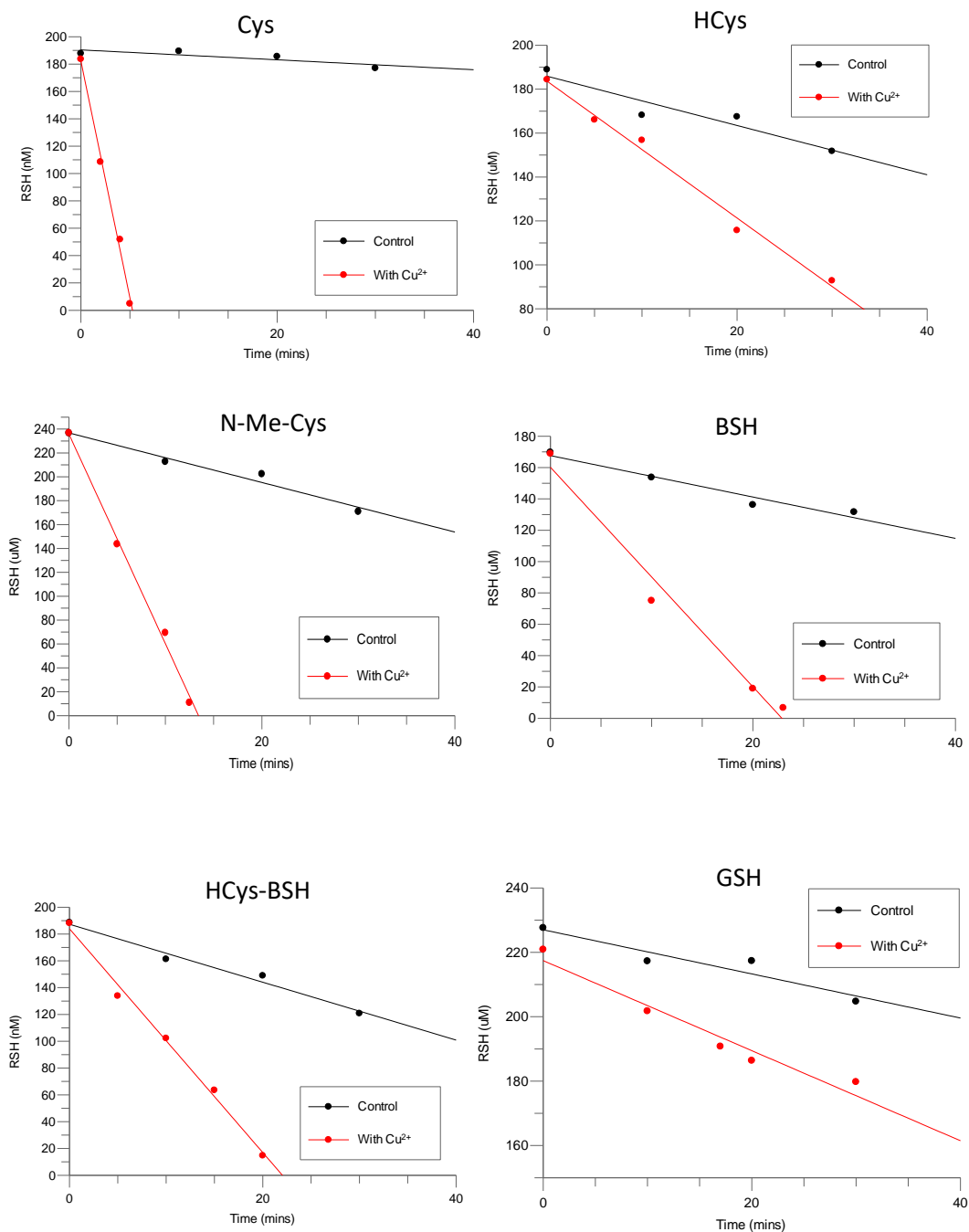


Figure 26. Differences in autoxidation rates for each thiol when incubated with and without CuSO₄. The gradient of the linear fit gives the rate of autoxidation.

Even though there are clear differences between the controls and the Cu²⁺ catalysed reactions, it is difficult to tell from the graphs in figure 26. how each thiol compares to another. Therefore, a linear fit was fitted to every set of data in order to identify the gradient

of each line graph. The gradients of these graphs corresponded to the autoxidation rate for each thiol. The rates and their standard errors are given in table 5. From there, the fastest rate (Cys) was normalised to 100% and the remainder given a percentage accordingly. These relative rates are given alongside the autoxidation rates in table 5. as well as being represented in a bar graph in figure 27. for a clearer comparison.

Table 5. The autoxidation rates of LMW thiols with and without CuSO₄, their rates relative to Cys when normalised to 100%, and their standard errors.

Thiol	Autoxidation Rate (μM/min)	Standard Error	Relative Rate (%)
Cys	34.63	1.90	100
HCys	3.12	0.19	9
N-Me-Cys	17.56	0.85	51
BSH	7.01	0.74	20
HCys-BSH	8.35	0.40	24
GSH	1.40	0.18	4
Cys Control	0.36	0.16	1
HCys Control	1.12	0.26	3
N-Me-Cys Control	2.08	0.27	6
BSH Control	1.32	0.21	4
HCys-BSH Control	2.16	0.22	6
GSH Control	0.68	0.17	2

When observing the published rates in previous papers, approximately 80% of Cys is consumed within five minutes when reacted in the presence of copper [143]. In comparison, the graph representing Cys in figure 26. shows that the reaction occurred at a faster rate with almost all of the thiol being consumed in the same amount of time. These results are more comparable to those published by Sundquist and Fahey in which 100% of the thiol was consumed in approximately five minutes [144]. The data presented in figure 26. for GSH sees 18% of thiol oxidised within thirty minutes of incubation with copper. One paper's data was similar to this with 13% consumption in the same time [144] but another paper's results claims a 75% drop in GSH after 30 minutes [143]. Studies performed with GASH found that its rate of autoxidation was far slower than that of GSH, making it more resistant to air oxidation than its similarly structured equivalent [51]. MSH also undergoes autoxidation at a slower rate than GSH, making it especially suitable as a cellular antioxidant [143]. Before the addition of the copper catalyst, the controls for each thiol were run to observe the natural autoxidation to ensure that there was no interference from the buffers. One buffer was treated with ethylenediaminetetraacetic acid (ETDA) to mop up any residual metal ions that could affect the rate of the reaction. The other buffer was chelated using a sodium form of chelex that desalts the solution by binding with the metal ions. The autoxidation rates for each control varied slightly as each reacts to the oxygen in the air at different speeds. The reasons behind these differences in both the controls and the copper catalysed reactions are speculated below.

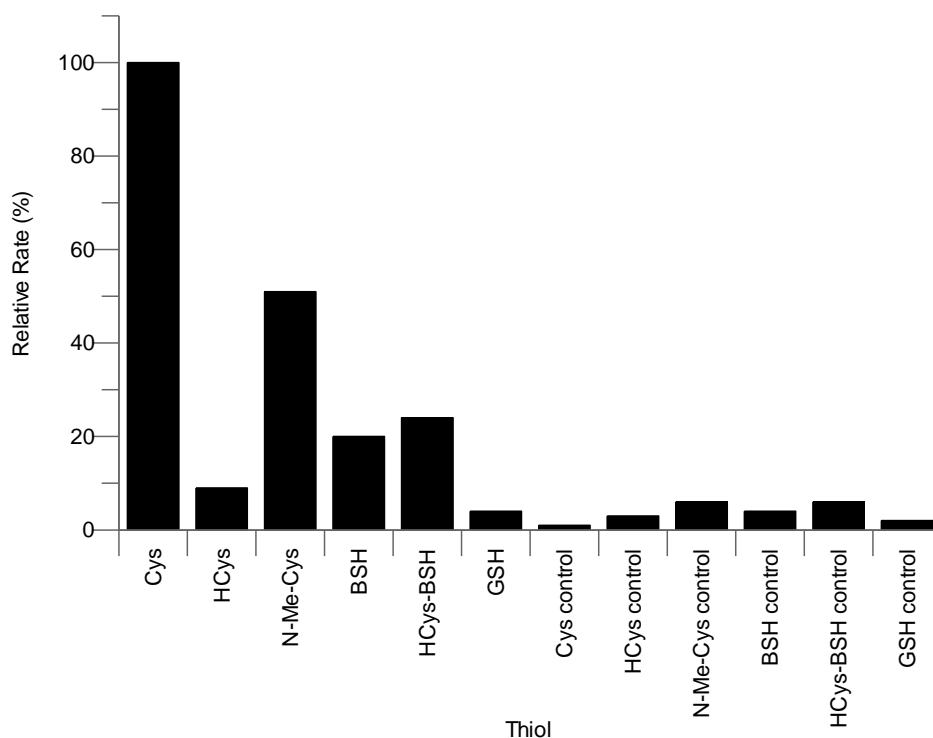


Figure 27. Rates of thiol autoxidation when incubated with and without CuSO₄ when compared to Cys (normalised to 100%).

The data presented in figure 27. presents the relative rates of each thiol and their controls. Each control has a slower rate of reaction than the copper catalysed reactions proving that the addition of copper speeds the reaction. Cys was by far the fastest thiol to be consumed, followed by N-Me-Cys which was consumed at half the rate Cys was. HCys-BSH was consumed at half the rate again followed closely by BSH which reacted at 20% of the speed of Cys. HCys reacted at double the speed BSH did but GSH was the slowest, reacting at 4% compared to Cys's 100%. The slowest copper catalysed autoxidation (GSH) was in line with some of the rates of the controls, but the reaction occurred twice as fast as its own control. The speed of the assays may vary slightly due to a few factors. First, the buffers that were treated to ensure that they were metal ion free may have had some ionic interference from ions that were added when the solutions were altered to their specific pH's after the addition of EDTA/they were chelated. Second, human error would play a significant role due to the accuracy required to run each assay. This had limitations due to the thiols tendency to slowly oxidise when exposed to oxygen. Precautions were taken every time stocks were used (they were exposed to air as little as possible) and kept on ice to preserve them as much as possible. The stock solutions of thiols were also dissolved in milli Q water so that no impurities would be present in solution and affect the results. To further aid the results of this study, a comparison of the controls with the addition of EDTA and the data displayed above would be useful as it would ensure that the controls were more accurate and did not contain any excess metal ions. An additional way to compare the affinity of metal catalysed autoxidation would be to conduct experiments using other metals such as iron. Such an experiment would provide insight into the individual effectiveness of each of them, the

mechanisms by which they occur and what factors certain metals have that can either aid or hinder the autoxidation process.

Furthermore, it was found that the distance between the free amino group and thiol group is important in thiol autoxidation [130]. Having the amino group close to the thiol group substantially increases the rate of oxidation through the site-specific binding of the copper ion. When the amino group is absent or blocked, the thiol is stable to autoxidation and there is a substantial decrease in the rate. This effect has been seen in Cys [130], GSH [124], N-acetylcysteine as well as dithiothreitol [145]. Cys is susceptible to autoxidation because of its exposed thiol, amino and carboxyl groups all being available for bonding to metal ions. The availability of both the amino and carboxyl groups during the initial binding of copper to Cys are crucial as when one or both are either blocked or missing, the complex is far less stable [130]. MSH undergoes autoxidation catalysed by copper ions around thirtyfold slower than autoxidation of Cys [143]. This is achieved by the amino and carboxyl groups on Cys being blocked by N-acetyl and GlcN-Ins moieties causing reduced metal-ion coordination strength [6]. The same can be said for the slow rate of oxidation of GSH as both the amino and carboxyl groups on its Cys residue are blocked and cannot bond with metal ions [143].

The structure of each thiol seems to bear great influence on the speed at which oxidation occurs. For example, in N-Me-Cys each of its potential binding sites (the thiol, amino and carboxyl groups) are available but the presence of the methyl group attached to the amino group hinders the binding enough that the rate (when compared to Cys) decreases by half. It appears that the bulk of the extra sidechain hinders the binding enough to slow down the rate but not by as much as it would if it was completely blocked. HCys, however, reacts at only a fraction of the speed of Cys and its rate of reaction more comparable to GSH. This is surprising but perhaps the distance between the thiol and amino groups is far enough to hinder the site-specific binding of the copper. The same cannot be said for HCys-BSH as its rate is more than three times faster than HCys. While it bears the same distance between its thiol and amino groups and its cysteinyl carboxyl group is blocked, these may be countered by the two carboxyl groups that are available for complex bonding potentially boosting its oxidation rate. Similar can be said for BSH as it contains the same two carboxyl groups as well as the free thiol and amino groups on its Cys sidechain. It is difficult to discern why the rate of oxidation for BSH is slower than that of HCys-BSH since the distance between its thiol and amino groups is smaller. If all the criteria mentioned above is met, then the rate would be expected to be quicker rather than slower for BSH.

The rate of autoxidation reactions varies depending on the pH of the solution. In other words, it depends upon the protonation state of both the thiol and the oxidant. When the oxidant is protonated, it accelerates the reaction due to its protonated form being a better electrophile. This is in contrast to the more favourable deprotonated state of the thiol [109]. The four graphs in figure 28. compare the relative rates of autoxidation of thiols compared to their individual microscopic pK_a values. Each graph is dedicated to a specific microscopic pK_a : pK_s , pK_n , pK_{ns} , and pK_{sn} . No graph shows any correlation between the two properties indicating that the pK_a values of thiols bear no influence on autoxidation activity when catalysed with copper.

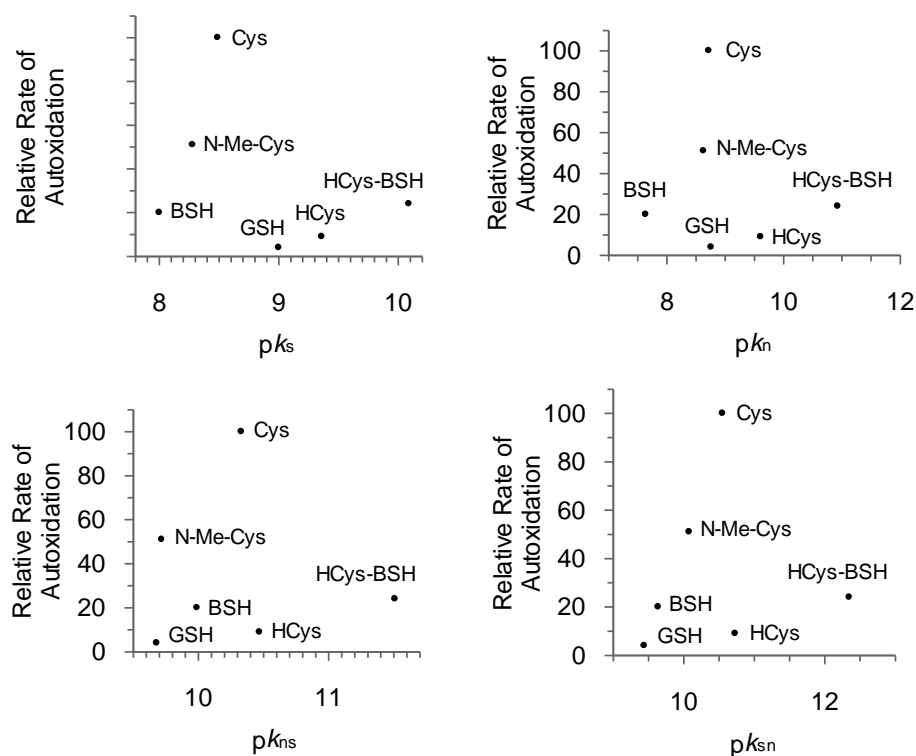


Figure 28. Graphs depicting the relationship between the relative rates of autoxidation and the microscopic pK_a values of Cys, HCys, N-Me-Cys, BSH, HCys-BSH and GSH.

For a thiol to function properly at millimolar concentrations in aerobic cells, it must be resilient to autoxidation in order to minimize its occurrence [1]. Anaerobic cells, such as the GSB, also require resilience to autoxidation, although perhaps not to such the same extent as aerobic cells. It is thought that bacteria in the past that couldn't adapt to aerobic environments remained confined to anaerobic environments. The lack of mechanisms that utilise oxygen meant that resistance to autoxidation was not as necessary [1]. Since Cys oxidises so quickly and is so toxic, it is maintained in the form of other less susceptible thiols in order to protect the cell and significantly slow down the process of autoxidation [22, 27]. Even though anaerobic cells do not require oxygen to respire, they still utilise alternatives that bear the same functions and still produce reactive species. It could then be predicted that the mechanism by which autoxidation occurs is very different from those of Cys and GSH in figure 24. and 25. It is presumed that, like all other LMW thiols, N-Me-BSH is also required for autoxidation in the GSB much the same as MSH in the actinomycetes. While the majority of its structure is the same as BSH, the presence of the methyl group of N-Me-Cys has been seen to slow the rate of autoxidation, so it is likely that the rate of reaction for N-Me-BSH will be slower than that of BSH. However, the rate may not be as slow as N-Me-Cys is compared to Cys due to the presence of the additional carboxyl group.

Chapter 5: Conclusions and Future Work

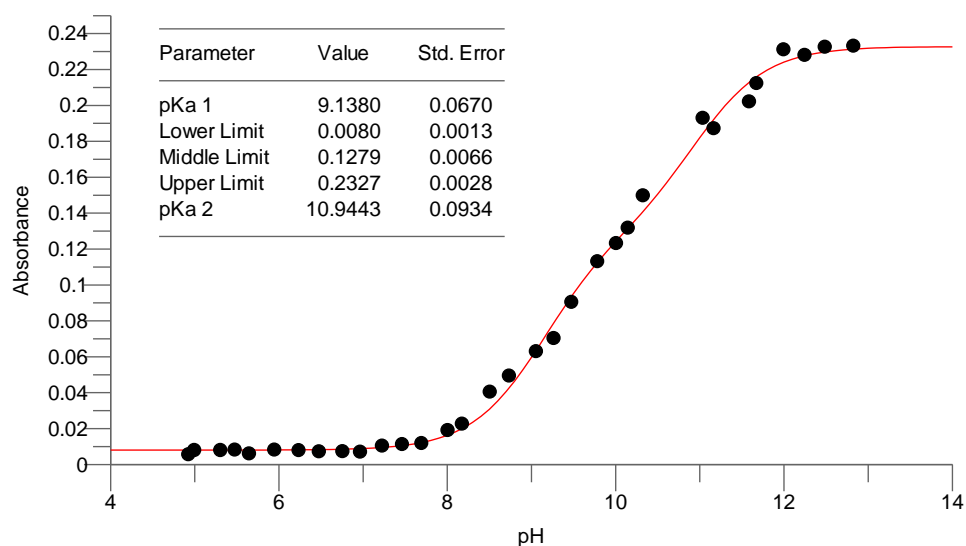
The main aim of this study was to expand on the knowledge of N-Me-BSH, the novel LMW thiol discovered in the GSB, and to determine the significance of its N-methylated sidechain. This was to be achieved through the observation of other LMW thiols with similar structures. By determining their biophysical properties, predictions could be made for N-Me-BSH's properties and speculation as to the impact of the presence of the N-methyl sidechain has on the rest of the molecule could be discussed. However, the only evidence of the thiol consisted of an as of yet unpublished paper, ensuring that very little is currently known about the bacteria and its thiol.

Data presented in chapter 2 revealed that many factors, not just the structure of sidechains, affect the macroscopic and microscopic pK_a values. The differences made it possible to predict accurate values for N-Me-BSH as well as create a graph depicting the percentage of thiolate present at specific pH's. Once the physiological pH is determined within some of the GSB, the proportions of thiol and amino protonation forms under normal conditions can be identified. At the physiological pH of 7.7 in *B.subtilis* (a BSH producing bacteria), the percentage thiolate of BSH is approximately 20%. At the same pH for N-Me-BSH, the percentage thiolate is approximately 30%. Data presented in chapter 3 revealed that N-Me-Cys is far more reactive than any of the other thiols utilised in this experiment. The addition of the methyl group seemed to greatly increase the speed of thiol-disulfide reactions. It could be deduced from this that N-Me-BSH would have the same effect as the bulkiness of the molecule did not seem to hinder its reactive capabilities when testing BSH. Data presented in chapter 4 revealed that the autoxidation rates vary greatly between thiols. No thiol is more prone to autoxidation than Cys but while the N-methylation of this thiol slows the process, it is still faster than any other thiols rate in this study. BSH is much slower but has the additional presence of another carboxylic group to consider. Therefore, it is difficult to give a definitive prediction of the rate of autoxidation for N-Me-BSH. Since the GSB are a group of anaerobic bacteria, they require less resistance to autoxidation as they do not utilise oxygen to photosynthesise. From this, it can be deduced that the rate could be around half the speed of BSH's.

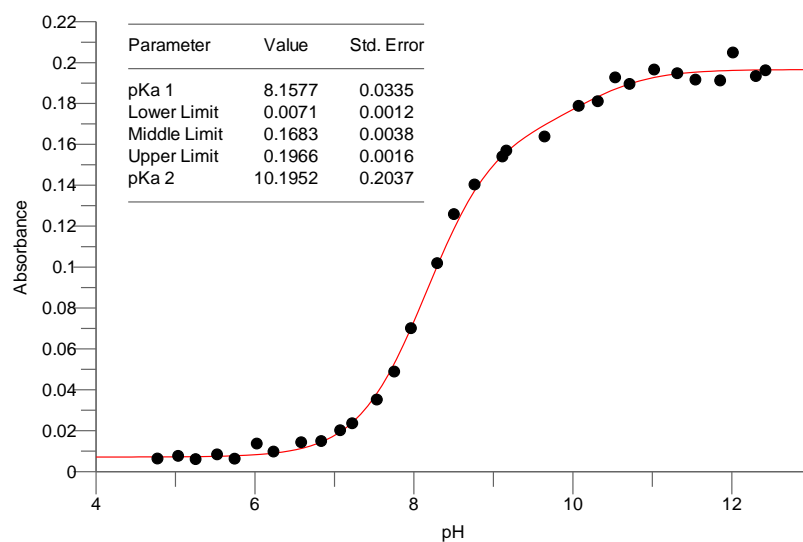
The analysis of co-occurring orthologs to BSH biosynthesis genes as well as BSH N-methyltransferase predicted thiol biosynthesis in phylogenetically distant genomes [85]. This indicates that BSH and its N-methylated counterpart may be the most widely distributed class of thiols. The results presented here focused on a chemical modification that is rare in biology. The N-methylation of BSH is only the fourth occurrence of cysteinyl nitrogen methylation in metabolism [85]. There is still much more to explore in relation to this unique modification. In future, the successful isolation of the LMW thiol would be required in order to either confirm or deny the findings of this study. This could be achieved through chemical synthesis, isolation of the thiol from the GSB or through the genetic modification of an organism that produces BSH. In theory, the additional step in the biosynthesis of N-Me-BSH could be introduced to a strain of bacteria such as *B. subtilis*. This could identify why the modification is so important to the GSB and whether it would affect the normal functions of the cell as in the bacteria that produce N-Me-BSH, BSH is also produced (although in smaller quantities). It could be that it makes no difference or that so little of it is produced that it doesn't have any effect. The results could also give insight into the thiols proposed role of trafficking sulfur atoms within phototrophic sulfur oxidising bacteria. Identification of the thiol in other organisms would also broaden the spectrum of knowledge.

Appendices

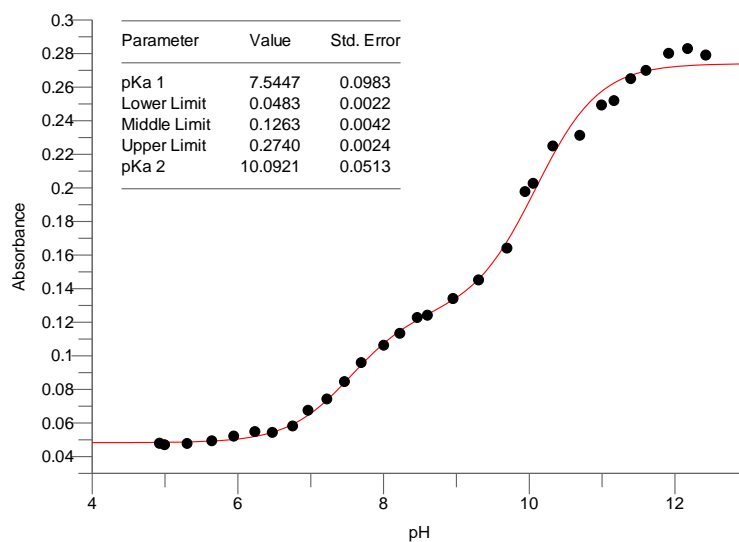
1.1 Additional pK_a graphs and standard errors



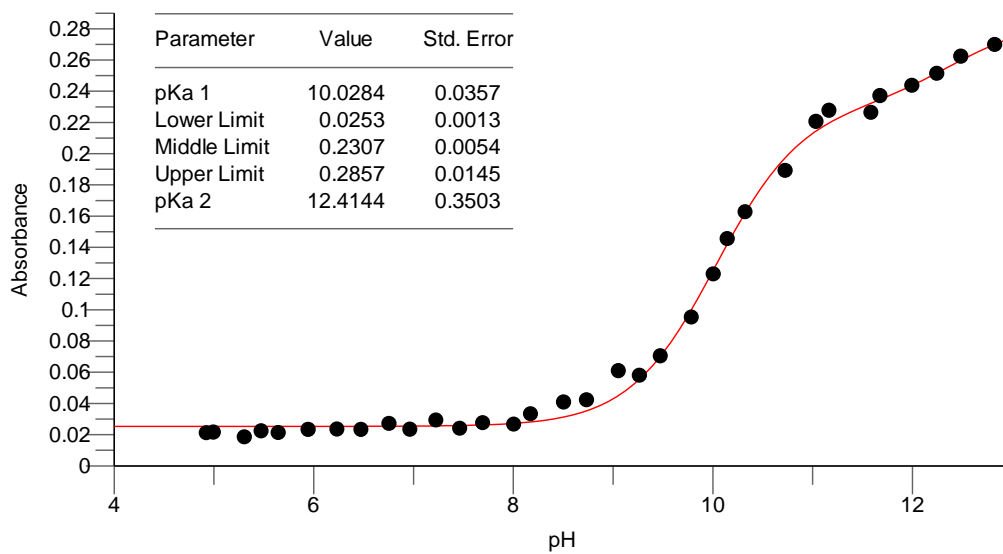
Appendix 1. The absorbance (at 232nm) vs pH plot determining the thiol and amino pK_a values of HCys. The standard error for each one was also calculated.



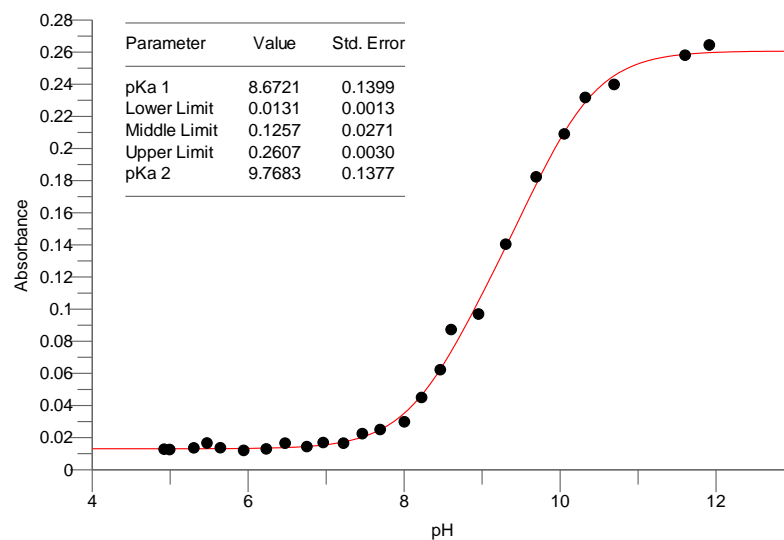
Appendix 2. The absorbance (at 232nm) vs pH plot determining the thiol and amino pK_a values of N-Me-Cys. The standard error for each one was also calculated.



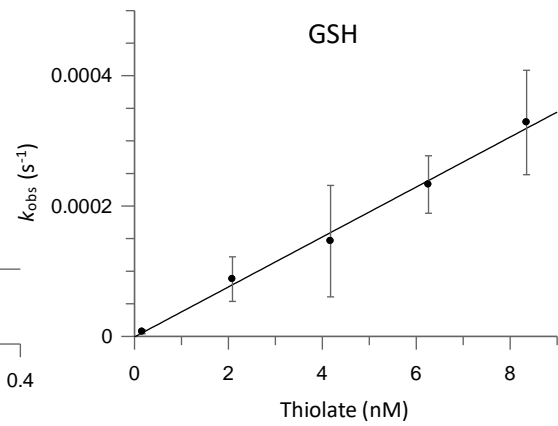
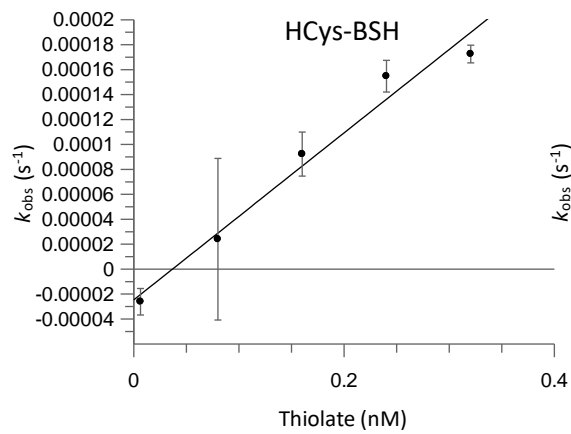
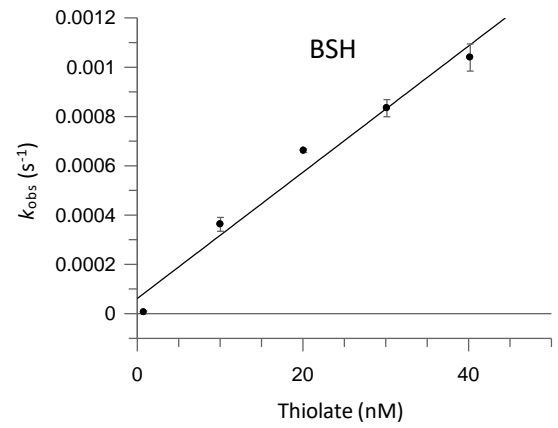
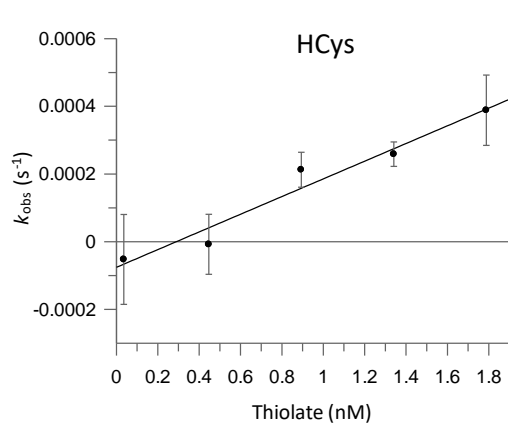
Appendix 3. The absorbance (at 232nm) vs pH plot determining the thiol and amino pK_a values of BSH. The standard error for each one was also calculated.



Appendix 4. The absorbance (at 232nm) vs pH plot determining the thiol and amino pK_a values of HCys-BSH. The standard error for each one was also calculated.



Appendix 5. The absorbance (at 232nm) vs pH plot determining the thiol and amino pK_a values of GSH. The standard error for each one was also calculated



Appendix 6. Graphs depicting the rate (k_1) of TNB formation (k_{obs}) vs thiolate concentration for the remaining LMW thiols when reacted with DTNB (40mM). Each data point was conducted in triplicate and the errors shown as error bars.

Abbreviations

β-ME	β-mercaptoethanol
BSH	Bacillithiol
BSSB	Bacillithiol disulfide
CO₂	Carbon dioxide
CoA	Coenzyme A
Cu⁺	Cuprous ion
Cu²⁺	Cupric ion
CuSO₄	Copper sulfate
Cys	Cysteine
DSR	Dissimilatory sulphite reductase enzyme
DTNB	5,5'-dithio-bis-[2-nitrobenzoic acid]
DTT	Dithiothreitol
dw	Dry weight
ETDA	Ethylenediaminetetraacetic acid
Fe²⁺	Ferrous ion
Fe³⁺	Ferric ion
GASH	Glutathione amide
GCS	γ-glutamylcysteine synthetase
Glc-N-Mal	Glucosaminyl-malate
Glc-NAc-Mal	N-acetylglucosaminyl-malate
GSB	Green sulfur bacteria
GSH	Glutathione
GSSG	Glutathione disulfide
H₂O₂	Hydrogen peroxide
HCys	Homocysteine
HCys-BSH	Homocysteinyl-bacillithiol
HIV	Human immune deficiency virus
LMW	Low molecular weight
mBBBr	Monobromobimane
Met	Methionine

MSH	Mycothiol
N-Me-BSH	N-methyl-bacillithiol
N-Me-Cys	N-methyl-cysteine
Na₂HPO₄	Sodium phosphate dibasic
NaH₂PO₄	Sodium phosphate monobasic
NADPH	Nicotinamide adenine dinucleotide phosphate
NMR	Nuclear magnetic resonance
O₂	Oxygen
PSB	Purple sulfur bacteria
SAM	S-adenosyl-methionine
SOX	Sulfide:quinone oxidoreductases
TCEP	Tris(2-carboxyethyl)phosphine
TNB⁻	2-nitro-5-thiobenzoate
TR	Trypanothione reductase
T(SH)₂	Trypanothione
TS₂	Trypanothione disulfide
TxN	Tryparedoxin
TxNPx	Tryparedoxin peroxidase
RSOH	Sulfenic acid
RSO₂H	Sulfinic acid
RSO₃H	Sulfonic acid
UDP-Glc-NAc	Uridine diphosphate n-acetylglucosamine

Bibliography

- [1] R. Fahey, "Novel Thiols of Prokaryotes," *Annual Review of Microbiology*, vol. 55, pp. 333-356, 2001.
- [2] Z. Fang and P. Santos, "Protective role of bacillithiol in superoxide stress and Fe-S metabolism in *Bacillus subtilis*," *Microbiology Open*, vol. 4, no. 4, pp. 616-631, 2015.
- [3] C. Hamilton, M. Arbach and M. Groom, "Beyond glutathione: Different low molecular weight thiols as mediators of redox regulation and other metabolic functions in lower organisms," *Book at Spiringer*, pp. 291-320, 2014.
- [4] G. Cody, N. Boctor, T. Filley, R. Hazen, J. Scott, A. Sharma and H. Yoder Jr, "Primordial Carbonylated Iron-Sulfur Compounds and the Synthesis of Pyruvate," *Science*, vol. 289, pp. 1337-1340, 2000.
- [5] W. Heinen and A. Lauwers, "Organic sulfur compounds resulting from the interaction of iron sulfide, hydrogen sulfide and carbon dioxide in an anaerobic aqueous environment," *Origins of Life and Evolution of the Biosphere*, vol. 26, pp. 131-150, 1996.
- [6] K. Laer, C. Hamilton and J. Messens, "Low-Molecular-Weight Thiols in Thiol-Disulfide Exchange," *Antioxidants & Redox Signaling*, vol. 18, no. 13, pp. 1642-1653, 2012.
- [7] L. Poole, "The Basics of Thiols and Cysteines in Redox Biology and Chemistry," *Free Radical Biology and Chemistry*, pp. 148-157, 2015.
- [8] A. Gaballa, G. Newton, H. Antelmann, D. Parsonage, H. Upton, M. Rawat, A. Claiborne, R. Fahey and J. Helmann, "Biosynthesis and functions of bacillithiol, a major low-molecular-weight thiol in Bacilli," *PNAS*, vol. 107, no. 14, pp. 6482-6486, 2010.
- [9] O. Zitka, S. Skalickova, J. Gumulec, M. Masarik, V. Adam, J. Hubalek, L. Trnkova, J. Kruseova, T. Eckschlager and R. Kizek, "Redox status expressed as GSH:GSSG ratio as a marker for oxidative stress in paediatric tumour patients," *Oncology Letters*, vol. 4, pp. 1247-1253, 2012.
- [10] J. Imlay, "The molecular mechanisms and physiological consequences of oxidative stress: lessons from a model bacterium," *Nature Reviews Microbiology*, vol. 11, pp. 443-454, 2013.
- [11] B. Ezraty, A. Gennaris, F. Barras and J. Collet, "Oxidative stress, protein damage and repair in bacteria," *Nature Reviews Microbiology*, vol. 15, pp. 385-396, 2017.
- [12] T. Nystrom, "Role of oxidative carbonylation in protein quality control and senescence," *EMBO Journal*, vol. 24, pp. 1311-1317, 2005.

- [13] M. Feeney and C. Schoneich, "Tyrosine modifications in aging," *Antioxidants & Redox Signalling*, vol. 17, pp. 1571-1579, 2012.
- [14] D. Traore, A. El Ghazouani, L. Jacquamet, F. Borel, J. Ferrer, D. Lascoux, J. Ravanat, M. Jaquinod, G. Blondin, C. Caux-Thang, V. Duarte and J. Latour, "Structural and functional characterization of 2-oxo-histidine in oxidized PerR protein," *Nature Chemical Biology*, vol. 5, no. 1, pp. 53-59, 2009.
- [15] H. Antelmann, M. Hecker and P. Zuber, "Proteomic signatures uncover thiol-specific electrophile resistance mechanisms in *Bacillus subtilis*," *Expert Review of Proteomics*, vol. 5, pp. 77-90, 2008.
- [16] N. Allocati, L. Federici, M. Masulli and C. Di Ilio, "Glutathione transferases in bacteria," *FEBS Journal*, vol. 276, pp. 58-75, 2009.
- [17] P. Sherratt and J. Hayes, "Glutathione S-transferases," in *Enzyme Systems that Metabolise Drugs and Other Xenobiotics*, John Wiley & Sons, 2001, pp. 319-352.
- [18] G. Lamoureux and D. Russness, "The role of glutathione and glutathione-S-transferases in pesticide metabolism, selectivity, and mode of action in plants and insects," in *Glutathione: Chemical, Biochemical and Medical Aspects. Parts A and B*, Wiley Interscience, 1989, pp. 153-196.
- [19] T. Lee, M. Wei, W. Chang, I. Ho, J. Lo, K. Jan and H. Huang, "Elevation of glutathione levels and glutathione S-transferase activity in arsenic-resistant Chinese hamster ovary cells," *In Vitro Cellular & Developmental Biology*, vol. 25, pp. 442-448, 1989.
- [20] C. Morrow and K. Cowan, "Glutathione-S-transferases and drug resistance," *Cancer Cells*, vol. 2, pp. 15-22, 1990.
- [21] D. Waxman, "Glutathione-S-transferases: role in alkylating agent resistance and possible target for modulation chemotherapy," *Cancer Research*, vol. 50, pp. 6449-6454, 1990.
- [22] G. Wu, Y. Fang, S. Yang, J. Lupton and N. Turner, "Glutathione Metabolism and Its Implications for Health," *Journal of Nutrition*, vol. 134, no. 3, pp. 489-492, 2004.
- [23] R. Fahey, R. Buschbacher and G. Newton, "The evolution of glutathione metabolism in phototrophic microorganisms," *Journal of Molecular Evolution*, vol. 25, pp. 81-88, 1987.
- [24] A. Meister and M. Anderson, "Glutathione," *Annual Review of Biochemistry*, vol. 52, pp. 711-760, 1983.
- [25] A. Meister, "Metabolism of sulfur compounds," in *Metabolic Pathways*, Elsevier, 1975, pp. 101-188.
- [26] B. Chance, H. Sies and A. Boveris, "Hydroperoxide metabolism in mammalian organs," *Physiological Reviews*, vol. 59, pp. 527-605, 1979.

- [27] H. Sies, "Glutathione and its role in cellular functions," *Free Radical Biology & Medicine*, vol. 27, no. 9/10, pp. 916-921, 1999.
- [28] P. Varandani, "Glutathione-insulin transhydrogenase (protein-disulfide interchange enzyme)," in *Glutathione: Chemical, Biochemical and Medical Aspects. Parts A and B*, Wiley Interscience, 1989, pp. 753-765.
- [29] M. Hsu, M. Muhich and J. Boothroyd, "A developmentally regulated gene of trypanosomes encodes a homologue of rat protein-disulfide isomerase and phosphoinositol-phospholipase C," *Biochemistry*, vol. 28, pp. 6440-6446, 1989.
- [30] M. Anderson, R. Bridges and A. Meister, "Direct evidence for inter-organ transport of glutathione and that the non-filtration renal mechanism for glutathione utilization involves γ -glutamyl transpeptidase," *Biochemical and Biophysical Research Communications*, vol. 96, pp. 848-853, 1980.
- [31] A. Meister, "On the Cycles of Glutathione Metabolism and Transport," *Current Topics in Cellular Regulation*, vol. 18, pp. 21-58, 1981.
- [32] I. Dalle-Donne, R. Rossi, D. Giustarini, R. Colombo and A. Milzani, "S-glutathionylation in protein redox regulation," *Free Radical Biology and Medicine*, vol. 43, pp. 883-898, 2007.
- [33] P. Ghezzi, "Regulation of protein function by glutathionylation," *Free Radical Research*, vol. 39, pp. 573-580, 2005.
- [34] R. Fahey, G. Newton, B. Arrick, T. Overdank-Bogart and S. Aley, "Entamoeba histolytica: a eukaryote without glutathione metabolism," *Science*, vol. 224, pp. 70-72, 1984.
- [35] R. Fahey and A. Sundquist, "Evolution of glutathione metabolism," *Advances in Enzymology and Related Areas of Molecular Biology*, vol. 64, pp. 1-53, 1991.
- [36] A. Fairlamb and A. Cerami, "Metabolism and Functions of Trypanothione in the Kinetoplastida," *Annual Review of Microbiology*, vol. 46, pp. 695-729, 1992.
- [37] A. Fairlamb and A. Cerami, "Identification of a novel, thiol-containing co-factor essential for glutathione reductase enzyme activity in trypanosomatids," *Molecular and Biochemical Parasitology*, vol. 14, pp. 187-198, 1985.
- [38] M. Moutiez, M. Aumercier, R. Schoneck, D. Mezianecherif, V. Lucas, P. Aumercier, A. Ouaisi, C. Sergheraert and A. Tartar, "Purification and characterization of a trypanothione-glutathione thioltransferase from *Trypanosoma cruzi*," *The Biochemical Journal*, vol. 310, pp. 433-437, 1995.
- [39] A. Fairlamb, G. Henderson and A. Cerami, "Trypanothione is the primary target for arsenical drugs against African trypanosomes," *PNAS*, vol. 86, pp. 2607-2611, 1989.
- [40] M. Dormeyer, N. Reckenfelderbaumer, H. Ludemann and R. Krauth-Siegel, "Trypanothione-dependent synthesis of deoxyribonucleotides by *Trypanosoma*

- brucei ribonucleotide reductase," *The Journal of Biological Chemistry*, vol. 276, pp. 10602-10606, 2001.
- [41] S. Awad, G. Henderson, A. Cerami and K. Held, "Effects of trypanothione on the biological activity of irradiated transforming DNA," *International Journal of Radiation Biology*, vol. 62, pp. 401-407, 1992.
- [42] A. Fairlamb, G. Henderson, C. Bacchi and A. Cerami, "In vivo effects of difluoromethylornithine on trypanothione and polyamine levels in bloodstream forms of *Trypanosoma brucei*," *Molecular and Biochemical Parasitology*, vol. 24, pp. 185-191, 1987.
- [43] A. Bitonti, C. Bacchi, P. McCann and A. Sjoerdsma, "Catalytic irreversible inhibition of *Trypanosoma brucei* ornithine decarboxylase by substrate and product analogs and their effect in murine trypanosomiasis," *Biochemical Pharmacology*, vol. 34, pp. 1773-1777, 1985.
- [44] N. Yarlett and C. Bacchi, "Effect of D,L- α -difluoromethylornithine on methionine cycle intermediates in *Trypanosoma brucei*," *Molecular and Biochemical Parasitology*, vol. 27, pp. 1-10, 1988.
- [45] A. Bitonti, J. Dumont and P. McCann, "Characterization of *Trypanosoma brucei* S-adenosyl-L-methionine decarboxylase and its inhibition by Berenil, pentamidine and methylglyoxal bis(guanylhydrazone)," *The Biochemical Journal*, vol. 237, pp. 685-689, 1986.
- [46] A. Bitonti, S. Kelly and P. McCann, "Characterization of spermidine synthase from *Trypanosoma brucei*," *Molecular and Biochemical Parasitology*, vol. 13, pp. 21-28, 1984.
- [47] B. Arrick, O. Griffith and A. Cerami, "Inhibition of Glutathione synthesis as a chemotherapeutic strategy for trypanosomiasis," *The Journal of Experimental Medicine*, vol. 153, pp. 720-725, 1981.
- [48] O. Griffith and A. Meister, "Potent and specific inhibition of glutathione synthesis by buthionine sulfoxamine (S-N-butyl homocysteine sulfoxamine)," *The Journal of Biological Chemistry*, vol. 254, pp. 7558-7560, 1979.
- [49] C. Bacchi, H. Nathan, P. McCann, P. McCann and A. Sjoerdsma, "Polyamine metabolism: a potential therapeutic target in trypanosomes," *Science*, vol. 210, pp. 332-334, 1980.
- [50] V. Bellofatto, A. Fairlamb, G. Henderson and G. Cross, "Biochemical changes associated with α -difluoromethylornithine uptake and resistance in *Trypanosoma brucei*," *Molecular and Biochemical Parasitology*, vol. 25, pp. 227-238, 1987.
- [51] R. Bartsch, G. Newton, C. Sherrill and R. Fahey, "Glutathione amide and its perthiol in anaerobic sulfur bacteria," *Journal of Bacteriology*, vol. 178, no. 15, pp. 4742-4746, 1996.

- [52] R. Steudel, "On the nature of the "elemental sulfur" (S₀) produced by sulfur-oxidizing bacteria—a model for S₀ globules," in *Autotrophic bacteria*, Berlin, Springer-Verlag, 1989, pp. 289-303.
- [53] N. Pfennig and H. Truper, "The family Chromatiaceae," in *The prokaryotes*, New York, Springer-Verlag, 1992, pp. 3200-3221.
- [54] H. Truper, "Physiology and biochemistry of phototrophic bacteria," in *Autotrophic bacteria*, Berlin, Springer-Verlag, 1989, pp. 267-281.
- [55] A. Pott and C. Dahl, "Sirohaem sulfite reductase and other proteins encoded by genes at the *dsr* locus of *Chromatium vinosum* are involved in the oxidation of intracellular sulfur," *Microbiology*, vol. 144, pp. 1881-1894, 1998.
- [56] G. Hageage, E. Eanes and R. Gherna, "X-ray diffraction studies of the sulfur globules accumulated by *Chromatium* species," *Journal of Bacteriology*, vol. 101, pp. 464-469, 1970.
- [57] C. Dahl, "Inorganic Sulfur Compounds as Electron Donors in Purple Sulfur Bacteria," in *Sulfur Metabolism in Phototrophic Organisms*, Springer, 2008, pp. 289-317.
- [58] R. Hurlbert, "Effect of oxygen on viability and substrate utilization in *Chromatium*," *Journal of Bacteriology*, vol. 93, pp. 1346-1352, 1967.
- [59] C. Kampf and N. Pfennig, "Chemoautotrophic growth of *Thiocystis violacea*, *Chromatium gracile* and *C. vinosum* in the dark at various O₂- concentrations," *Journal of Basic Microbiology*, vol. 26, pp. 517-531, 1986.
- [60] J. Overmann and N. Pfennig, "Continuous chemotrophic growth and respiration of Chromatiaceae species at low oxygen concentrations," *Archives of Microbiology*, vol. 158, pp. 59-67, 1992.
- [61] G. Newton, K. Arnold, M. Price, C. Sherrill, S. Delcardayre, Y. Aharonowitz, G. Cohen, J. Davies, R. Fahey and C. Davis, "Distribution of Thiols in Microorganisms: Mycothiol Is a Major Thiol in Most Actinomycetes," *Journal of Bacteriology*, vol. 178, no. 7, pp. 1990-1995, 1996.
- [62] H. Spies and D. Steenkamp, "Thiols of intracellular pathogens. Identification of ovoid thiol A in *Leishmania donovani* and structural analysis of a novel thiol from *Mycobacterium bovis*," *European Journal of Biochemistry*, vol. 224, pp. 203-213, 1994.
- [63] G. Newton and R. Fahey, "Mycothiol biochemistry," *Archives of Microbiology*, vol. 178, pp. 388-394, 2002.
- [64] M. Misset-Smits, P. van Ophem, S. Sakuda and J. Duine, "Mycothiol, 1-O-(2'-[N-acetyl-L-cysteinyl]amido-2'-deoxy- α -D-glucopyranosyl)-D-myo-inositol, is the factor of NAD/factor-dependent formaldehyde dehydrogenase," *FEBS Letters*, vol. 409, pp. 221-222, 1997.

- [65] A. Norin, P. van Ophem, S. Piersma, B. Persson, J. Duine and H. Jornvall, "Mycothiol-dependent formaldehyde dehydrogenase, a prokaryotic medium-chain dehydrogenase/reductase, phylogenetically links different eukaryotic alcohol dehydrogenases—primary structure, conformational modelling and functional correlations," *European Journal of Biochemistry*, vol. 248, pp. 282-289, 1997.
- [66] G. Newton, Y. Av-Gay and R. Fahey, "A novel mycothiol-dependent detoxification pathway in mycobacteria involving mycothiol S-conjugate amidase," *Biochemistry*, vol. 39, pp. 10739-10746, 2000.
- [67] G. Newton, Y. Av-Gay and R. Fahey, "N-Acetyl-1-D-myo-inosityl-2-amino-2-deoxy- α -D-glucopyranoside deacetylase (MshB) is a key enzyme in mycothiol biosynthesis," *Journal of Bacteriology*, vol. 182, pp. 6958-6963, 2000.
- [68] G. Newton, P. Ta, K. Bzymek and R. Fahey, "Biochemistry of the initial steps of mycothiol biosynthesis," *Journal of Biological Chemistry*, vol. 281, pp. 33910-33920, 2006.
- [69] C. Bornemann, M. Jardine, H. Spies and D. Steenkamp, "Biosynthesis of mycothiol: elucidation of the sequence of steps in *Mycobacterium smegmatis*," *Biochemical Journal*, vol. 325, pp. 623-629, 1997.
- [70] S. Anderberg, G. Newton and R. Fahey, "Mycothiol biosynthesis and metabolism: cellular levels of potential intermediates in the biosynthesis and degradation of mycothiol," *Journal of Biological Chemistry*, vol. 273, pp. 30391-30397, 1998.
- [71] F. Fan, M. Vetting, P. Frantom and J. Blanchard, "Structures and mechanisms of the mycothiol biosynthetic enzymes," *Current Opinion in Chemical Biology*, vol. 13, pp. 451-459, 2009.
- [72] R. Fahey, "Glutathione analogs in prokaryotes," *Biochimica et Biophysica Acta*, pp. 3182-3198, 2013.
- [73] K. Reddie and K. Carroll, "Expanding the functional diversity of proteins through cysteine oxidation," *Current Opinion in Chemical Biology*, vol. 12, pp. 746-754, 2008.
- [74] E. Marcucci, N. Bayo-Puxan, J. Tulla-Puche, J. Spengler and F. Albericio, "Cysteine-S-trityl a Key Derivative to Prepare N-Methyl Cysteines," *Journal of Combinatorial Chemistry*, vol. 10, pp. 69-78, 2008.
- [75] P. Chandrangsu, W. Loi, H. Antelmann and J. Helmann, "The role of Bacillithiol in Gram-positive Firmicutes," *Antioxidants & Redox Signalling*, vol. 28, no. 6, pp. 445-462, 2018.
- [76] X. Wang and M. Cyander, "Pyruvate released by astrocytes protects neurons from copper-catalyzed cysteine neurotoxicity," *Journal of Neuroscience*, vol. 21, pp. 3322-3331, 2001.
- [77] H. Beinert, "Iron-sulfur proteins: ancient structures, still full of surprises," *Journal of Biological Inorganic Chemistry*, vol. 5, pp. 2-15, 2000.

- [78] J. Burkhead, K. Reynolds, S. Abdel-Ghany, C. Cohu and M. Pilon, "Copper homeostasis," *New Phytologist*, vol. 182, pp. 799-816, 2009.
- [79] G. Newton, M. Rawat, J. La Clair, V. Jothivasan, T. Budiarto, C. Hamilton, A. Claiborne, J. Helmann and R. Fahey, "Bacillithiol as an antioxidant thiol produced in Bacilli," *Nature Chemical Biology*, vol. 5, no. 9, pp. 625-627, 2009.
- [80] D. Parsonage, G. Newton, R. Holder, B. Wallace, C. Paige, C. Hamilton, P. Dos Santos, M. Redinbo, S. Reid and A. Claiborne, "Characterization of the N-Acetyl-R-D-glucosaminyl L-Malate Synthase and Deacetylase Functions for Bacillithiol Biosynthesis in *Bacillus anthracis*," *Biochemistry*, vol. 49, pp. 8398-8414, 2010.
- [81] H. Upton, G. Newton, M. Gushiken, K. Lo, D. Holden, R. Fahey and M. Rawat, "Characterization of BshA, bacillithiol glycosyltransferase from *Staphylococcus aureus* and *Bacillus subtilis*," *FEBS Letters*, vol. 586, no. 7, pp. 1004-1008, 2012.
- [82] K. Winchell, P. Egeler, A. van Duinen, L. Jackson, M. Karpen and P. Cook, "A structural, functional, and computational analysis of BshA, the first enzyme in the bacillithiol biosynthesis pathway," *Biochemistry*, vol. 55, pp. 4654-4665, 2016.
- [83] S. Sharma, M. Arbach, A. Roberts, C. Macdonald, M. Groom and C. Hamilton, "Biophysical Features of Bacillithiol, the Glutathione surrogate of *Bacillus subtilis* and other Firmicutes," *ChemBioChem*, vol. 14, pp. 2160-2168, 2013.
- [84] N. Frigaard and C. Dahl, "Sulfur Metabolism in Phototrophic Sulfur Bacteria," *Advances in microbial Physiology*, vol. 54, pp. 103-200, 2009.
- [85] J. Hiras, S. Sharma, V. Raman, R. Tinson, M. Arbach, D. Rodrigues, J. Norambuena, C. Hamilton and T. Hanson, "Physiological studies of Chlorobiaceae suggest that bacillithiol derivatives are the most widespread thiols in bacteria.," *mBio*, vol. 9, no. 6, pp. 1603-1618, 2018.
- [86] J. Overmann, "The Prokaryotes," pp. 359-378, 2006.
- [87] J. Rodriguez, J. Hiras and T. Hanson, "Sulfite oxidation in *Chlorobaculum tepidum*," *Frontiers in Microbiology*, vol. 2, p. 112, 2011.
- [88] L. Falkenby, M. Szymanska, C. Holkenbrink, K. Habicht, J. Andersen, M. Miller and N. Frigaard, "Quantitative proteomics of *Chlorobaculum tepidum*: insights into the sulfur metabolism of a phototrophic green sulfur bacterium," *FEMS Microbiology Letter*, vol. 323, pp. 142-150, 2011.
- [89] J. Hiras, "Characterization of a Novel Redox Active Thiol from *Chlorobaculum Tepidum*," *PhD Thesis*, 2012.
- [90] E. Ruggles, S. Flemer Jr and R. Hondal, "A Viable Synthesis of N-Methyl Cysteine," *Biopolymers*, vol. 90, no. 1, pp. 61-68, 2008.
- [91] F. Romero, F. Espliego, J. Baz, T. De Quesada, D. Gravalos, F. De La Calle and J. Fernandez-Puentes, "Thiocoraline, a New Depsipeptide with Antitumor Activity

Produced by a Marine Micromonospora," *Journal of Antibiotics*, vol. 50, no. 9, pp. 734-737, 1997.

- [92] E. Erba, D. Bergamaschi, S. Ronzoni, M. Faretta, S. Taverna, M. Bonfanti, C. Catapano, G. Faircloth, J. Jimeno and M. D'Incalci, "Mode of action of thiocoraline, a natural marine compound with anti-tumour activity," *British Journal of Cancer*, vol. 80, no. 7, pp. 971-980, 1999.
- [93] F. Aslund, K. Berndt and A. Holmgren, "Redox Potentials of Glutaredoxins and Other Thiol-Disulfide Oxidoreductases of the Thioredoxin Superfamily Determined by Direct Protein-Protein Redox Equilibria," *The Journal of Biological Chemistry*, vol. 272, no. 49, pp. 30780-30786, 1997.
- [94] V. Jothivasan and C. Hamilton, "Mycothiols: synthesis, biosynthesis and biological functions of the major low molecular weight thiol in actinomycetes," *Natural Product Reports*, vol. 25, pp. 1091-1117, 2008.
- [95] S. Park and J. Imlay, "High levels of intracellular cysteine promote oxidative DNA damage by driving the Fenton reaction," *Journal of Bacteriology*, vol. 185, pp. 1942-1950, 2003.
- [96] D. Keire, E. Strauss, W. Guo, B. Noszal and D. Rabenstein, "Kinetics and equilibria of thiol/disulfide interchange reactions of selected biological thiols and related molecules with oxidized glutathione," *The Journal of Organic Chemistry*, vol. 57, pp. 123-127, 1992.
- [97] P. Jocelyn, *Biochemistry of the SH group: the occurrence, chemical properties, metabolism and biological function of thiols and disulphides*, Academic Press, 1972.
- [98] J. Ippolito, R. Alexander and D. Christianson, "Hydrogen bond stereochemistry in protein structure and function," *Journal of Molecular Biology*, vol. 215, pp. 457-471, 1990.
- [99] D. Pal and P. Chakrabarti, "Different Types of Interactions Involving Cysteine Sulfhydryl Group in Proteins," *Journal of Biomolecular Structure and Dynamics*, vol. 15, no. 6, pp. 1059-1072, 1998.
- [100] A. Streitwieser, "Solvolytic Displacement Reactions At Saturated Carbon Atoms," *Chemical Reviews*, vol. 56, no. 4, pp. 571-752, 1956.
- [101] R. Benesch and R. Benesch, "The Acid Strength of the -SH Group in Cysteine and Related Compounds," *Journal of the American Chemical Society*, vol. 77, no. 22, pp. 5877-5881, 1955.
- [102] P. Riddles, R. Blakeley and B. Zerner, "Reassessment of Ellman's reagent," *Methods in Enzymology*, vol. 91, pp. 49-60, 1983.
- [103] G. Clement and T. Hartz, "Determination of the microscopic ionization constants," *Journal of Chemical Education*, vol. 48, no. 6, pp. 395-397, 1971.

- [104] A. Splittgerber and L. Chinander, "The spectrum of a dissociation intermediate of cysteine: a biophysical chemistry experiment," *Journal of Chemical Education*, vol. 65, no. 2, pp. 167-170, 1988.
- [105] M. Shaik and S. Gan, "Rapid resolution liquid chromatography method development and validation for simultaneous determination of homocysteine, vitamins B 6 , B 9 , and B 12 in human serum," *Indian Journal of Pharmacology*, vol. 45, no. 2, pp. 159-167, 2013.
- [106] R. Dawson, D. Elliott, W. Elliott and K. Jones, "Data for Biochemical Research," *Oxford University Press*, vol. 3, pp. 16-17, 1987.
- [107] C. Aakeroy and K. Seddon, "The hydrogen bond and crystal engineering," *Chemical Society Reviews*, vol. 22, pp. 397-407, 1993.
- [108] A. Glushchenko and D. Jacobsen, "Molecular Targeting of Proteins by L-Homocysteine: Mechanistic Implications for Vascular Disease," *Antioxidants & Redox Signalling*, vol. 9, no. 11, pp. 1883-1898, 2007.
- [109] P. Nagy, "Kinetics and Mechanisms of Thiol–Disulfide Exchange Covering Direct Substitution and Oxidation-Mediated Pathways," *Antioxidants & Redox Signaling*, vol. 18, no. 13, pp. 1623-1641, 2013.
- [110] T. Liu, "The Role of Sulfur in Proteins," in *The Proteins*, Academic Press, 1977, p. 239.
- [111] G. Whitesides, J. Houk and M. Patterson, "Activation parameters for thiolate-disulfide interchange reactions in aqueous solution," *Journal of Organic Biochemistry*, vol. 48, pp. 112-115, 1983.
- [112] D. Ziegler, "Role of reversible oxidation-reduction of enzyme thiols-disulfides in metabolic regulation," *Annual Review of Biochemistry*, vol. 54, pp. 305-329, 1985.
- [113] H. Gilbert, "Redox control of enzyme activities by thiol/disulfide exchange," *Methods in Enzymology*, vol. 107, pp. 330-351, 1984.
- [114] J. Houk, R. Singh and G. Whitesides, "Measurement of Thiol-Disulfide Interchange Reactions and Thiol pKa Values," *Methods in Enzymology*, vol. 143, pp. 129-140, 1987.
- [115] G. Whitesides, J. Lilburn and R. Szajewski, "Rates of thiol-disulfide interchange reactions between mono- and dithiols and Ellman's reagent," *Journal of Organic Chemistry*, vol. 42, pp. 332-338, 1977.
- [116] J. Wilson, R. Bayer and D. Hupe, "Structure-reactivity correlations for thiol-disulfide interchange reaction," *Journal of the American Chemical Society*, vol. 99, pp. 7922-7926, 1977.
- [117] P. Nagy and C. Winterbourn, "Redox chemistry of biological thiols," in *Advances in Molecular Toxicology*, Amsterdam, Elsevier, 2010, pp. 183-222.

- [118] G. Roos, N. Foloppe and J. Messens, "Understanding the pKa of redox cysteines: the key role of hydrogen bonding," *Antioxidants & Redox Signalling*, vol. 18, pp. 94-127, 2012.
- [119] X. Chen and J. Brauman, "Hydrogen bonding lowers intrinsic nucleophilicity of solvated nucleophiles," *Journal of the American Chemical Society*, vol. 130, pp. 15038-15046, 2008.
- [120] G. Ferrer-Sueta, B. Manta, H. Botti, R. Radi, M. Trujillo and A. Denicola, "Factors affecting protein thiol reactivity and specificity in peroxide reduction," *Chemical Research in Toxicology*, vol. 24, pp. 434-450, 2011.
- [121] T. DeCollo and W. Lees, "Effects of Aromatic Thiols on Thiol-Disulfide Interchange Reactions That Occur during Protein Folding," *Journal of Organic Chemistry*, vol. 66, pp. 4244-4249, 2001.
- [122] P. Fernandes and M. Ramos, "Theoretical insights into the mechanism for thiol/disulfide exchange," *Chemistry: A European Journal*, vol. 6, pp. 63-74, 2004.
- [123] R. Singh and G. Whitesides, "Comparisons of rate constants for thiolate-disulfide interchange in water and in polar aprotic-solvents using dynamic ¹H NMR line-shape analysis," *Journal of the American Chemical Society*, vol. 112, pp. 1190-1197, 1990.
- [124] A. Kachur, C. Koch and J. Biaglow, "Mechanism of Copper-Catalyzed Oxidation of Glutathione," *Free Radical Research*, vol. 28, no. 3, pp. 259-269, 1998.
- [125] H. Seko, K. Tsuge, A. Igashira-Kamiyama, T. Kawamoto and T. Konno, "Autoxidation of thiol-containing amino acid to its disulfide derivative that links two copper(II) centers: the important role of auxiliary ligand," *Chemical Communications*, vol. 46, pp. 1962-1964, 2010.
- [126] W. Rauser, "Phytochelatin," *Annual Review of Biochemistry*, vol. 59, pp. 61-86, 1990.
- [127] D. Hamer, "Metallothionein," *Annual Review of Biochemistry*, vol. 55, pp. 913-951, 1986.
- [128] G. Saez, P. Thornalley, H. Hill, R. Hems and J. Bannister, "The production of free radicals during the autoxidation of cysteine and their effect on isolated rat hepatocytes," *Biochimica et Biophysica Acta*, vol. 719, pp. 24-31, 1982.
- [129] A. Searle and A. Tomasi, "Hydroxyl free radical production in iron-cysteine solutions and protection by zinc," *Journal of Inorganic Biochemistry*, vol. 17, pp. 161-166, 1982.
- [130] A. Kachur, C. Koch and J. Biaglow, "Mechanism of copper-catalyzed autoxidation of cysteine," *Free Radical Research*, vol. 31, no. 1, pp. 23-34, 1999.

- [131] D. Cavallini, C. De Marco, S. Dupre and G. Rotilio, "The copper catalyzed oxidation of cysteine to cystine," *Archives of Biochemistry and Biophysics*, vol. 130, pp. 354-361, 1969.
- [132] G. Buettner, "The pecking order of free radicals and antioxidants: lipid peroxidation, α -tocopherol and ascorbate," *Archives of Biochemistry and Biophysics*, vol. 300, pp. 535-543, 1993.
- [133] C. Koch and S. Evans, "Cysteine concentrations in rodent tumors: unexpectedly high values may cause therapy resistance," *International Journal of Cancer*, vol. 67, pp. 661-667, 1996.
- [134] A. Lehmann, H. Hadberg, O. Orwar and M. Sandberg, "Cysteine sulphinate and cysteate: mediators of cysteine toxicity in the neonatal rat brain?," *European Journal of Neuroscience*, vol. 5, pp. 1398-1412, 1993.
- [135] N. Zhang, H.-P. Schuchmann and C. von Sonntag, "The reaction of superoxide radical anion with dithiothreitol: a chain process," *Journal of physical Chemistry*, vol. 95, pp. 4718-4722, 1991.
- [136] L. Sjoberg, T. Eriksen and L. Revesz, "The reaction of the hydroxyl radical with glutathione in neutral and alkaline aqueous solution," *Radiation Research*, vol. 89, pp. 255-263, 1982.
- [137] C. Winterbourn and D. Metodiewa, "The reaction of superoxide with reduced glutathione," *Archives of Biochemistry and Biophysics*, vol. 314, pp. 284-290, 1994.
- [138] G. Buettner, "The pecking order of free radicals and antioxidants: lipid peroxidation, α -tocopherol and ascorbate," *Archives of Biochemistry and Biophysics*, vol. 300, pp. 535-543, 1993.
- [139] L. Milne, P. Nicotera, S. Orrenius and M. Burkitt, "Effect of glutathione and chelating agents on copper-mediated DNA oxidation: pro-oxidant and antioxidant properties of glutathione," *Archives of Biochemistry and Biophysics*, vol. 304, pp. 102-109, 1993.
- [140] J. Brunet, M. Boily, S. Cordeau and C. des Rosiers, "Effect of N-acetylcysteine in the rat heart reperfused after low-flow ischemia: evidence for a direct scavenging of hydroxyl radical and nitric oxide-dependent increase in coronary flow," *Free Radical Biology and Medicine*, vol. 19, pp. 627-638, 1995.
- [141] M. Ciriolo, A. Palamara, S. Incerpi, E. Lafavia, M. Bue, P. de Vito, E. Garaci and G. Rotilio, "Loss of GSH, oxidative stress, and decrease of intracellular pH as sequential steps in viral infection," *Journal of Biological Chemistry*, vol. 272, pp. 2700-2708, 1997.
- [142] A. Stark and G. Glass, "Role of copper and ceruloplasmin in oxidative mutagenesis induced by the glutathione-gamma-glutamyl transpeptidase system and by other thiols," *Environmental & Molecular Mutagenesis*, vol. 29, pp. 63-72, 1997.

- [143] G. Newton, C. Bewley, T. Dwyer, R. Horn, Y. Aharonowitz, G. Cohen, J. Davies, D. Faulkner and R. Fahey, "The structure of U17 isolated from *Streptomyces clavuligerus* and its properties as an antioxidant thiol," *European Journal of Biochemistry*, vol. 230, pp. 821-825, 1995.
- [144] A. Sundquist and R. Fahey, "The function of gamma-glutamylcysteine and bis-gamma-glutamylcysteine reductase in *Halobacterium halobium*," *Journal of Biological Chemistry*, vol. 264, pp. 719-725, 1989.
- [145] A. Kachur, K. Held, C. Koch and J. Biaglow, "Mechanism of production of hydroxyl radicals in the copper-catalyzed oxidation of dithiothreitol," *Radiation Research*, vol. 147, pp. 409-415, 1997.
- [146] M. Arbach, "Diallyl Polysulfides from Garlic: Mode of Action and Applications in Agriculture," *PhD Thesis*, 2014.
- [147] T. Fiskerstrand, H. Refsum, G. Kvalheim and P. Ueland, "Homocysteine and Other Thiols in Plasma and Urine: Automated Determination and Sample Stability," *Clinical Chemistry*, vol. 39, no. 2, pp. 236-271, 1993.
- [148] B. Mannervick, I. Carlberg and K. Larson, "Glutathione: general review of mechanism of action," in *Glutathione: Chemical, Biochemical and Medical Aspects. Parts A and B*, Wiley Interscience, 1989, pp. 475-516.
- [149] T. Stevenson, B. McDonald and S. Roston, "Colorimetric method for determination of erythrocyte glutathione," *Journal of Laboratory and Clinical Medicine*, vol. 56, p. 157, 1960.
- [150] K. Shimada, K. Fujikawa, K. Yahara and T. Nakamura, "Antioxidative Properties of Xanthan on the Autoxidation of Soybean Oil in Cyclodextrin Emulsion," *Journal of Agriculture and Food Chemistry*, vol. 40, pp. 945-948, 1992.